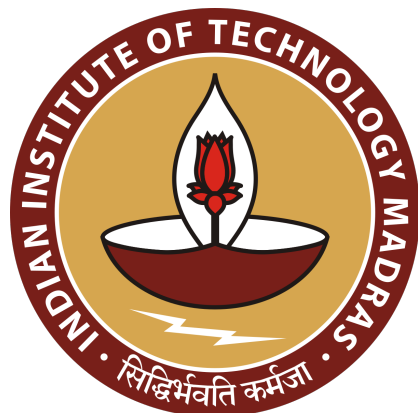

AERIAL SEARCH AND RELIEF UAV

AS5213: DESIGN OF UAV AND MAV

GROUP-1



PROF. DEVAPRAKASH MUNIRAJ AND

PROF. SATADAL GHOSH

AE21B108 REVA DHILLON

AE23M047 VINAY B A

AE21B102 AKASH THAKUR

AE21B062 TONGARIA BHAVESH

AE23M802 MOHAMMAD SARWAR

AE23M012 CHINMAY GOURKHEDE

AE23M020 KHUSHBOO RAJENDRA THAKUR

Contents

1 Mission profile	10
1.1 Abstract:	10
1.2 Mission Objective and Motivation:	11
1.2.1 Mission Objective:	11
1.2.2 Mission Motivation: Why does marine SAR need UAVs?	11
1.3 Mission Profile:	13
1.3.1 Performance Parameters' Characteristics (Mission requirements):	14
1.3.2 Payload requirements:	14
1.3.3 Configuration:	14
1.4 Previous Aircraft Study:	16
2 Preliminary weight estimate	17
2.1 Detailed Mission Profile for power estimation:	17
2.2 Preliminary Weight Estimate:	18
2.2.1 Empty weight fraction as a function of DTOW:	18
2.2.2 Payload Weight:	20
2.2.3 Battery Weight:	21
2.2.4 Empty Weight and DTOW:	23
2.3 Summary:	25
3 Propulsion system selection	26
3.1 Flowchart for this week's process	26
3.2 Requirement of L/D estimation	26
3.3 Power Requirements - Refined Estimate:	28
3.3.1 Power for Climb - 1:	28
3.3.2 Power for Cruise:	29
3.3.3 Power for Loiter:	29
3.3.4 Power for Climb - 2:	30
3.3.5 Power required for Takeoff, Descent and Landing:	30
3.3.6 Total Power requirement:	30
3.4 Power-plant specification and configuration	31
3.4.1 Motor	31
3.4.2 Propellers	31
3.4.3 ESC	31
3.4.4 Battery	32
3.4.5 Powerplant position	32
3.5 Summary	34
4 Wing Loading	35
4.1 Stall velocity:	36

4.2	Maximum range cruise:	36
4.3	Maximum rate of climb:	36
4.4	Maximum endurance loiter:	37
4.5	Maximum Velocity:	38
4.6	Absolute ceiling:	38
4.7	Summary	39
5	Secondary Weight Estimate:	40
5.1	Power loading based on wing loading:	40
5.1.1	Propeller efficiency(η_p):	41
5.1.2	Power-plant Weight	41
5.1.3	Power loading for cruise:	41
5.1.4	Power loading for climb - 1:	42
5.1.5	Power loading for loiter:	42
5.1.6	Power loading for Climb-2:	43
5.2	Secondary Weight Estimate:	44
5.3	Summary	45
6	Re-estimation of design parameters.	46
6.1	Detailed mission profile	46
6.2	Weight estimate	47
6.3	Power requirements	48
6.4	Power-plant	48
7	Wing Design	49
7.1	Airfoil Selection	49
7.1.1	Parameters previously estimated for the aircraft:	49
7.1.2	Airfoil Thickness	50
7.1.3	Airfoil Selection Criteria	51
7.2	Wing Vertical Location	55
7.2.1	High wing	55
7.2.2	Low wing	55
7.2.3	Mid wing	56
7.3	Wing Dihedral	56
7.4	Aspect Ratio	57
7.5	Taper Ratio (λ)	58
7.6	Sweep Angle (Λ)	58
7.7	Twist	59
7.8	Wingtips	60
7.9	Wing angle of incidence (i_w)	60
7.10	Control Surfaces	60
7.11	High Lift Devices	61
7.12	Summary	62
8	Fuselage Design	63
8.1	Fuselage Dimensions:	64
8.1.1	Fuselage Length:	64
8.1.2	Mid-section of Fuselage:	64
8.1.3	Up-sweep angle:	66
8.1.4	Nose Section	66
8.1.5	Rear fuselage length:	66

8.2	Summary	67
9	Tail Design and Preliminary Sizing	68
9.1	Tail Configuration	68
9.2	Average values for parameters	69
9.3	Horizontal Tail	69
9.3.1	Area S_h :	69
9.3.2	Aspect Ratio AR_h :	69
9.3.3	Taper Ratio λ_h and Sweep Angle Λ_h :	69
9.3.4	Horizontal Tail Airfoil Selection:	69
9.3.5	Horizontal Tail Incidence Angle:	70
9.4	Vertical Tail:	70
9.4.1	Vertical Tail Area	70
9.4.2	Aspect Ratio of vertical tail	70
9.4.3	Vertical tail Sweep Λ_v and Taper Ratio λ_v	70
9.4.4	Airfoil selection	70
9.5	Inverted V-tail:	71
9.6	Summary	72
10	Landing System Design	73
10.1	Different landing mechanisms	73
10.2	Takeoff mechanism	74
10.2.1	How it works:	74
10.3	Terminal velocity and altitude of deployment	75
10.3.1	The terminal velocity:	75
10.3.2	The altitude of parachute deployment:	75
10.3.3	Mathematical model used:	75
10.3.4	Results:	77
10.4	Parachute selection	79
10.5	CAD Models:	80
10.6	Summary	81
11	Internal Layout & CG Estimate	82
11.1	Introduction	82
11.2	Internal Layout	82
11.2.1	Nose	82
11.2.2	Mid-Fuselage	82
11.2.3	Rear Fuselage	82
11.2.4	Payload-drop Mechanism	82
11.2.5	Access Doors	83
11.2.6	Parachute deployment door	84
11.3	CG Estimation	84
11.3.1	Structural Mass Approximation	84
11.3.2	CG calculation	84
11.3.3	CAD Figures	85
11.4	Summary	87
12	Static Stability Analysis	88
12.1	Longitudinal Static Stability	88
12.1.1	Static Pitch Stability and Neutral Point	89
12.1.2	Lift coefficient slopes - Wing and Tail	90

12.1.3 Effect of the Fuselage	91
12.1.4 Effect of Downwash	92
12.1.5 Tail contribution	93
12.1.6 Neutral Point and Static Margin:	96
12.2 Gust Strength:	97
12.3 Horizontal and Vertical Control Surfaces	98
12.3.1 The Elevator	98
12.3.2 The Rudder	99
12.4 Summary	101
12.5 Tail parameters (updated)	101
13 Performance Analysis	104
13.1 Parasite drag estimation:	104
13.1.1 Skin friction coefficient:	104
13.1.2 Wetted area(S_{wet}):	105
13.1.3 Form factor:	105
13.1.4 Final calculations:	106
13.2 Drag Polar:	106
13.3 The $V - n$ diagram	107
13.4 Gust load diagram	108
13.5 The Drag Bucket	109
13.6 Power requirement	110
13.6.1 Maximum velocity estimate	111
13.6.2 Rate of climb	111
14 Summary	112
14.1 Mission Profile	112
14.2 Payload	112
14.3 Preliminary weight estimate	113
14.4 Wing Loading	113
14.5 Secondary weight estimate	114
14.6 Powerplant Description	114
14.7 Wing Design	115
14.8 Fuselage Design and Tail Design	116
14.9 Internal Layout	118
14.10 Takeoff and Landing Mechanisms	119
14.11 CG Location & Masses	120
14.12 Stability Analysis	122
14.13 Performance Analysis	123
14.14 CAD model	123
Bibliography	124
Website References	124
Book References	124
Image References	124
UAV References	125
Battery & ESC References	125
Gimbal References	125
Life Jacket References	125
Motor References	125
Propeller References	125

Parachute References	126
15 Appendix	127

List of Figures

1.1	South Korea ferry disaster	12
1.2	Mission Profile	13
1.3	Fixed wing [UAVL] and Tilt Rotor UAVs [16]	15
2.1	$\frac{W_e}{W_0}$ VS. DTOW (log - log scale).	18
2.2	$\frac{W_e}{W_0}$ VS. DTOW	19
2.3	Weight Estimation Vs iterations	23
3.1	Estimation of L/Dmax	28
5.1	Variation in DTOW with iterations.	44
6.1	Mission Profile	46
6.2	Flyby height calculations	47
6.3	Revised weight estimate	48
7.1	Thickness ratio - Historical trend [13]	50
7.2	GA 35A015	52
7.3	C_l vs Angle of Attack for Reynolds no. of 500k	52
7.4	C_d vs Angle of Attack for Reynolds no. of 500k	53
7.5	C_l/C_d vs Angle of Attack for Reynolds no. of 500k	53
7.6	C_l/C_d vs C_l for Reynolds no. of 500k	54
7.7	GA 35A015 Airfoil in XFLR5	54
7.8	Effect of Aspect Ratio on C_L vs α curve [13]	57
7.9	Sweep Angle & Mach Angle [5]	59
7.10	Wingtip types	60
7.11	Wing CAD	62
8.1	Plots for regression	65
8.2	Fuselage Isometric View	66
8.3	Fuselage dimension	67
9.1	Tail config, ref pg.68 [13]	68
9.2	Inverted V-tail diagrams	71
9.3	Tail CAD	72
10.1	Bungee Chord Mechanism.	74
10.2	Two-degree of freedom trajectory system model	76
10.3	The x location variation with time.	77
10.4	The z location variation with time.	77
10.5	\dot{x} variation with time.	78
10.6	\dot{z} variation with time.	78

10.7 UAV Trajectory	79
10.8 CAD model of the UAV design proposed	80
11.1 Payload-drop Mechanism	83
11.2 Three View diagram of Internal Layout and CG locations	86
11.3 CG location	86
12.1 Forces acting on the aircraft.	89
12.2 τ variation plot - A is the aspect ratio and $a_0 = C_{l_\alpha}$	90
12.3 CL vs Alpha using XFLR5	91
12.4 K_f vs. Position of 1/4 root chord	92
12.5 Downwash estimation	93
12.6 New tail CAD	94
12.7 C_{N_β} plot	95
12.8 C_{L_β} plot	96
12.9 CM vs Alpha plot using XFLR5	97
12.10 C_{M_α} updated plot	102
12.11 C_{N_β} updated plot	103
12.12 C_{L_β} updated plot	103
13.1 Drag Polar	107
13.2 $V - n$ Diagram	108
13.3 Flight Envelope	109
13.4 $\frac{C_L}{C_D}$ vs C_L	110
13.5 Power-velocity curve	111
14.1 Mission Profile	112
14.2 Wing	115
14.3 Fuselage	116
14.4 Tail	117
14.5 Internal Layout of Components	118
14.6 Parachute deployment - Two degree-of-freedom model results.	119
14.7 UAV CG location	120
14.8 Isometric view of the UAV model	123

List of Tables

1.1 Comparison Fixed Wing v/s Hybrid	14
1.2 Aircraft data	16
2.1 Gimbals' Weight Estimate	20
2.2 Life Jackets' Weight Estimate	20
2.3 Weight of Components Required for GPS	21
2.4 Power requirements for initial W_0	23
2.5 Summary Week 2 Tasks	25
3.1 Wing configuration data	27
3.2 Revised Energy Requirements	30
3.3 Power and Thrust Requirements	31
3.4 Motor-Propeller-ESC-Battery	33
3.5 Summary	34
4.1 Parameters	35
4.2 Wing Loading Summary	39
5.1 Selected wing loading.	40
5.2 Parameters to be used in power estimate	40
5.3 Chapter 5 Summary	45
5.4 Secondary Power estimate	45
6.1 Power estimates	48
7.1 Airfoil Data	51
7.2 Comparison of Wing vertical location configuration	56
7.3 Summary	62
8.1 Component Volume Estimation	63
8.2 Comparable UAV data - DTOW and fuselage length	64
8.3 Fuselage Dimensions	67
9.1 Summary	72
10.1 Parachute specifications	80
10.2 Parachute specifications	81
11.1 Structural Mass estimation	84
11.2 CG location of Structural Components	85
11.3 Components' Masses	85
11.4 Components' CG location	86
11.5 Summary - Chapter 11	87

12.1 Summary	94
12.2 Average wind speeds and the corresponding gust speeds	97
12.3 Summary : Stability	101
13.1 Skin friction coefficient	105
13.2 Wetted area	105
13.3 Form factor	106
13.4 Component build-up for parasite drag calculation	106

Chapter 1

Mission profile

1.1 Abstract:

We aim to design a UAV for near-shore aerial search and relief missions. An analysis of conventional maritime search and rescue operations and methodologies revealed the need to incorporate UAVs in the SAR efforts.

We aim to fabricate a UAV that may locate people lost in sea and deliver a payload comprising basic survival items.

We believe that this objective may also be extended to a UAV swarm that will allow for quicker location of the lost party and facilitate a speedy rescue, we can find about that in [15].

Drowning ranks as the 3rd leading cause of unintentional injury death worldwide, according to the World Health Organization (WHO)[6]

It accounts for roughly 7% of all injury-related deaths.

An estimated 236,000 people drown annually worldwide, with over 90% of these deaths occurring in low- and middle-income countries.

While this data includes all natural water bodies, it clearly emphasizes the need to improve the current SAR operations. We believe that the use of UAVs will prove to be a valuable addition to conventional SAR methods.

1.2 Mission Objective and Motivation:

1.2.1 Mission Objective:

To design a UAV for near-shore aerial search and relief missions. The mission comprises surveillance of the sea and payload delivery. The payload consists of basic equipment to ensure survival, giving a rescue team enough time to reach the person in need.

1.2.2 Mission Motivation: Why does marine SAR need UAVs?

The Search:

- Current marine search and rescue methods involve the use of helicopters - amphibious and non-amphibious, rescue vessels, or any other appropriate vessel to return the lost party to land safely.
- All of the conventional vehicles listed above are heavy vehicles that are slow and consume relatively high amounts of fuel in locating the lost people and their subsequent rescue.
- We propose to reduce both the fuel consumption and the time taken in the location process by the use of UAVs.
- The lighter UAVs can swiftly cover large expanses of water ensuring a quicker response, potentially saving lives.
- Due to the moving currents and winds in an oceans a floating body may not be in the same location after sometime. So covering a particular patch doesn't guarantee that the body won't be there after some time. This is a very interesting challenge and requires advanced path planning techniques.
- Moreover, tasks that are identified as able to be performed by UAS may also benefit from the ability of a swarm of UAS to operate in a cooperative and parallel manner. Parallelization implies that several parts of the search area can be covered at the same time, reducing the overall task completion time.
- UAVs also reduce unnecessary human risks during rescue operation in adverse weather and in remote or hazardous locations.

Payload Delivery:

- The next objective that we propose is the delivery of a payload comprised on a life-jacket or float to the distressed person.
- This is aimed at enabling the survival of the person till a rescue party reaches them.
- We also propose that the payload delivery capability of the UAV be utilised in cases of ships sinking and other situations where lifeboats cannot reach the distressed victims.
- The need for this is best explained with the example of the South Korea ferry disaster of April 2014.

Life buoy delivering UAVs could have save hundreds of lives during the fatal accident if the ferry or the rescue vessels were equipped with such UAVs.

The sinking ferry is shown in Figure 1. Among the 476 people on board, almost 300 people drowned with most of them being Danwon High School students. Some survivors claimed that they had not received any help from the ferry crews which abandoned the ship when there were still hundreds of passengers trapped inside[15].



Figure 1.1: South Korea ferry disaster

The ferry also tilted at an angle that rendered lifeboats on board unreachable for the passengers as it listed and started to sink.

With autonomous UAVs, additional life buoys could have been provided on scene during the critical moments for the passengers to cling to and wait for rescue. It would have provided an alternative to crew directed instructions and given more passengers a chance of survival.” [4]

To summarise, UAVs can serve as a valuable lifesaving technology while racing against time in offshore and nearshore SAR operations.

1.3 Mission Profile:

The mission profile of the UAV can be described in the following sequence:

- Takeoff - Based on the configuration.
- Climb
- Cruise - Involves scanning the area and searching for the target.
- Descent to the required altitude.
- Loiter
- Payload drop
- Climb back to cruise altitude.
- Descent
- Landing

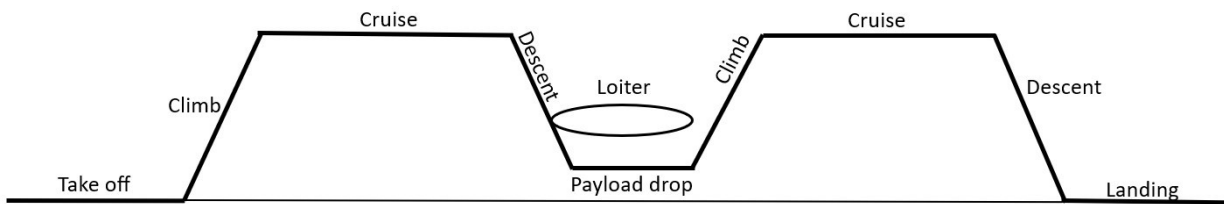


Figure 1.2: Mission Profile

The takeoff of the UAV can be done either by hand launch or it can be facilitated by a catapult. It is then followed by a climb to the desired altitude. Once the desired altitude is reached, the UAV would be in cruise mode. This phase involves scanning the area and sending the live feed to the crew on ground. Once the location is identified, the UAV begins its descent to a predetermined altitude. Upon reaching the required altitude, payload drop will be carried out. A loiter phase is also included in the mission profile in case it is unable to reach the precise location in the first attempt. After the payload drop, the UAV begins a slow climb back to its cruise altitude followed by cruise, descent and landing.

The above mission profile identifies the basic set of tasks that we aim to accomplish.

1.3.1 Performance Parameters' Characteristics (Mission requirements):

The key mission requirements that we focus on are:

- Range : The range of the UAV is aimed at around **45 to 50 kilometres** to be able to carry out the required surveillance of the ocean.
- Endurance : Maximum endurance of approximately **1 hour** is targeted, so as to carry out required SAR operation.
- Cruise altitude : Cruise altitude will be decided based on payload considerations as well as power plant specifications.
- Speed : This involves cruise speed, speed during payload drop and maximum speed attainable. The wind speeds must also be factored in while estimating the speed of the UAV.
- Payload : This is a key parameter in design. The payload weight will be decided based on the payload requirements as detailed below.

1.3.2 Payload requirements:

The payload on the aircraft consists of:

- **Visual surveillance equipment** like a high definition camera to identify the target.
- **Navigation equipment** to identify the UAV's current location with respect to its surroundings like a GPS system.
- **Communication equipment** to relay important information to the base station.
- **Response kit** which would be dropped at the rescue location for the person. This kit will consist of: a GPS tracker to mark the exact location in moving sea currents and winds, a safety response kit and a life jacket.

1.3.3 Configuration:

The two possible configuration for the UAV in our project are :

1. Fixed-wing UAV
2. Hybrid of fixed-wing and VTOL.

	Fixed-Wing	Hybrid
Pros	- Long range	- Reduced take-off distance
	- High endurance	- Increased accuracy of payload drop
Cons	- Stability against gusts	- Flexibility of landing/take-off location
	- Low maneuverability w.r.t. hybrid	- Increased system complexity
	- Longer take-off and landing distance	- Expensive build

Table 1.1: Comparison Fixed Wing v/s Hybrid



Figure 1.3: Fixed wing [UAVL] and Tilt Rotor UAVs [16]

A few examples of marine search and rescue (SAR) UAVs available commercially are :

1. **TEKEVER AR3 VTOL** - A small fixed-wing + VTOL UAV with a span of 3.5 meters & length of 1.5 meters, designed for long endurance flights of 8 hrs (VTOL) or 16 hrs (fixed-wing) with swappable VTOL capabilities.
2. **ElevonX Tango VTOL** - 3 x 1.9 meter fixed-wing + VTOL with payload capacity of 5 kg and range of 420 kms. Its fixed-wing counterparts require a runway length of 150 meters.

From the above Comparison and Commercial Data we can make the following conclusions about the target configuration of our UAV,

- For a SAR mission with Payload delivery, accuracy of Drop-off and Prompt take-off capability makes Hybrid configuration most suitable for the mission.
- Additionally with combined Fixed wing, we get both High Range and Endurance.
- Commercially available UAV with only Fixed wing require a runway length of 150-200 meters or a additional Slingshot system.
- VTOL also helps in maintaining the UAV attitude when faced with strong winds which adds to why a Hybrid configuration is suitable and reliable for Marine SAR missions.

1.4 Previous Aircraft Study:

We started by looking for specifications of general UAVs which are used for surveys and payload deliveries and their Maximum take-off weight lies between 5 to 25 kg as this data would be useful for us in interpolation to get a preliminary weight estimate.

Considering the fabrication we decided not to look for heavier UAVs due to fabrication feasibility constraints.

Aircraft Name	MTOW (Kg)	Payload (Kg)	Empty wt. (Kg)	Range (Km)	Endurance (hr)	Ceiling (m)
Deltaquad pro [22]	6.2	1.2	5	120	2	4000
Blackswift [20]	9.5	2.3	7.2	110	1.5	6000
MH900 Mav Tech [23]	1.2	20.25	0.95	5	0.5	-
SQA eVTOL [24]	9.8	1.3	8.5	40	2.5	4000
Atlas AS90X [19]	2.4	0.3	2.1	15	1	5000
Bramor C4eye [21]	4.5	1	3.5	150	3	5000
AR1-TEKEVER [18]	5	1.5	3.5	20	2	-
Albatros Fixed-wing [17]	10	4.4	9	100	4	3000
V220 [25]	13.5	3	10.5	200	3	-

Table 1.2: Aircraft data

Chapter 2

Preliminary weight estimate

2.1 Detailed Mission Profile for power estimation:

Initial Values for First weight estimate.

- MTOW(W_0) = 8 kg (Considering feasibility in fabrication we decided to keep W_0 low)
- Range (R) = 50 km (table 1.2)
- Endurance (E)= 60 minutes (table 1.2)
- Cruise Speed (V)= 18 m/s (table 1.2)
- Cruise altitude = 200 m (Typical altitude of a surveillance UAV)
- Climb rate = 2.5 m/s (table 1.2)
- Payload weight (W_p) = 1.5 Kg
- Climb angle (γ) = 5° (Calculated from speed and climb rate)
- Wing span (b)= 2.5 m (Typical wingspan from the data sheet)
- $C_{d_0} = 0.04-0.07$ [14]

Time required for each phase:

- Takeoff/Climb = 120 s
- Cruise/surveillance = 2700 s
- Descent to drop altitude = 120 s
- Climb back =120 s
- Buffer = 540 s

2.2 Preliminary Weight Estimate:

The section details the weight estimates for the empty weight, the payload weight, the battery weight and the total design take-off weight.

The empty weight fraction has been derived as a function of the DTOW.

The payload details have been enumerated and an average weight for the payload has been estimated from the same.

The power requirements for the various flight phases has been calculated to arrive at an estimate for the battery weight.

Using these values, we have obtained a preliminary estimate for the DTOW.

2.2.1 Empty weight fraction as a function of DTOW:

We formulate the empty weight fraction as a function of the DTOW W_0 .

$$\frac{W_e}{W_0} = AW_0^L \quad (2.1)$$

Given that the design take-off weight(DTOW) and the maximum take-off weight(MTOW) are similar, the maximum take-off weights of previous aircrafts have been utilised to get a conservative estimate for our DTOW.

To find the constants A and L in the relation above, linear regression has been performed on the data points available from previous aircraft data. (Octave code in appendix 15.)

The figures below display the curves that have been fit. The results are as follows:

$$L = -0.086047 \\ A = 0.894172$$

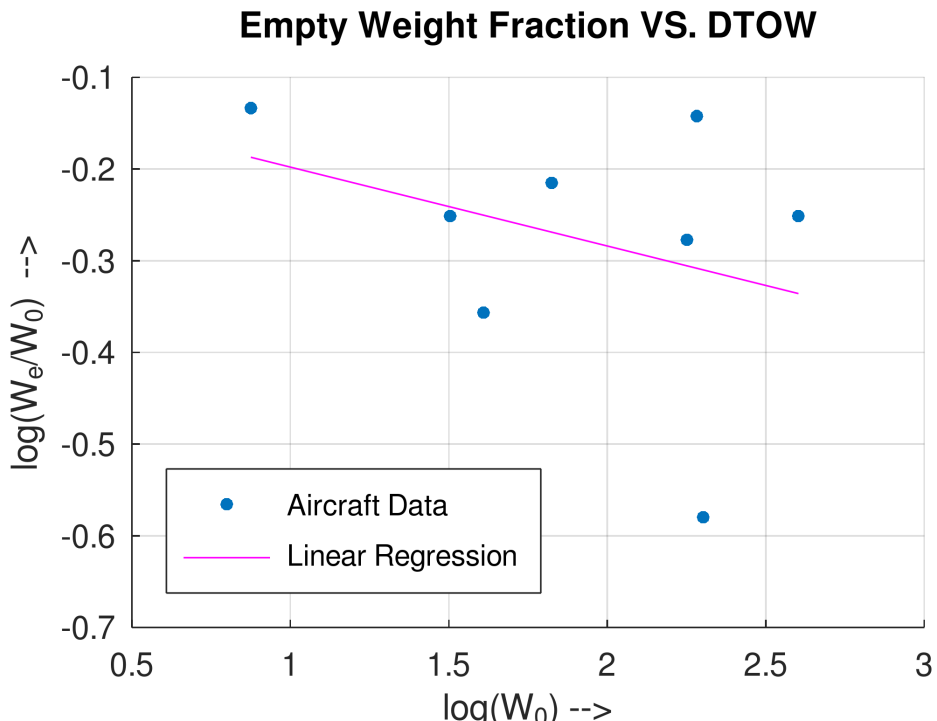


Figure 2.1: $\frac{W_e}{W_0}$ VS. DTOW (log - log scale).

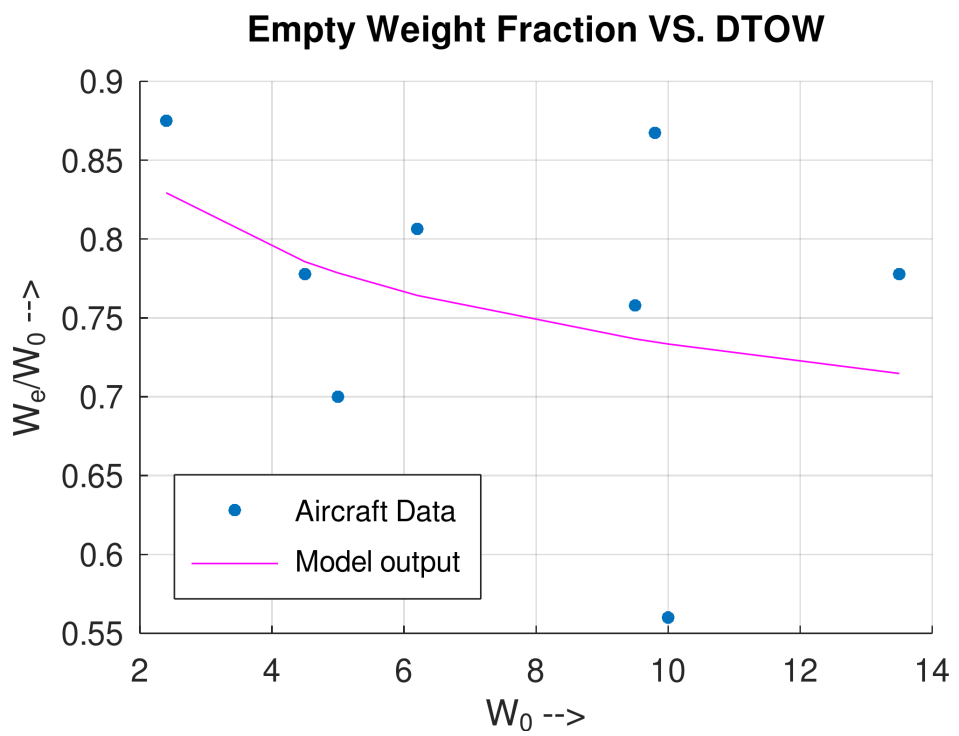


Figure 2.2: $\frac{W_e}{W_0}$ VS. DTOW

Therefore, the final function for the empty weight fraction is as follows:

$$\frac{W_e}{W_0} = 0.894172 \times W_0^{-0.086047} \quad (2.2)$$

Note: Extreme data points were removed e.g. UAVs with very high or very low DTOW.

2.2.2 Payload Weight:

The payloads considered for Search and Recuse mission over the Sea are :

1. Gimbal - Non deliverable
2. Personal Flotation Device (PFD) or Life Jacket - Deliverable
3. GPS Tracker - Deliverable

The weight estimation for the above three required market survey to obtain the general trends which will be utilised to get a good first estimate of our Payload Weight (W_P).

Gimbals	Weight (g)
Trillium HD 25 [32]	340
Trillium HD 40 [33]	840
Trillium HD 45 [34]	1280
SIYI A8 mini [30]	95
SIYI ZR10 [31]	381
SIYI A2 mini [29]	85
Average Gimbal Weight	503.5

Table 2.1: Gimbals' Weight Estimate

Life Jacket Brand	Weight (g)
Onyx	660
Sea choice	480
Absolute Outdoor	997
Solas [35]	952
Average Weight	772.25

Table 2.2: Life Jackets' Weight Estimate

First Estimate for Payload Weight is calculated as,

$$W_P = W_{gimbal} + W_{PFD} + W_{GPS}$$

$$W_P \approx 772.25 + 503.5 + 63 \approx 1500 \text{ grams}$$

GPS and Communication	Weight (g)
Neo 6M	12
Arduino nano	7
Small battery for gps	36
SX1278 LoRa Module (10km range)	8
Total Weight of Components	63

Table 2.3: Weight of Components Required for GPS

2.2.3 Battery Weight:

Battery estimate is done by considering the power requirements for each phase as given in the mission profile. Before proceeding with the power estimates we require certain aerodynamic data. However since this is a first estimate, we rely on correlations, previous data and equations. The following are the data used for power requirement estimation.

- Aspect ratio(AR) = 9 [7]
- $C_{d_0} = 0.04-0.07$ [14]
- $K = \frac{1}{\pi e A R}$
- $e = 1.78(1 - 0.045 AR^{0.68}) - 0.64$ [7]

The power requirements are quite substantial at time of climbing as well as during the cruise as can be seen from our mission profile. Further since our mission also has loitering phase we also need to account for the power requirement during that phase as well.

Power required for cruise:

The cruise phase of our mission is the longest as it involves surveillance and hence the power requirement will also be higher.

During cruise we consider the UAV to be in a steady level flight, hence the thrust is directly equal to drag and is given in Eq.(3)[7]

$$P_{cruise} = VT_{cruise}, \text{ where, } T_{cruise} = D = q_\infty S C_D \quad (2.3)$$

$$P_{cruise} = 145.7119368 + 0.5774166W_0^2 \quad (2.4)$$

Power required for climb:

The thrust required for climb is determined by using the constant rate of climb as defined in the mission requirement.

$$T - W \sin \gamma - D = 0 \quad (2.5)$$

The power required is then obtained by multiplying the thrust with the speed of the climb given by Eq(7)[8].

$$P_{climb} = [(W \sin \gamma) + C_D q_\infty S] V_{climb} \quad (2.6)$$

$$V_{climb} = 1.2 \sqrt{\frac{(2W_0)}{S \rho_{sl} C_{Lmax}}} \quad (2.7)$$

$$P_{climb} = (0.9479 W_0^{1.25}) + (9.12966 W_0^{0.25}) + (0.053 W_0^{1.25}) \quad (2.8)$$

Power required for loiter:

The loiter phase in our mission involves dropping the payload once the location identification is done. This phase takes roughly about 540s of time. Further even during this phase we assume the UAV is in a steady level condition and the corresponding velocity during this phase is obtained by taking maximum (L/D) condition resulting in a much lower velocity than cruise velocity[12]. So, the power requirement during loiter phase is:

$$P_{loiter} = VT_{loiter} \quad (2.9)$$

$$V_{loiter} = \sqrt{\frac{2}{\rho_\infty} \sqrt{\frac{K}{C_{d0}} \frac{W_0}{S}}} \quad (2.10)$$

$$P_{loiter} = (0.343 W_0^{1.5}) + (4.6884 W_0^{0.5}) \quad (2.11)$$

Power required for other mission phases:

The power required during takeoff and landing phases are not included in the initial estimate as takeoff will mostly be by catapult launching method, while for descend phase we have considered the power requirement to be similar to the climb phase. This is done so, because we want the maximum power that would be required during the mission based on which we can select the battery weight.i.e, we are looking at the maximum power requirements.

Total Power requirement:

The total power required for the entire mission is obtained by combining the power requirements for individual phases. An initial estimate of the power requirement is shown in the below table for a W_0 value of 8 Kg.

The above obtained power requirement is multiplied by a factor of 1.2 so as to take into account the other requirements that might need power such as on board camera etc.

Now that we have the power requirements, we need to identify a battery with sufficient specific energy density in order to obtain the battery weight. We have chosen Li-ion battery for this purpose as they have a specific energy density of around 160wh/kg [28]. After the iterations and obtaining convergence the battery weight came out to be 1.8838 kg.

Mission Phase	Power requirement (Wh)
Climb	28.82
Cruise	182.666
Loiter	21.022
Miscellaneous requirements	46.502
Total power requirement($W_0 = 8Kg$)	279.01

Table 2.4: Power requirements for initial W_0

2.2.4 Empty Weight and DTOW:

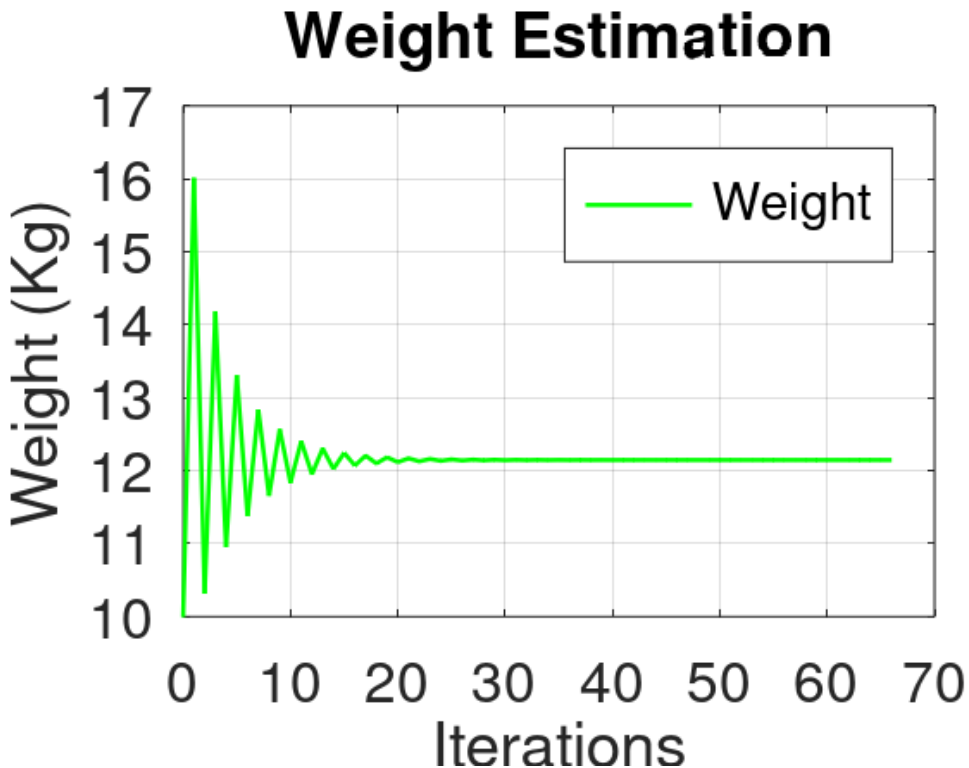


Figure 2.3: Weight Estimation Vs iterations

In the above figure 2.3 what we can see is the total weight convergence, the convergence was implemented using the code from section 15. The code considers two major constraints while converging.

$$w = \frac{w_p}{1 - \frac{w_b}{w} - Aw^L} \quad (2.12)$$

First the weight equation (2.12) is followed and since the battery weight is also varying based on the total weight that leads to divergence of the algorithm if we just do a fixed point iteration. To make it converge we had to make sure that the power consumption is being calculated after each iteration to get the new battery weight based on the new total weight.

The process might look tedious but it's simply to resolve the energy consumption by the UAV in

different phases in terms of the total weight and then add them up to get the total energy. Dividing this total energy by the energy density of a suitable battery can give use the weight of that particular type of the battery. That can be further put in the loop with some initial estimate to start the loop to hit the convergence.

The convergence value comes out to be **12.142 Kg** total weight and **1.8838 Kg** for the battery weight, it took 67 iterations to get the total weight and 47 to get the battery weight.

Important thing to notice is that the estimated weight might have been more than 10 Kg, but since it is a very preliminary weight estimation it can be better as the process evolves. Also here it depends a lot on the data of past aircraft which will later be replaced by the actual estimation of the structures and payloads.

Based on the current payload and battery weight, the empty weight comes out to be **8.7581 Kg**

2.3 Summary:

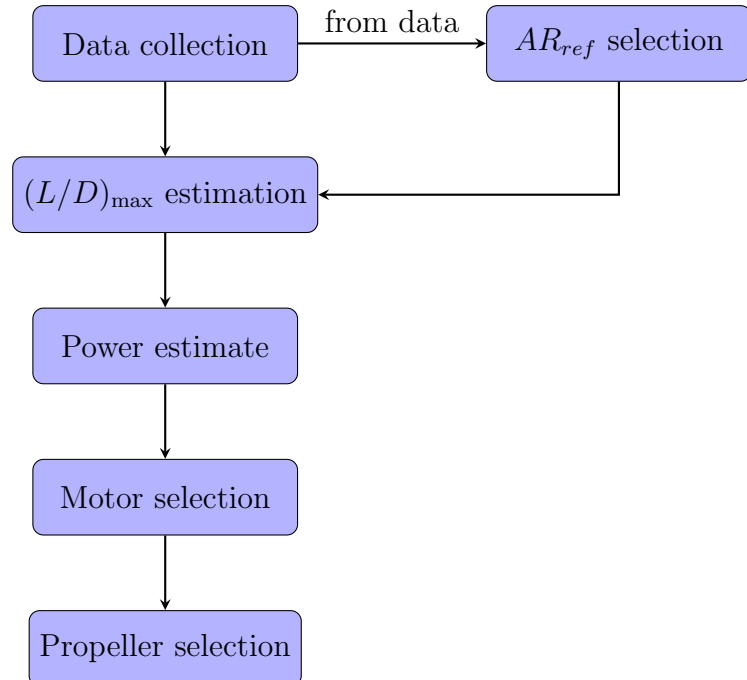
Task	Result
Payload Weight Estimation (W_p)	1.5 kg
Power consumption for $W_0 = 8Kg$	279.01 Wh
Power consumption for $W_0 = 12.142Kg$	301.4163 Wh
Battery Weight estimation (W_B)	1.8838 kg
Empty Weight estimation (W_e)	8.7581 kg
Take off weight estimation (W_o)	12.142 kg

Table 2.5: Summary Week 2 Tasks

Chapter 3

Propulsion system selection

3.1 Flowchart for this week's process



3.2 Requirement of L/D estimation

In order to select a suitable propulsion system we require the thrust to weight ratio($\frac{T}{W}$).

To get the $\frac{T}{W}$ we need to know the Thrust/Power requirements for our UAV. The power estimates in the previous section were based mainly on the aerodynamic data obtained from comparable aircraft. In this section before carrying out the analysis of power requirements we first estimate the $(L/D)_{\max}$.

For the calculation of L/D, previous UAV's were considered. The geometrical parameters of these UAV's like span(b) were already given while other geometric parameters like S_{ref} and S_{wet} were obtained from the three view diagrams of these UAV's. The reference aspect ratio AR_{ref} and the wetted aspect ratio AR_{wet} were calculated using the following relations.

$$AR_{ref} = \frac{b^2}{S_{ref}} \quad (3.1)$$

$$AR_{wet} = \frac{b^2}{S_{wet}} \quad (3.2)$$

Once these data were obtained the $(L/D)_{\max}$ for all the comparable UAV's were calculated using the following relations

$$(L/D)_{\max} = \frac{1}{\sqrt{4C_{D0}k}} \quad (3.3)$$

Where C_{D0} was calculated based on $(L/D)_{\max}$ condition i.e., $C_{D0} = K C_L^2$ and K is calculated as follows

$$K = \frac{1}{\pi e AR_{ref}} \quad (3.4)$$

Based on these values a plot of $(L/D)_{\max}$ versus $\sqrt{AR_{wet}}$ is plotted as shown in figure 3.1. By do-

Aircraft Name	Span(b) (m)	S_{ref} (m^2)	S (m^2)	AR_{ref}	\sqrt{AR}	$(L/D)_{\max}$
Blackswift [20]	3	0.76	2.10	4.29	2.07	20.33
MH900 Mav Tech [23]	0.9	*0.21	0.62	1.31	1.15	13.75
SQA eVTOL [24]	2.9	0.69	2.07	4.06	2.02	18.85
Atlas AS90X [19]	1.55	0.48	1.65	1.46	1.21	20.06
Bramor C4eye [21]	2.3	*0.49	1.49	3.56	1.89	21.49
AR1-TEKEVER [18]	1.8	0.33	1.50	2.16	1.47	12.04
Albatros Fixed-wing [17]	3	0.72	1.98	4.54	2.13	30.49
V220 [25]	3.64	0.72	2.28	5.79	2.41	22.06

Table 3.1: Wing configuration data

ing a linear regression the following relation between $(L/D)_{\max}$ and $\sqrt{AR_{wet}}$ is obtained.

$$\left(\frac{L}{D}\right)_{\max} = 5.339\sqrt{AR_{wet}} + 9.0769 \quad (3.5)$$

An important thing to note in the plot 3.1 is that we have not used all the points in the data collection, a point for the UAV Delta quad pro is removed as it had exceptional values, which was deviating the line from the rest of the data-set.

Now, in order to obtain $(L/D)_{\max}$ for our design, we decided to have a constraint on our reference aspect ratio. The maximum AR_{ref} we have chosen is 12, which corresponds to a $\sqrt{AR_{wet}}$ of 2, this serves as our upper bound, while $\sqrt{AR_{wet}}$ of 1 is chosen as the lower bound. Between these limits we have chosen $\sqrt{AR_{wet}}$ of 1.5492, this corresponds to

$$\left(\frac{L}{D}\right)_{\max} = 5.339\sqrt{AR_{wet}} + 9.0769 = 17.3480 \quad (3.6)$$

- Assuming the wings to have no sweep and taper (rectangular wings)
- We chose a value for $\frac{S_{wet}}{S_{ref}}=3$ based on the data from the book [13].

We used the following Desmos code to find power requirements for cruise:<https://www.desmos.com/calculator/rxuwourqxp>

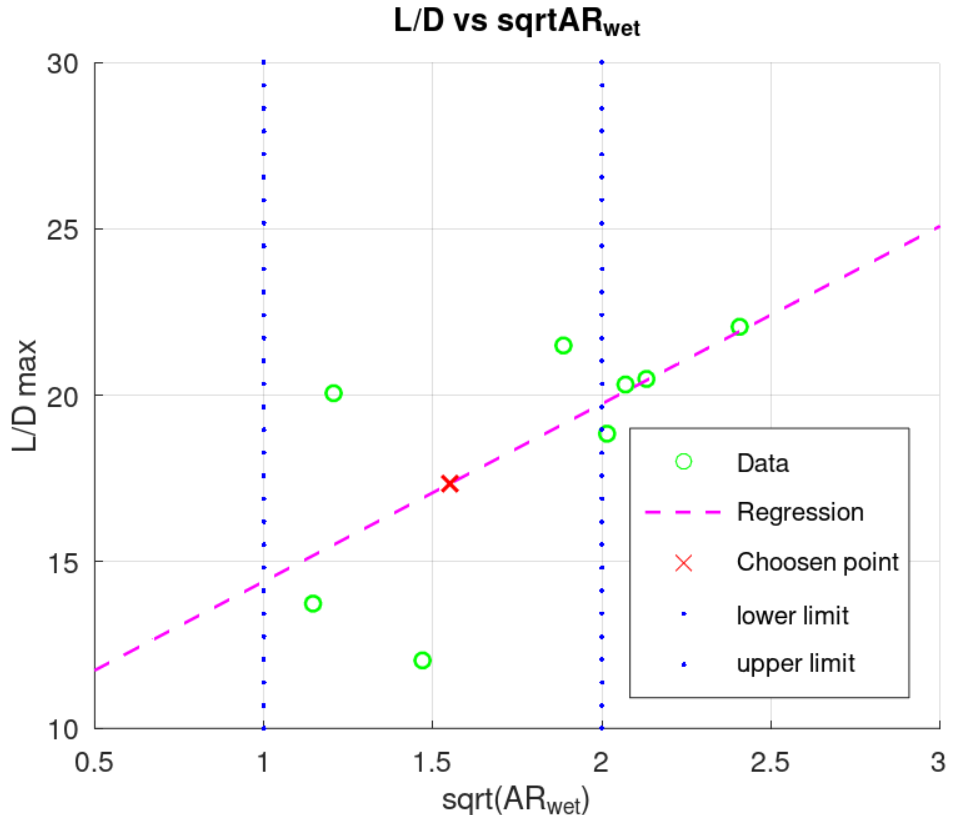


Figure 3.1: Estimation of L/Dmax

3.3 Power Requirements - Refined Estimate:

Based on the $(\frac{L}{D})_{\max}$ vs. $\sqrt{AR_{wet}}$ plot, the power required by the fixed-wing UAV is recalculated.

Given that the value chosen for $\sqrt{AR_{wet}} = 1.55$, the corresponding value for $(\frac{L}{D})_{\max} = 5.4 \times \sqrt{AR_{wet}} + 9.1 = 17.35$.

Based on the empirical relation [7],

$$e = 1.78(1 - 0.045AR^{0.68}) - 0.64 = 0.83 \quad (3.7)$$

$$K = \frac{1}{\pi e AR} = 0.05 \quad (3.8)$$

$$C_{D_0} = \frac{1}{4K(\frac{L}{D})_{\max}^2} = 0.016 \quad (3.9)$$

$$C_{L_{\max}} = 1.5 \text{ (Assumed based on past data.)} \quad (3.10)$$

These are the new values based on which the power requirements have been re-estimated.

3.3.1 Power for Climb - 1:

During climb, the density is assumed to be constant at 1.225 kg/m^3 . The variation in density for the target altitude is less than 2%. Hence, this assumption is reasonable. The power required for climb is given by:

$$P = T \times v_{climb} \quad (3.11)$$

$$v_{climb} = 1.2v_{stall} = 1.2\sqrt{\frac{2W}{\rho SC_{L_{max}}}} = 14.7 \text{ m/s} \quad (3.12)$$

$$L = W \cos \gamma = 118.7 \text{ N} \quad (3.13)$$

$$C_L = \frac{L}{\frac{1}{2}\rho v^2 S} = 1.04 \quad (3.14)$$

$$D = q_\infty S(C_{D_0} + KC_L^2) = 8.32 \text{ N} \quad (3.15)$$

$$T = W \sin \gamma + D = 18.7 \text{ N} \quad (3.16)$$

Therefore,

$$P_{climb} = 274.2 \text{ W} \quad (3.17)$$

3.3.2 Power for Cruise:

The power required for cruise is given by:

$$P = T \times v_{cruise} \quad (3.18)$$

$$L = W \quad (3.19)$$

$$C_L = \frac{W}{q_\infty S} = 0.7 \quad (3.20)$$

$$T = D = q_\infty S(C_{D_0} + KC_L^2) = 7.1 \text{ N} \quad (3.21)$$

Therefore,

$$P_{cruise} = 127.6 \text{ W} \quad (3.22)$$

3.3.3 Power for Loiter:

For the loiter phase, we assume that the flight is level and steady and that we are operating at a velocity equal to 1.2 times the stall velocity. This value is an estimate of the low speed at which the UAV will actually loiter.

$$v_{loiter} = 1.2v_{stall} = 1.2\sqrt{\frac{2W}{\rho SC_{L_{max}}}} = 14.7 \text{ m/s} \quad (3.23)$$

$$L = W = 119.1 \text{ N} \quad (3.24)$$

$$C_L = \frac{L}{\frac{1}{2}\rho v^2 S} = 1.04 \quad (3.25)$$

$$D = q_\infty S(C_{D_0} + KC_L^2) = 8.4 \text{ N} \quad (3.26)$$

$$T = D = 8.4 \text{ N} \quad (3.27)$$

Therefore,

$$P_{loiter} = T v_{loiter} = 122.7 \text{ W} \quad (3.28)$$

3.3.4 Power for Climb - 2:

For the second climb phase, the UAV is no longer carrying the payload. Therefore the weight $W = 10.642$ kg. Using the same formulae as in Climb - 1,

$$v_{climb} = 1.2 \sqrt{\frac{2W}{\rho SC_{L_{max}}}} = 13.7 \text{ m/s} \quad (3.29)$$

$$L = W \cos \gamma = 104.00 \text{ N} \quad (3.30)$$

$$C_L = \frac{L}{\frac{1}{2}\rho v^2 S} = 1.04 \quad (3.31)$$

$$D = q_\infty S(C_{D_0} + KC_L^2) = 7.3 \text{ N} \quad (3.32)$$

$$T = W \sin \gamma + D = 16.4 \text{ N} \quad (3.33)$$

Therefore,

$$P_{climb} = 225 \text{ W} \quad (3.34)$$

3.3.5 Power required for Takeoff, Descent and Landing:

The power required during takeoff and landing phases are not included in the estimate as take-off will mostly be by catapult launching method, while for descent phase we have considered the power requirement to be similar to the climb phase. This is done to get an estimate of the maximum power that would be required during the mission based on which we can select the battery weight i.e, we are looking at the maximum power requirements.

3.3.6 Total Power requirement:

The total power required for the entire mission is obtained by combining the power requirements for individual phases. The time required to complete each climb phase has been assumed to be the same to account for other losses of energy. The requirements have been tabulated below.

Mission Phase	Energy requirement (Wh)
Climb - 1	9.14
Cruise (Both phases included)	95.7
Loiter	18.4
Climb - 2	7.50
Descent (Both phases included)	9.14
Total Energy Requirement	139.9
Miscellaneous requirements	20 % of total Energy = 28
Final Energy Requirement	167.8

Table 3.2: Revised Energy Requirements

The miscellaneous requirements are taken as 20 % of the total energy required so as to account for any losses and the other requirements that might need power such as on board camera etc.

Now that we have the power and thrust requirements, we can select the battery, motor, ESC and propellers.

Mission Phase	Power (Watts)	Thrust(N)
Climb - 1	274.2	18.7
Cruise (Both phases included)	127.6	7.1
Loiter	122.7	8.4
Climb - 2	225	16.4
Miscellaneous requirements	28	

Table 3.3: Power and Thrust Requirements

3.4 Power-plant specification and configuration

3.4.1 Motor

The Function of the Motor is to rotate the Propeller at the designated RPM so that the Propeller can generate Thrust. The selection of the Motor hence depends on its capability of providing the required range of RPMs and also the KV rating of the Motor. KV rating defines the sensitivity of RPM with respect to Voltage provided. The motor should provide sufficient torque for the propeller at our operating RPM.

The MN 4112 UAV Multi-motor KV320 [37] satisfies all these requirements with a rated max current of 54A and works with a 6S battery.

3.4.2 Propellers

Propeller selection is based on Satisfying the Thrust requirements obtained from the Power Estimate for each Phase. The maximum thrust required is 18.698 N during steady climb. Acceleration during take-off and climb would require even more thrust hence we find a power plant that can provide 20% more thrust i.e. 22.44N. [38]

The database for Motors corresponds to the tests conducted for Propellers suitable and most Optimal for the respective Motors.

3.4.3 ESC

ESCs connect Battery to Motors and are responsible for controlling the RPM for the Motor. The Motors usually have ESCs ratings in Amperes specified already. This rating should be higher than the maximum current which the motor can take which is at 100% throttle to ensure safe operation. Considering the motor specifications, a 40A rated ESC would be ideal for our case. It's burst current capacity is 60A, well over our maximum requirement.

3.4.4 Battery

The Battery selection here is solely based on the Objective to satisfy the Power requirements of the motor propeller; the Power consumption of other equipment like Gimbal and Communication systems has not been considered. We have decided to use 18650 Li-ion cells due to their higher energy density and the ability to make our own custom battery pack.

Based on the Motors selected earlier, each of them has a specification which simply the task of Battery selection :

1. As each Li-ion cell has a nominal voltage of 3.7V[27], a 6S battery is 22.2V nominal and would be compatible with our motor as well. Hence, considering our total energy requirement of 167.8453 Wh we will need a 7.56 Ah capacity battery pack.
2. Each Li-ion cell has 3.5Ah capacity therefore we will require to keep at least 3 of them in parallel.
3. So our battery pack configuration becomes 6S3P with voltage of 22.2V and capacity of 10.5Ah. 18 cells in total
4. The extra capacity allows us leeway in power for camera and gimbal requirements.

3.4.5 Powerplant position

Comparison and acceptance In general, push propellers may be more widely accepted and have a higher design standard in certain applications, particularly for high-performance aircraft, military aircraft, and modern commercial airliners. Push propellers offer advantages such as improved aerodynamic efficiency, reduced noise levels, reduced fuselage drags and better safety in the event of propeller failure. They are commonly used in turbofan engines, which are prevalent in modern jet aircraft. On the other hand, pull propellers are still widely used in various aircraft types, including general aviation, light aircraft, and some turboprop aircraft. Pull propellers offer advantages such as simplicity, visibility, and ease of maintenance, making them suitable for a wide range of applications. They are commonly used in piston-engine aircraft and some turboprop aircraft designs. Ultimately, the choice between push and pull propellers depends on the specific requirements and constraints of the aircraft design and mission profile. Design standards for both configurations are well-established, and aircraft manufacturers and designers carefully consider factors such as performance, efficiency, safety, and reliability when selecting the appropriate propeller configuration for a particular aircraft.

- A 3-blade propeller usually offers top speed performance while a 4-blade propeller provides maximum thrust and smooth cruising operation.
- The pusher design is more efficient, because the suction forward of the prop reduces flow separation, and the accelerated flow behind it is not streaming around the fuselage (or wing), where it would create additional friction drag.

Assets:

- Reduced Noise and Vibrations: Pusher propellers tend to produce less noise and vibration compared to tractor propellers (those mounted at the front of the aircraft) since they operate in undisturbed airflow behind the aircraft.
- Improved Safety: In case of an engine failure, a pusher propeller configuration may offer better safety as the propeller is located away from the main fuselage and occupants.
- Enhanced Visibility: Pusher propeller configurations often provide better forward visibility for pilots and passengers, as there are no propeller blades obstructing the view.

- Reduced Risk of Foreign Object Damage: Pusher propellers are less susceptible to damage from debris on the runway during takeoff and landing compared to tractor propellers.
- Reduced fuselage drag: Because of the favorable pressure gradient produced by the propeller in the stream-wise direction.

Liabilities:

- Complexity of Design: Pusher propeller configurations can be more complex to design and engineer compared to tractor configurations due to the need for additional structural support and aerodynamic considerations.
- Cooling Challenges: Cooling the engine can be more challenging with a pusher propeller configuration since the propeller may obstruct airflow to the engine, requiring additional cooling systems.
- Handling Characteristics: Pusher configurations may have different handling characteristics compared to tractor configurations, which may require additional pilot training and experience to operate safely.
- Maintenance Accessibility: Accessing and performing maintenance on a pusher propeller system can be more challenging compared to a tractor configuration, as the propeller is located behind the engine and may require more disassembly to reach.

Assets are more than Liabilities

In the table 3.4 , the highlighted powerplant is the one selected as it satisfies our requirements. If after further calculations and designing the requirements change, then a more/less powerful powerplant options are also mentioned.

Motor	Propeller	ESC	Battery
MN 4110 [36] UAV Multi-Motor KV300	16" x 8" [40]	2-6S, 40 A [26]	6S4P Li-ion [27]
MN 4112 [37] UAV Multi-motor KV320	16" x 5.4" [39]	2-6S, 40 A [26]	6S4P Li-ion [27]
MN 4110 [36] UAV Multi-Motor KV400	16" x 5.4" [39]	2-6S, 40 A [26]	6S4P Li-ion [27]

Table 3.4: Motor-Propeller-ESC-Battery

3.5 Summary

Tasks	Results
$(L/D)_{\max}$	17.3
AR_{wet}	2.4
Total Energy required	167.8 Wh
Configuration	Pusher

Table 3.5: Summary

Chapter 4

Wing Loading

Before proceeding with the calculations of wing loading, we will summarize the parameters as well as their corresponding values obtained so far.

Aspect ratio	7.2
Cruise Velocity	18 m/s
Stall Velocity	12.22 m/s
Maximum Velocity	22m/s
$C_{L_{max}}$	1.5
C_{D_0}	0.016
K	0.05
Cruise altitude	200m
Absolute Ceiling	\approx 2300m
Maximum Takeoff Weight	12.14 kg

Table 4.1: Parameters

This chapter details a procedure to obtain a range for the wing loading ($\frac{W}{S}$) given the following constraints:

- Stall velocity
- Maximum range cruise
- Maximum rate of climb (ROC)
- Absolute ceiling
- Maximum endurance loiter
- Maximum velocity

The formulae used are for propeller-driven aircraft.[13] The design constraints are as listed in the detailed mission profile.

4.1 Stall velocity:

The constraint on stall velocity is placed using the values from the previous chapter on revised power requirements. The values of $C_{L_{\max}} = 1.5$ and $\rho = 1.225 \text{ kg/m}^3$ are assumed.

$$v_{\text{stall}} = 12.2 \text{ m/s} \quad (4.1)$$

$$W = L = \frac{1}{2}\rho v_{\text{stall}}^2 S C_{L_{\max}} \quad (4.2)$$

$$\left(\frac{W}{S}\right)_{\text{stall}} = \frac{1}{2}\rho v_{\text{stall}}^2 C_{L_{\max}} \quad (4.3)$$

$$\left(\frac{W}{S}\right)_{\text{stall}} = 137.2 \text{ N/m}^2 \quad (4.4)$$

4.2 Maximum range cruise:

We aim to find the wing loading that allows us to maximise the range of the fixed-wing UAV. Maximum range is obtained when the aircraft is operating at $(L/D)_{\max}$. The density at cruise altitude is taken to be $\rho = 1.207 \text{ kg/m}^3$.

$$v_{\text{cruise}} = 18 \text{ m/s} \quad (4.5)$$

As operation at $(L/D)_{\max}$ is considered, the value of C_L is,

$$C_L = \sqrt{\frac{C_{D_0}}{K}} = 0.54 \quad (4.6)$$

The value of wing loading is obtained as follows:

$$W = L = \frac{1}{2}\rho v_{\text{cruise}}^2 S C_L \quad (4.7)$$

$$\left(\frac{W}{S}\right)_{\text{cruise}} = \frac{1}{2}\rho v_{\text{cruise}}^2 C_L \quad (4.8)$$

$$\left(\frac{W}{S}\right)_{\text{cruise}} = 106.3 \text{ N/m}^2 \quad (4.9)$$

4.3 Maximum rate of climb:

To climb to the cruise altitude as quickly as possible, operation at maximum rate of climb ROC_{\max} is required. Given that the flight path angle γ for maximum rate of climb depends on maximum power delivered, density and other constraints still unknown, we assume that $\gamma = 5^\circ$. This assumption is reasonable as it is known that γ is a small angle. The density taken is $\rho = 1.225 \text{ kg/m}^3$.

$$L = W \cos \gamma \simeq W \quad (4.10)$$

$$T = D + W \sin \gamma \quad (4.11)$$

$$ROC = \frac{P - DV}{W} \quad (4.12)$$

Differentiating the rate of climb with respect to velocity, we obtain the following condition for maximum ROC ,

$$v^4 = \frac{4KW^2}{3\rho^2 S^2 C_{D_0}} \quad (4.13)$$

From equation (4.10),

$$KC_L^2 = 3C_{D_0} \quad (4.14)$$

$$\frac{P}{W} = \frac{Tv}{W} = \frac{Dv + Wv \sin \gamma}{W} \quad (4.15)$$

$$\frac{P}{W} = \frac{\frac{1}{2}\rho v^3 S(C_{D_0} + KC_L^2) + Wv \sin \gamma}{W} \quad (4.16)$$

Substituting the variables,

$$\frac{P}{W} = \left(\sin \gamma + \frac{1.1547}{(L/D)_{\max}} \right) \sqrt{\frac{2}{\rho \sqrt{\frac{3C_{D_0}}{K}}} \left(\frac{W}{S} \right)} \quad (4.17)$$

Where,

$$(L/D)_{\max} = \frac{1}{\sqrt{4KC_{D_0}}} = 17.4 \quad (4.18)$$

The final results are as follows:

$$\left(\frac{W}{S} \right)_{\text{climb-1}} = 129.4 \text{ N/m}^2 \quad (4.19)$$

$$\left(\frac{W}{S} \right)_{\text{climb-2}} = 113.4 \text{ N/m}^2 \quad (4.20)$$

4.4 Maximum endurance loiter:

As our mission profile involves hovering at a certain place for payload drop, we should also look at the wing loading required for such a phase. An optimum wing loading for loiter is obtained when the induced drag is three times the parasite drag. This also corresponds to wing loading at minimum power required.

$$v_{\text{loiter}} = 14.7 \text{ m/s} \quad (4.21)$$

$$KC_L^2 = 3C_{D_0} \quad (4.22)$$

The corresponding wing loading is obtained as per the following formula.[13]

$$\left(\frac{W}{S}\right)_{\text{loiter}} = 0.5\rho v_{\text{loiter}}^2 \sqrt{3\pi A Re C_{D_0}} \quad (4.23)$$

$$\left(\frac{W}{S}\right)_{\text{loiter}} = 124.05 \text{ N/m}^2 \quad (4.24)$$

4.5 Maximum Velocity:

In order to obtain the wing loading for maximum velocity, we make use of the same equation as in cruise, except that the velocity,

$$v_{\max} = 22 \text{ m/s} \quad (4.25)$$

This velocity was considered based on the maximum velocities of comparable UAV's as given in our previous aircraft study.

As operation at $(L/D)_{\max}$ is considered, the value of C_L is,

$$C_L = \sqrt{\frac{C_{D_0}}{K}} = 0.54 \quad (4.26)$$

The value of wing loading is obtained as follows:

$$W = L = \frac{1}{2}\rho v_{\max}^2 S C_L \quad (4.27)$$

$$\left(\frac{W}{S}\right)_{\max} = \frac{1}{2}\rho v_{\max}^2 C_L \quad (4.28)$$

$$\left(\frac{W}{S}\right)_{\max} = 158.8 \text{ N/m}^2 \quad (4.29)$$

4.6 Absolute ceiling:

Based on our mission profile, the altitude at which we fly is around 200m. However, this is not the absolute ceiling for the UAV. Comparable UAV's have an absolute ceiling in the range of 3000 - 6000m. For the purpose of wing loading calculation we take the absolute altitude to be around 3000m, based on the previous aircraft data considered in our report.

$$ROC = \frac{P - DV}{W} \quad (4.30)$$

At absolute ceiling ROC is zero. Hence from the above equation,

$$P = (0.5\rho_{ac}v^2 S(C_{D_0} + KC_L^2)) \times v \quad (4.31)$$

$$\frac{P}{W} = \frac{1.1547}{(L/D)_{\max}} \sqrt{\frac{2}{\rho_{ac} \sqrt{\frac{3C_{D_0}}{K}}}} \left(\frac{W}{S}\right) \quad (4.32)$$

Substituting the variables,

$$\left(\frac{W}{S}\right)_{\text{ac}} = 17.61 \text{ N/m}^2 \quad (4.33)$$

The wing loading obtained here is too low and almost impractical. Hence for such case as suggested in [13], the wing loading should be compared with the wing loading required to fly at a given lift coefficient. Here we consider a lift coefficient of 0.54357 as it corresponds to better efficiency.

$$\left(\frac{W}{S}\right)_{ac} = \frac{1}{2} \rho_{ac} v^2 C_L \quad (4.34)$$

$$\left(\frac{W}{S}\right)_{ac} = 53.16 \text{ N/m}^2 \quad (4.35)$$

Since our UAV is mainly focused on surveillance and rescue, based on the mission profile, we see that cruise and loiter are our critical phases. Hence we need to optimize the wing loading for these phases. We can go a step further and say that based on our mission duration since the loiter requirement is only a fraction of the cruise, it will be better if we optimize the wing loading for the cruise.

4.7 Summary

Segments	Wing Loading (N/m ²)
Climb-1	129.4
Cruise	106.4
Stall	137.2
Climb-2	113.4
Loiter	124.1
Maximum velocity constraint	158.8
Absolute ceiling constraint	53.16
Range of wing loading	53.16 - 158.8

Table 4.2: Wing Loading Summary

- The wing loading in the power calculation section is assumed to be 137.2 N/m². This lies within the range calculated and is reasonable for the power calculations.
- The powerplant configuration was changed and a new configuration was decided as the previous one lacked sufficient efficiency. (3.4)

Chapter 5

Secondary Weight Estimate:

In the previous chapter we obtained a range of wing loading's corresponding to different mission phases. Of these values of wing loading, we are picking a wing loading corresponding to cruise phase of our mission. The reasoning behind this is, as our mission is primarily surveillance, we would be spending considerable amount of time in cruise phase. We also have loiter as our secondary mission, but since loiter is only a fraction of cruise and the value of wing loading during loiter is also closer to cruise. Hence we would like to optimize our wing loading for cruise.

Wing loading corresponding to cruise	106.3 N/m ²
Wing loading with 5% tolerance	101 N/m ² - 111.6 N/m ²

Table 5.1: Selected wing loading.

5.1 Power loading based on wing loading:

Now that we have a wing loading, we go back and calculate the S_{ref} , AR_{ref} , $(\frac{L}{D})_{max}$, C_{D_0} and K. These values are reported in the following table.

Parameter	Value
Wing loading	111.6 N/m ²
S_{ref}	1.07 m ²
AR_{ref}	5.84
$(L/D)_{max}$	16.54
K	0.062
C_{D_0}	0.015

Table 5.2: Parameters to be used in power estimate

Before getting started with power estimates, there is one last factor to be considered. In our previous estimate, we had not considered the propeller efficiency(η_p).

5.1.1 Propeller efficiency(η_p):

The Theoretical Propeller efficiency was estimated for Maximum Thrust of 19.82 N which is required during the Climb phase.

1. Calculating L/D for the Climb Thrust,

$$\left(\frac{L}{D}\right)_{climb} = \frac{C_L|_{climb}}{C_{D_o} + K \cdot C_L|_{climb}^2}$$

$$L/D = 12.57 \quad (5.1)$$

2. Calculating Theoretical efficiency using [11]

$$\eta_p = \frac{W \cdot V_{inf}}{((L/D)_{climb} \cdot P|_{climb})}$$

$$a\eta_p = 0.48 \quad (5.2)$$

here,

- W is the Weight of the UAV
- V_{inf} is the Airspeed
- P is the Mechanical Power

5.1.2 Power-plant Weight

The selected Power-plant , mentioned in (3.4) has the following weight distribution,

$$\begin{aligned} W_{plant} &= W_{motor} + W_{propeller} + W_{ESC} \\ &= 172 + 25 + 26 \text{ grams} \end{aligned}$$

$$W_{plant} = 223 \text{ grams} \quad (5.3)$$

5.1.3 Power loading for cruise:

Now that we have the propeller efficiency, we can go ahead and calculate the power loading. For a propeller driven aircraft.

$$\eta_p \times P_{cruise} = T \times V_{cruise} \quad (5.4)$$

$$L = W \quad (5.5)$$

$$C_L = \frac{W}{q_\infty S} = 0.57 \quad (5.6)$$

$$T = D = q_{\infty} S (C_{D_0} + K C_L^2) = 7.3 \text{ N} \quad (5.7)$$

$$\eta_p \times P_{cruise} = 131.8 \text{ W} \quad (5.8)$$

Therefore,

$$P_{cruise} = 275.8 \text{ W} \quad (5.9)$$

Power loading is;

$$\left(\frac{W}{P} \right)_{\text{Cruise}} = 0.43 \text{ N/W} \quad (5.10)$$

5.1.4 Power loading for climb - 1:

During climb, the density is assumed to be constant at 1.225 kg/m^3 . The power required for climb is given by:

$$\eta_p \times P = T \times v_{climb} \quad (5.11)$$

$$v_{climb} = 1.2v_{stall} = 1.2 \sqrt{\frac{2W}{\rho S C_{L_{max}}}} = 13.1 \text{ m/s} \quad (5.12)$$

$$L = W \cos \gamma = 118.7 \text{ N} \quad (5.13)$$

$$C_L = \frac{L}{\frac{1}{2} \rho v^2 S} = 1.06 \quad (5.14)$$

$$D = q_{\infty} S (C_{D_0} + K C_L^2) = 9.5 \text{ N} \quad (5.15)$$

$$T = W \sin \gamma + D = 19.82 \text{ N} \quad (5.16)$$

Therefore,

$$\eta_p \times P_{climb} = 259.2 \text{ W} \quad (5.17)$$

$$P_{climb} = 542.2 \text{ W} \quad (5.18)$$

Power loading is;

$$\left(\frac{W}{P} \right)_{\text{Climb-1}} = 0.22 \text{ N/W} \quad (5.19)$$

5.1.5 Power loading for loiter:

For the loiter phase, we assume that the flight is level and steady and that we are operating at a velocity equal to 1.2 times the stall velocity.. This value is an estimate of the low speed at which the UAV will actually loiter.

$$v_{loiter} = 1.2v_{stall} = 1.2 \sqrt{\frac{2W}{\rho S C_{L_{max}}}} = 13.68 \text{ m/s} \quad (5.20)$$

$$L = W = 119.1 \text{ N} \quad (5.21)$$

$$C_L = \frac{L}{\frac{1}{2}\rho v^2 S} = 0.97 \quad (5.22)$$

$$D = q_\infty S(C_{D_0} + KC_L^2) = 8.9 \text{ N} \quad (5.23)$$

$$T = D = 8.9 \text{ N} \quad (5.24)$$

Therefore,

$$\eta_p \times P_{loiter} = T v_{loiter} = 122.8 \text{ W} \quad (5.25)$$

$$P_{loiter} = 256.8 \text{ W} \quad (5.26)$$

Power loading is;

$$\left(\frac{W}{P}\right)_{\text{Loiter}} = 0.46 \text{ N/W} \quad (5.27)$$

5.1.6 Power loading for Climb-2:

For the second climb phase, the UAV is no longer carrying the payload. Therefore the weight $W = 10.642 \text{ kg}$. Using the same formulae as in Climb -1,

$$v_{climb} = 1.2 \sqrt{\frac{2W}{\rho S C_{L_{max}}}} = 12.4 \text{ m/s} \quad (5.28)$$

$$L = W \cos \gamma = 104 \text{ N} \quad (5.29)$$

$$C_L = \frac{L}{\frac{1}{2}\rho v^2 S} = 1.04 \quad (5.30)$$

$$D = q_\infty S(C_{D_0} + KC_L^2) = 8.2 \text{ N} \quad (5.31)$$

$$T = W \sin \gamma + D = 17.32 \text{ N} \quad (5.32)$$

Therefore,

$$\eta_p \times P_{climb-2} = 214.2 \text{ W} \quad (5.33)$$

$$P_{climb-2} = 448 \text{ W} \quad (5.34)$$

Power loading is;

$$\left(\frac{W}{P}\right)_{\text{Climb-2}} = 0.27 \text{ N/W} \quad (5.35)$$

5.2 Secondary Weight Estimate:

Using the new values that have been chosen for winging loading and $(L/D)_{\max}$, a secondary weight estimate is run that gives a better value for the design take-off weight and battery weight.

The procedure followed is the same as that enumerated in 2.2.4.

- Set the values of the aircraft parameters that remain constant and the value of the DTOW (W_0) to start the iterations.
- For each value of W_0 , calculate the power requirements to obtain the battery weight as well as the number of batteries. Note that the number of batteries must be a whole number. This procedure is carried out based on the battery selected.[27]
- Substitute the weights obtained in the right hand side of the following equation to obtain the next guess for the DTOW (W_0).

$$W_0 = \frac{W_p}{1 - \frac{W_b}{W_0} - AW_0^L} \quad (5.36)$$

- Repeat the procedure for each new value of W_0 until the DTOW converges.

The following image shows the variation of DTOW with the number of iterations. At convergence, the variation between successive weights is less than 30 grams.

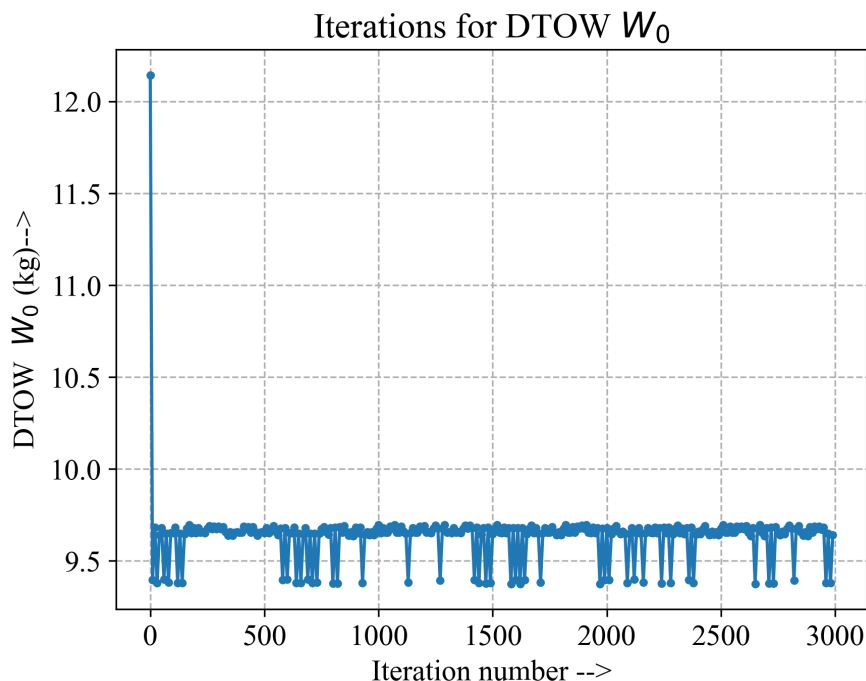


Figure 5.1: Variation in DTOW with iterations.

The code to obtain the DTOW can be found in the appendix 15. The final results are as follows:

- Final DTOW: 9.4 kg
- Final number of batteries: 21
- Final battery weight: 1.008 kg

5.3 Summary

Propeller Efficiency	0.48
Wing Loading (N/m^2)	111.6
$(L/D)_{max}$	16.54
$S_{ref} (m^2)$	1.07

Table 5.3: Chapter 5 Summary

Phase	Power (Watts)	Energy (Wh)	Thrust (N)	W/P
Cruise (both phase)	275.8	206.8	7.32	0.43
Climb - 1	542.2	9.04	19.82	0.22
Loiter	256.8	38.52	8.9	0.46
Climb - 2	448	7.5	17.32	0.27
Miscellaneous (20% of Energy)		54.17		
Total Energy		316		

Table 5.4: Secondary Power estimate

NOTE: The changes recommended based on feedback on the presentation will be included in next week's report.

Chapter 6

Re-estimation of design parameters.

Based on the feedback we received during our mid-term presentation, there were certain changes we needed to incorporate. An important feedback was to have the mission profile defined in detail with all the design constraints defined. We have addressed these issues in the following chapter, starting with a detailed mission profile, new weight estimate, power requirements and power-plant selection. Finally, we have picked a value of wing loading and new weight, which will be used for all calculations in the subsequent chapters.

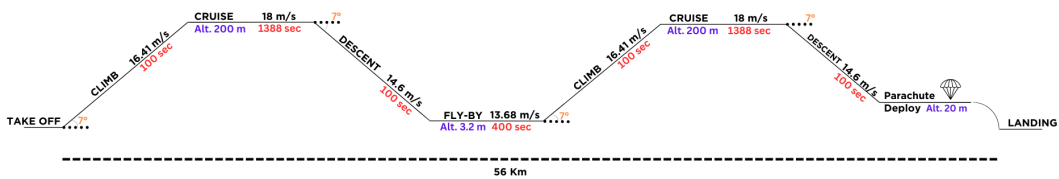


Figure 6.1: Mission Profile

6.1 Detailed mission profile

The main objective of our UAV is aerial search and relief operations. The mission profile would typically consist of takeoff from a ship, climb to its cruising altitude, carrying out aerial search for potential survivors, a descent to drop relief payload, followed by a climb back to return cruise and land. The parameters and the constraints in each of these phases are detailed below.

1. Phase-1 : Takeoff - This will be done through a system capable of being mounted on any ship. The takeoff is assumed to be using a catapult. The type of catapult mechanism is not yet finalized.
2. Phase-2 : Climb-1 - For the first climb to cruise altitude, we are fixing our rate of climb to be 2 m/s and climb angle to be 7 degrees. Both these values are considered based on the data of comparable UAV's.

$$V_{climb} = \frac{R.O.C}{\sin\theta} = \frac{2}{\sin(7)} = 16.41 \text{ m/s}[12].$$

Further, the time required to climb to 200m cruise altitude is obtained by dividing the altitude by rate of climb which turns out to be 100s.

3. Phase-3 : Cruise - We have identified the cruise altitude to be 200m and the cruise distance to be 50Km. The rationale behind this is that we should be able to search a reasonable distance, in order to identify the survivors. The cruise velocity is fixed at 18 m/s, and the time

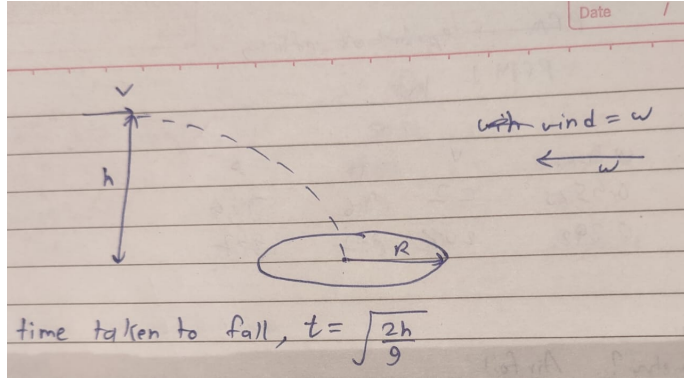


Figure 6.2: Flyby height calculations

taken for this phase is calculated by dividing the distance by velocity, which comes out to be around 2800s.

4. Phase-4 : Descend to drop altitude - The descend angle is considered similar to climb angle. However the velocity in this phase is calculated using $V_{descend} = 0.76 \times V_{cruise} = 13.68m/s$ [12].
5. Phase-5 : Flyby: The flyby velocity was taken to be $1.2 \times V_{stall}$ as the objective in this phase is to drop the payload. The altitude was selected by considering the range of error we can allow from the drop location. We decided that the payload should drop within a radius of 4m and found that the maximum wind speed near sea level is 5m/s. Therefore the payload should touch the ground within 0.8s of release. From this, we found an altitude for which it takes 0.8s to reach the ground and that is 3.2m.
6. Phase-6 : The remaining phases include climb back to return cruise and land. The climb and cruise parameters are still the same, the exception being now the weight would have reduced as we have dropped the payload.

The above description is illustrated in the mission profile.

6.2 Weight estimate

Based on this new mission profile we had a revised weight estimate to ensure that the used quantities are consistent, to proceed with, in the first weight estimate we didn't have much information about the aircraft, whereas for the second weight estimation we still used the same equation but changed the conditions for convergence as stated in the later portion

$$W_0 = \frac{W_p}{1 - \frac{W_b}{W_0} - AW_0^L} \quad (6.1)$$

This equation is the main equation for the estimate, as we have some knowledge of our power-plant now, so we can also try a similar equation which considers that mass as fixed and performs the iterations. As we have mentioned earlier the power-plant mass is not that significant so to avoid all those changes we retained the same equation for iteration.

In the previous task we tried to get the wing loading for all the phases and were suppose to take a value which can provide us a maximum wing area that can handle that wing loading throughout that phase. To get that we chose the cruise loading to be the wing loading which we'll be considering in the estimate.

The code 15 was used to perform the convergence. This considers the fact that after each iteration our weight is changed and based on that the wing loading for the cruise is changed,

this is because after each iteration when we get the required wing loading, we assume that if we had this wing loading for our aircraft then using that wing loading we get the required planform area(S), this provides us the new Aspect Ratio as there is a constraint on the span(b) of 2.5 m

So all the quantities that depends on the AR will change including the C_{D_0} , e , $(L/D)_{(max)}$, etc. Thus the power consumption gets changed and due to which we now get a new battery weight and total weight, this iterations go on till the point of convergence. As we are trying to get the battery weight, we try to ensure that all the power is coming from integer number of cells this makes the iteration to not properly converge is what we think, and leaves us with a higher tolerance that is compared to the one without considering it.

Finally,

we get the total weight as **9.65 Kg**

Total battery weight as **1.056 Kg** which means **22** Li-ion cells of 48 grams each. We'll consider adding two more cells for having a proper arrangement of 6×4

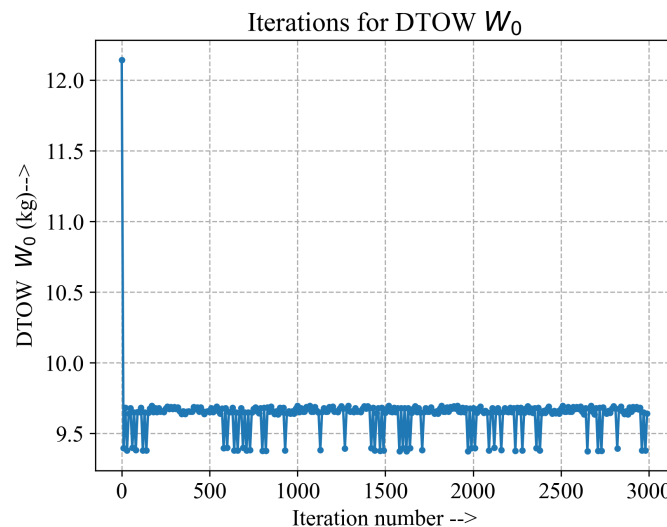


Figure 6.3: Revised weight estimate

6.3 Power requirements

Phases	Energy(Wh)	Thrust(N)
Climb-1	281.7	17.2
Climb-2	237	14.4
Cruise	100	5.6
Flyby	85.9	6.3

Table 6.1: Power estimates

6.4 Power-plant

The Power-plant remains the same as the Thrust requirements are well within the current selection.

Chapter 7

Wing Design

7.1 Airfoil Selection

The first step in wing design is to select an appropriate airfoil for the wing that satisfies the lift requirements estimated in the previous chapters for all mission segments. This section describes the points taken into consideration and the final airfoil selected.

7.1.1 Parameters previously estimated for the aircraft:

- Planform Area $S = 0.92 \text{ m}^2$.
- Wingspan $b = 2.5 \text{ m}$.
- Chord $c = S/b = 0.37 \text{ m}$.
- Using the secondary weight estimate code 15, the actual values of C_L required are obtained.
 - $C_{L_{\text{climb-1}}} = 0.62$
 - $C_{L_{\text{cruise}}} = 0.53$
 - $C_{L_{\text{fly-by}}} = 0.90$
 - $C_{L_{\text{climb-2}}} = 0.53$

From this data, it can be observed that the value of $C_{L_{\max}} = 0.90$ is required. These give the requirements the airfoil must satisfy.

- Assuming an operating temperature of $T = 288 \text{ K}$ at cruise, the Mach number of operation at cruise,

$$M_{\text{cruise}} = \frac{v_{\text{cruise}}}{a_{\text{cruise}}} = \frac{v_{\text{cruise}}}{\sqrt{\gamma RT}} = 0.053 \quad (7.1)$$

- As the longest flight segment is a cruise, the airfoil is selected based on the Reynolds number at the cruise. The kinematic viscosity of air at $T = 288 \text{ K}$ is $\nu = 1.48 \times 10^{-5}$. Therefore, the Reynolds number is,

$$Re = \frac{v_{\text{cruise}} c}{\nu} = 4.46 \times 10^5 \simeq 5 \times 10^5 \quad (7.2)$$

7.1.2 Airfoil Thickness

The thickness of the airfoil has a major influence on the drag, maximum lift, structural weight, and stall characteristics.

- Stall characteristics:
 - Fat airfoils (round leading edge and t/c greater than about 14%) stall from the trailing edge. The boundary layer begins to separate, starting at the trailing edge and moving forward as the angle of attack is increased over about 10° . The loss of lift is gradual. The pitching moment changes only a small amount.
 - Thinner airfoils stall from the leading edge. If the airfoil is of moderate thickness (about 6-14%), the flow separates near the nose at a very small angle of attack and immediately reattaches itself so that little effect is felt. At some higher angle of attack the flow fails to reattach, which almost immediately stalls the entire airfoil. This causes an abrupt change in lift and pitching moment.
- Drag: The drag increases with increasing thickness due to increased separation.
- Structural weight: Thickness also affects the structural weight of the wing. Statistical equations for wing weight show that the wing structural weight varies approximately inversely with the square root of the thickness ratio. Halving the thickness ratio will increase wing weight by about 41%.
- The historical trend shown in the figure below is used to select the thickness ratio. The method followed is as given in [13].

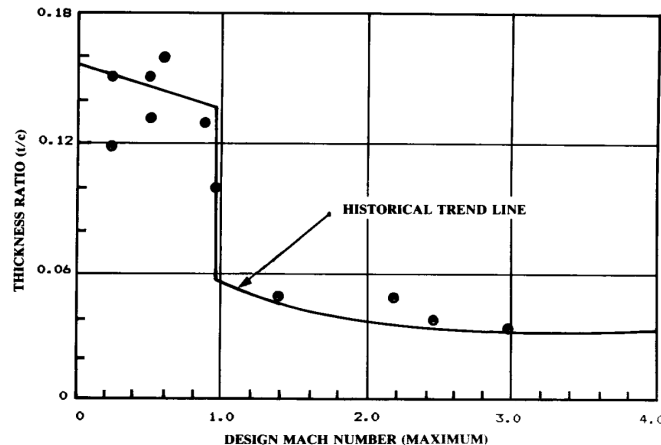


Figure 7.1: Thickness ratio - Historical trend [13]

- As the Mach number at cruise for our aircraft is 0.053, the thickness ratio must lie approximately between 15% - 16% from the figure. Airfoils with thickness ratio values in this range will be further examined.

7.1.3 Airfoil Selection Criteria

The following quantities are investigated to select the airfoil.

- Maximum lift coefficient $C_{l_{\max}}$
- Ideal or design lift coefficient C_{l_d}
- Maximum lift-to-drag ratio $(C_l/C_d)_{\max}$ (Maximum aerodynamic efficiency)
- Angle of attack (α) for maximum aerodynamic efficiency
- Stall angle

Using the factor to isolate wing contribution to lift as recommended in [14],

- During cruise, $C_{L_w} = \frac{C_{L_{\text{cruise}}}}{0.95} = 0.56$.
- For maximum lift coefficient contributed by the wing, $C_{L_{\max_w}} = \frac{C_{L_{\max}}}{0.95} = 0.95$.

To shortlist airfoils, a starting assumption of $C_{L_w} = C_{l_d}$ is made. The table below lists the various possibilities based on the thickness ratio values and C_{l_d} requirement. We will pick the airfoil that best suits our requirements.

Airfoil	$C_{l_{\max}}$	Stall Angle	Maximum $\frac{C_l}{C_d}$	α for $\left(\frac{C_l}{C_d}\right)_{\max}$	Ideal $C_l = C_{l_d}$
GOE 738	1.3	19.5°	87.3	6.0°	0.88
EPPLER 478	1.3	15.0°	75.6	8.0°	0.93
EPPLER 502	1.04	15.5°	87.9	6.5°	0.83
GA 30-315	1.4	16.5°	90	5.5°	0.96
GA 30A315	1.5	16.0°	89.5	5.5°	0.93
GA 30A215	1.5	17.0°	81.2	5.5°	0.87
GA 35A015	1.15	14.5°	66.6	5.5°	0.6
GA35A215	1.3	15.5°	100.5	6.0°	0.9
GA35A016	1.15	16.0°	67.3	5.5°	0.6
GA 37-215	1.3	17.5°	98.3	6.5°	0.9

Table 7.1: Airfoil Data

After careful analysis, the airfoil **GA 35A015** has been selected for our UAV. The shape of the airfoil is shown in the figure below.

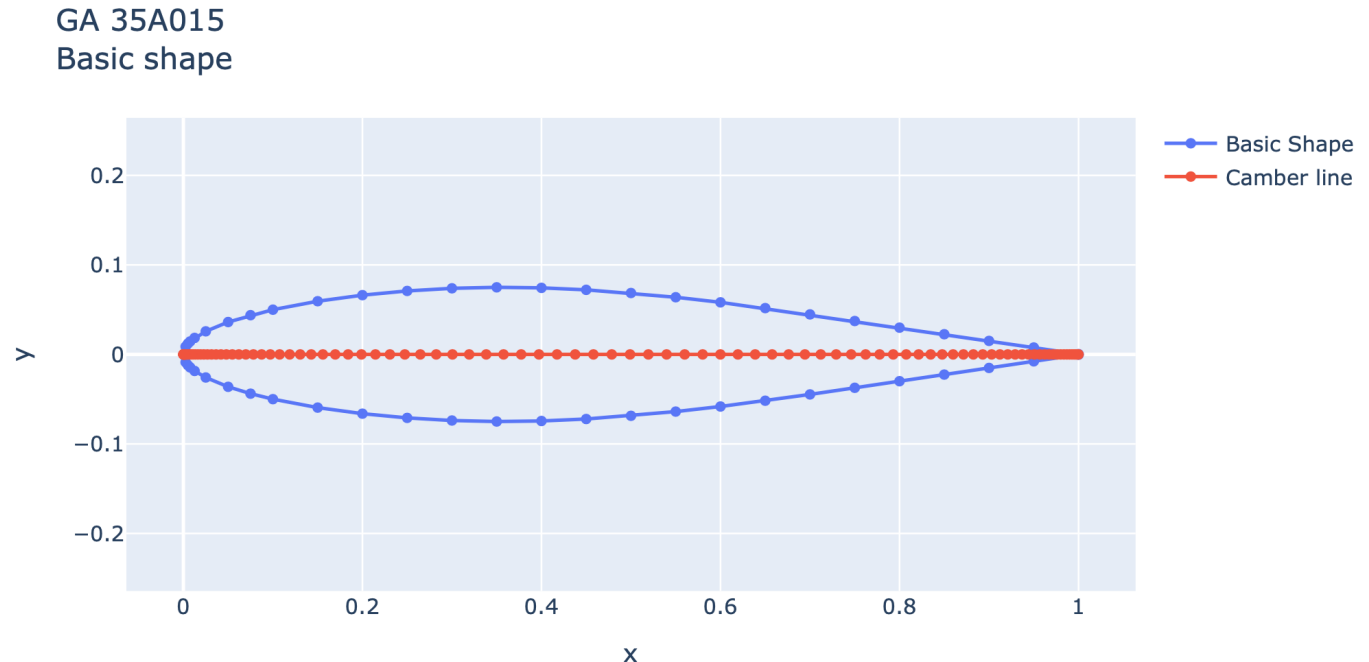


Figure 7.2: GA 35A015

The following characteristic graphs have been included:

- C_l vs. α
- C_d vs. α
- C_l/C_d vs. α
- C_l/C_d vs. C_l

GA 35A015

Basic data from JavaFoil for smooth airfoil at Mach 0, and windtunnel data if available
Section lift coefficient vs angle of attack

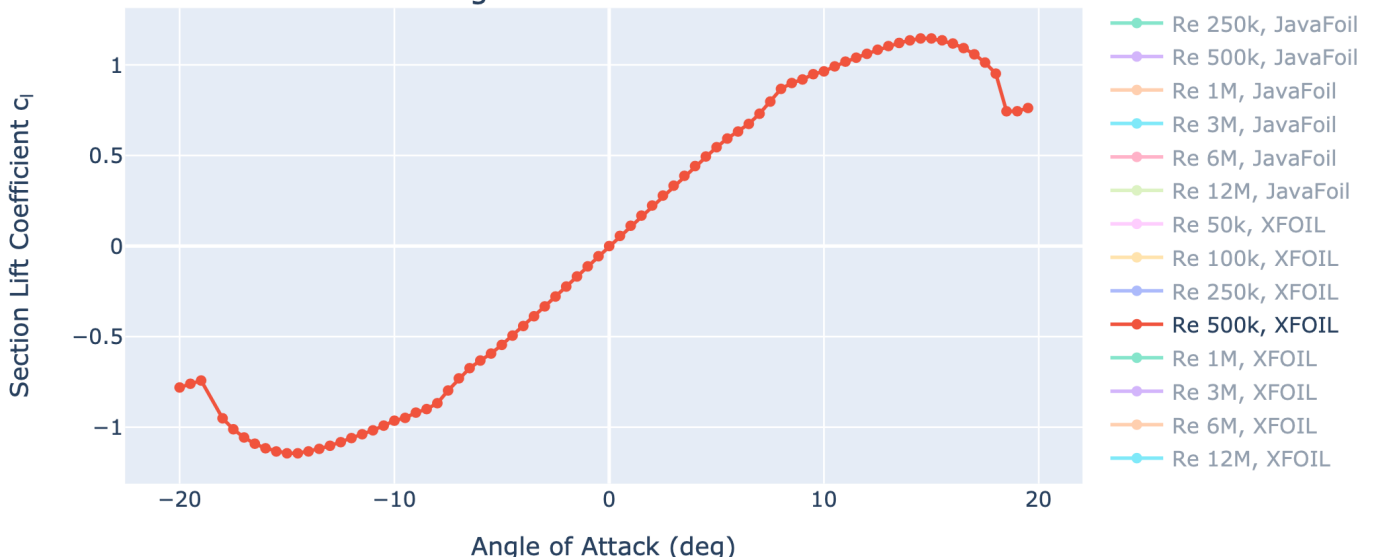


Figure 7.3: C_l vs Angle of Attack for Reynolds no. of 500k

GA 35A015

Basic data from JavaFoil for smooth airfoil at Mach 0, and windtunnel data if available
 Section drag coefficient vs angle of attack

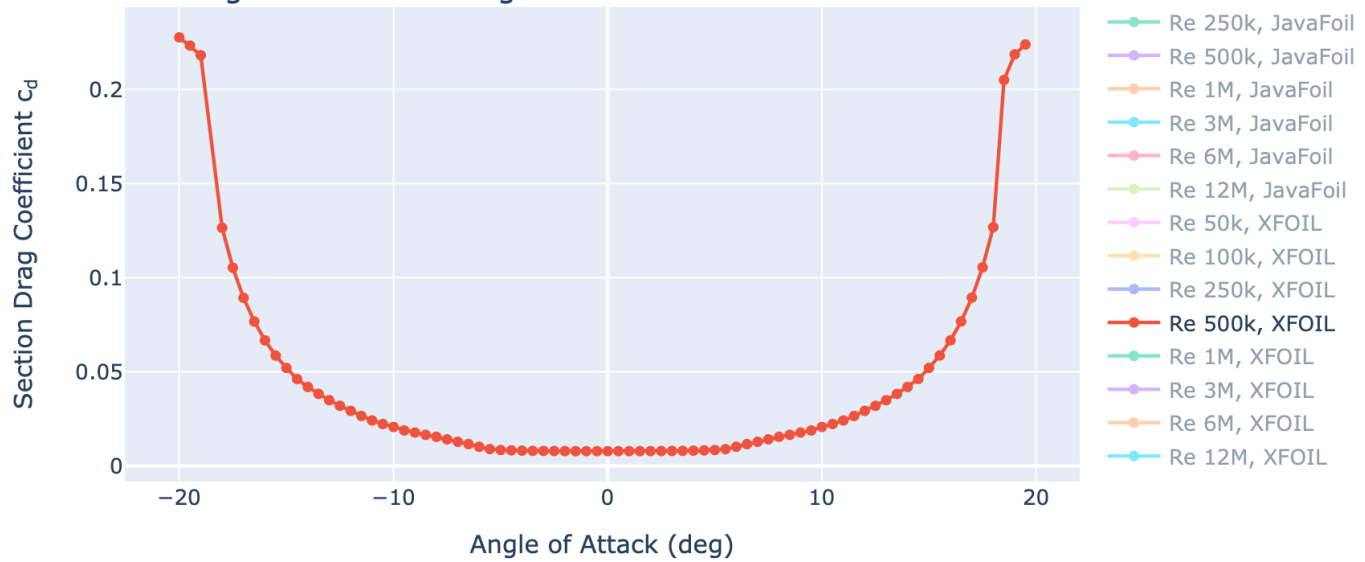


Figure 7.4: C_d vs Angle of Attack for Reynolds no. of 500k

GA 35A015

Basic data from JavaFoil for smooth airfoil at Mach 0, and windtunnel data if available
 Section lift/drag ratio vs angle of attack

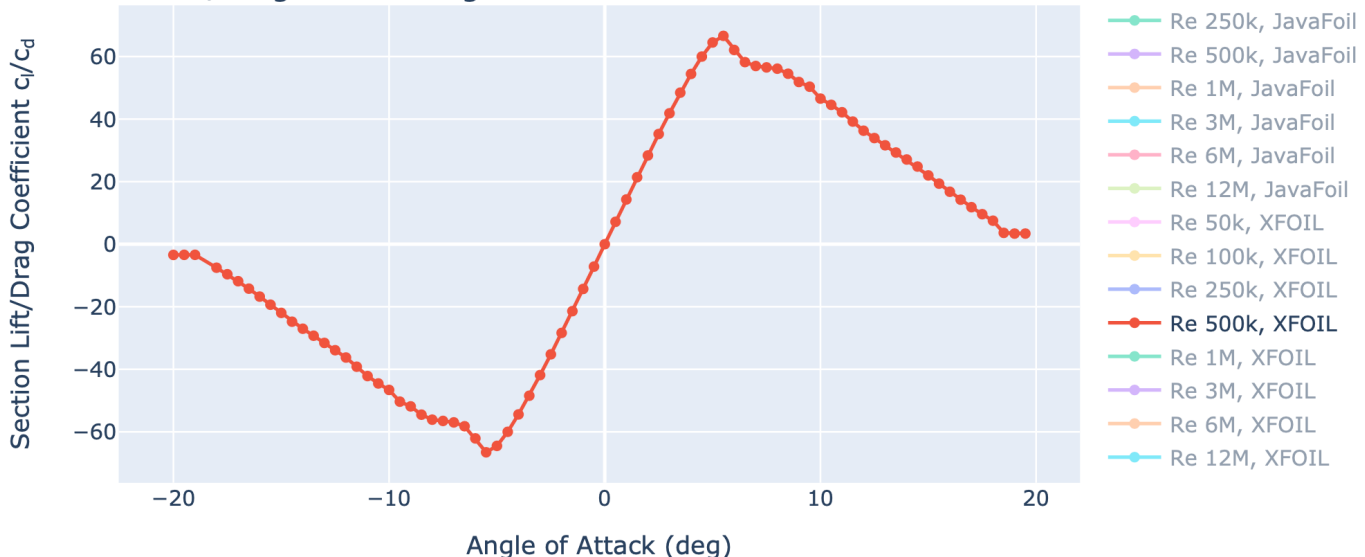


Figure 7.5: c_l/c_d vs Angle of Attack for Reynolds no. of 500k

GA 35A015

Basic data from JavaFoil for smooth airfoil at Mach 0, and windtunnel data if available

Section lift/drag ratio vs section lift coefficient

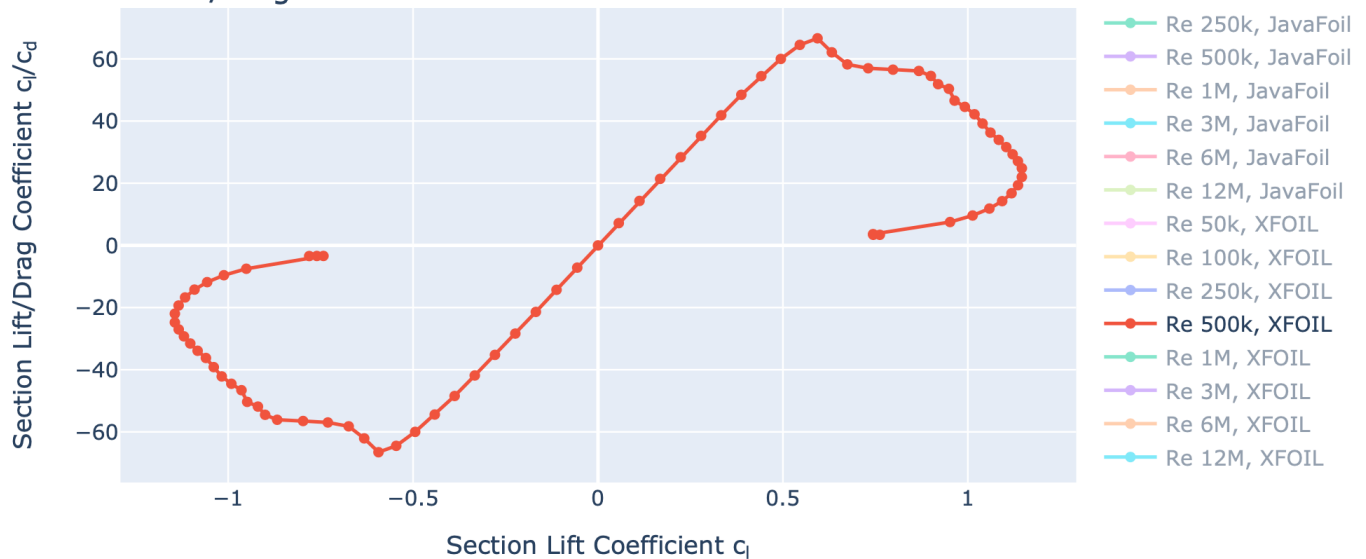
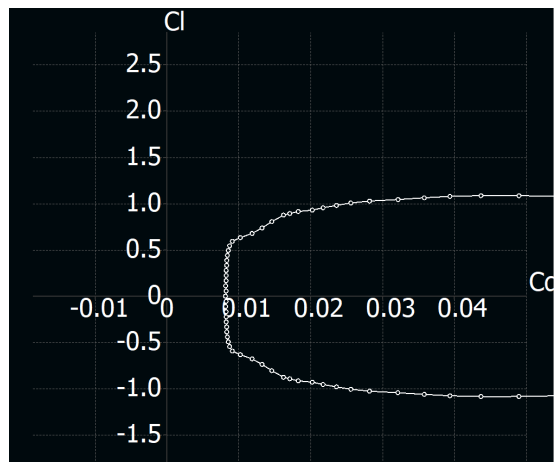
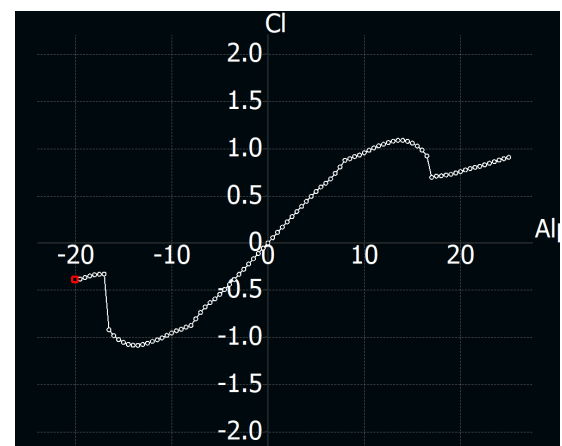


Figure 7.6: C_l/C_d vs C_l for Reynolds no. of 500k



(a) C_l vs C_d for Reynolds no. of 446k using XFLR5



(b) C_l vs Angle of Attack for Reynolds no. of 446k using XFLR5

Figure 7.7: GA 35A015 Airfoil in XFLR5

7.2 Wing Vertical Location

The location of the wing with respect to the fuselage center line is determined by the operating environment. This will have an influence on the design of other aircraft components such as tail design, and center of gravity. Before going ahead with the configuration suited for our mission, let us look at the advantages and disadvantages of the different possible configurations. In general, there are three possible options for the vertical location of the wing, namely:

1. High wing
2. Mid wing
3. Low wing

7.2.1 High wing

Advantages:

1. The propellers will have sufficient ground clearance.
2. Having the wing box passing through the fuselage, will require the fuselage to be stiffened, thereby contributing to the weight. This can be avoided by using a high wing where the wing box is carried over the top of the fuselage rather than passing through it.
3. If needed, a high wing allows for the use of large wing flaps for a high lift coefficient.
4. High wing prevents "floating" tendency (ground effect increases lift as the UAV approaches ground), which makes it difficult to hover/ drop payload at a desired spot.
5. Increases the dihedral effect C_{l_β} . It makes the aircraft laterally more stable.

Disadvantages:

1. We had mentioned that the wing box passing over the fuselage, reduces weight. However, there is a drag penalty to this as the frontal area increases.
2. Further since the high wing has more lateral stability, the lateral control is weaker.

7.2.2 Low wing

Advantages:

1. The low-wing configuration offers better aerodynamic performance and higher cruise speed than the high-wing configuration.
2. While flying over water bodies, in case of any crash or emergency if it is required to land on water, the low wing provides a better surface area and reduces the impact received by the fuselage and payload carried by it

Disadvantages:

1. Low wing configurations have ground clearance difficulties, which affects the propellers. This usually increases the interference effects between the wing and propellers and increases fuel consumption.
2. The low wing configuration dihedral angle will not be set by aerodynamics, but by the necessity to avoid the wing tip striking the ground.

3. It may increase the vertical tail size to avoid Dutch roll.

7.2.3 Mid wing

Advantages:

1. Mid-wing offers some of the ground clearance benefits as mentioned in high-wing configuration.
2. It has superior acrobatic maneuverability.

Disadvantages:

1. Structural carry-through is the major problem with mid-wing configuration. The wing carry-through box passes through the fuselage, splitting the fuselage.

	High Wing	Mid Wing	Low Wing
Ground Clearance for Propellers	High	average	Low
Interference drag	Average	Low	High
Stability about longitudinal axis	Stable	Neutral	Unstable (requires dihedral)
Ease of Payload drop	Easy	-	Average
Floating Tendency	Low	-	High
Downwash effect	Significant	Average	Low

Table 7.2: Comparison of Wing vertical location configuration

Comparing the three-wing vertical location and also considering our mission requirement, we find that it would be better for us to use **high wing** configuration as this allows for ease of payload drop and also has better stability characteristics.

7.3 Wing Dihedral

- The angle that the wing makes with the horizontal as seen from the front is called the dihedral angle. The position of the wing on the fuselage influences the effective dihedral.
- For our UAV we have decided to go ahead with high wing configuration. The high wing has a more pronounced dihedral effect.
- As the fuselage sideslips, it pushes the air over and under itself. If the wing is high mounted, the air being pushed over the top of the fuselage pushes up on the forward wing, providing an increased dihedral effect.
- Excessive dihedral effect produces "dutch-roll".

Hence because we are already using high wing configuration, we have decided not to have wing dihedral.

7.4 Aspect Ratio

Aspect Ratio is a measure of the Slenderness of the Wing. It is defined as Span squared by Wing Area.

$$AR = \frac{b^2}{S} \quad (7.3)$$

Effects of Aspect Ratio :

- Increasing the Aspect Ratio is similar to reducing the 3D effects on the wing. This is due to the increase in span which reduces the span affected by sideways flow due to flow leaks at Wingtip.
- Increasing aspect ratio has the following results,
 1. Increase in Aircraft $C_{L_{max}}$
 2. C_L increases for the same Angle of Attack
 3. Reduction in Stall Angle
 4. Increase in Aircraft L/D
 5. Increase in Aircraft Weight

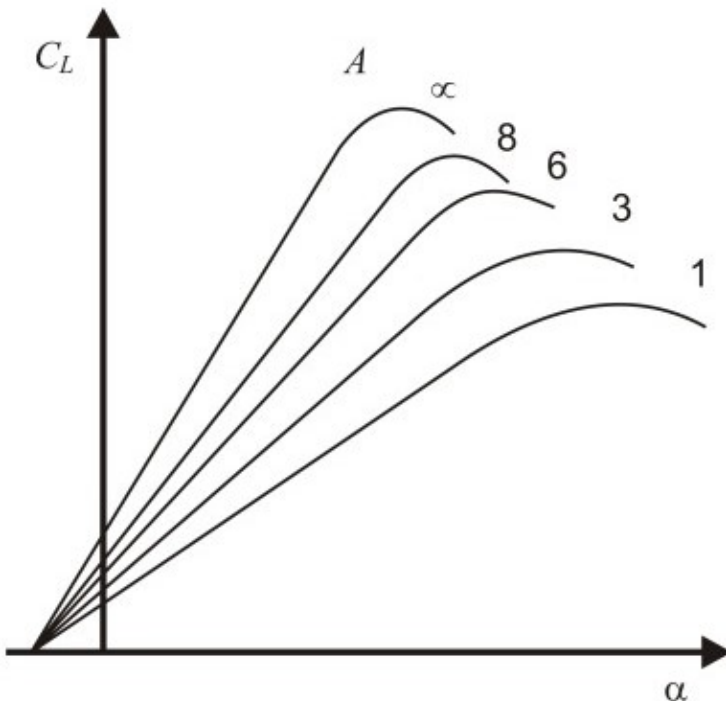


Figure 7.8: Effect of Aspect Ratio on C_L vs α curve [13]

From our previous estimates, AR for the aircraft was selected as **6.8** and we will be continuing with it for now.

7.5 Taper Ratio (λ)

- Taper ratio is Tip chord by Root chord. It is required as Prandlt's Wing Theory suggests that Elliptical lift distribution has minimum Induced drag implying an Elliptical wing.

$$\lambda = \frac{c_{tip}}{c_{root}}$$

- But the Issue with Elliptical wings is Difficulty in manufacturing. Hence Taper is used to alter the wing shape and hence the lift distribution.
- For Rectangular wings, tips having greater chords compared to the Elliptical wing which leads to more lift generation at the tip but also leads to more Induced Drag.
- It is hence preferred to try to incorporate a taper to bring the Lift distribution as close to the Elliptical distribution.

Considering the Manufacturing feasibility of our UAV we chose a Taper ratio of 1 or have No taper for our Wing.

7.6 Sweep Angle (Λ)

- The Function of the Sweep Angle is to reduce or delay the Adverse effects of Transonic & Supersonic flight regimes.
- Shock formation is determined by the flow velocity perpendicular to the Leading edge of the wing.
- Sweeping the wing aft or forward of the Mach cone angle changes the perpendicular velocity component and can reduce the loss of lift in Supersonic flows.

$$\text{Mach Angle } (\mu) = \arcsin \left(\frac{1}{M} \right)$$

- Sweeping the wing either aft or forward is theoretically the same. But forward sweep has structural difficulties.
- Sweep Angle is defined aft of the line perpendicular to flight direction whereas Mach angle is defined concerning flight direction. Hence we include $(90 - \mu)$ in the plots. This implies that the wing must be swept by this angle for the leading edge to be exactly at the Mach Cone.
- Sweep angle can be measured with respect to the Leading Edge or Quarter Chord line.

For our UAV, Evaluating the Mach no.

$$u = 25 \text{ m/s}$$

$$M = \frac{25}{339.5} = 0.07$$

For Flows under the Transonic regime, there is no requirement for a Sweep angle. Hence No Sweep Angle for our UAV wing.

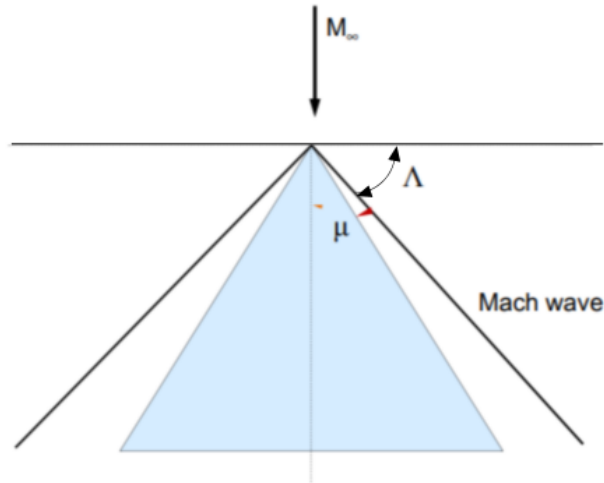


Figure 7.9: Sweep Angle & Mach Angle [5]

7.7 Twist

1. Twist helps to prevent tip stall before the root
2. Helps to redistribute lift to over-the-wing
3. Reduction in the lift which is limited by $|\alpha_t| + i_w \geq |\alpha_0|$, α_0 is the zero lift angle for any airfoil in the wing, α_t is tip AOA and i_w is the wing incidence at the root.

As we are dealing with a smaller Aspect Ratio we have to rely on the principle of lifting lines(vortex lines), as the down-wash created by the wing tip changes in span-wise direction we can have different stall conditions for the airfoils in the wing, generally the wings are designed in such a way that the root stalls first and then the tip.

Twist also helps us to redistribute the entire lift of the wing as per our requirement, we try to make the lift distribution close to the elliptical distribution so that the wing efficiency(e) stays high.

To achieve this we can have two types of twists along the span.

- Geometric (α)
- Aerodynamic (α_{eff})

These two can be obtained from the below equations, assuming an elliptical distribution.

For a position which is at y_0 from the mid is given as

$$L(y_0) = \rho V_\infty \Gamma(y_0)$$

$$\alpha(y_0) = \frac{\Gamma(y_0)}{\pi V_\infty(y_0)} + \alpha_{L=0}|_{y_0} + \frac{1}{4\pi V_0} \int \frac{(\frac{\partial \Gamma}{\partial y}) dy}{y_0 - y} \quad (7.4)$$

$$\alpha_{eff}(y_0) = \frac{\Gamma(y_0)}{\pi V_\infty C(y_0)} + \alpha_{l=0}(y_0) \quad (7.5)$$

The geometric twists we apply are generally linearly decreasing in a spanwise direction. This is to ensure that the tip doesn't stall before rooting. In practice these angles lie between -1° to -4° .

Based on this, we plan to have a twist of -2.5° , which is the average; however, the exact value depends on how we distribute the load.

7.8 Wingtips

Having looked at different types of winglet designs from the literature, we concluded that having a Hoerner-type wing tip would be helpful as it is the most common type of low-drag winglet, which is also easy to manufacture. An endplate or a winglet would be beneficial if we have constraints in the wingspan; otherwise, their drag penalty would be higher. [13]

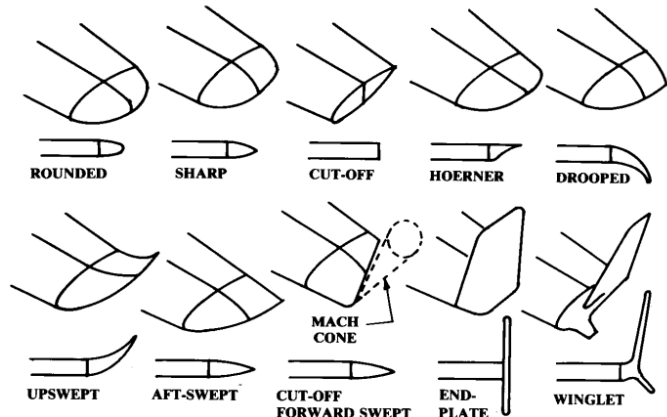


Fig. 4.27 Wing tips.

Figure 7.10: Wingtip types

7.9 Wing angle of incidence (i_w)

Talking about the incidence angle(i_w) is the angle that the chord makes with the fuselage reference line. This angle is used to optimize the lift and drag characteristics of our wing, for general purposes, we try to make the changes such that the AOA for $(L/D)_{(max)}$ happens when the aircraft is in cruise. There are other parameters also to describe this angle, those are the requirement of minimum drag in cruise, etc.

These can be achieved by two kinds of arrangement of the (i_w)

- Variable i_w
- Fixed i_w

For simplicity, we are going to have a fixed i_w which has a typical range of 0° to 4° , for the time being, we are going with the average value of 2° but we'll find the actual i_w based on the equations and lift distributions if required, based on the consideration of taper ratio we need. We can further provide an estimate for that in later stages.

7.10 Control Surfaces

For all types of aircraft like commercial, fighter, remote control, or model aircraft, control surfaces play a vital role. The reason behind this scene, without designing an accurate control surface no aircraft can fly safely, and not able to guide the aircraft with proper directory facilities. Control surfaces highly assist in the stability of an aircraft. As we know three axes of force (roll, pitch,

yaw) are must required to control and maneuver an aircraft. Hence, it brings a obligatory concern to aircraft design. There are two types of control systems in aircraft design:

- Primary control system(Aileron,Elevator,Rudder)
- Secondary control system(Slat,Flaps,Spoiler,Trim tab)

Here, to design a UAV it barely required a primary control system, which included an aileron, elevator, and rudder. To ensure the stability of an aircraft with the assistance of a control surface, we need to take into account to mount of these three primary control systems, where the aileron causes roll motion, the elevator causes pitch motion and the rudder causes yaw motion. It has to be found the geometric dimensions of these three obligatory control systems.

To design an aileron, we have to find the ratio of the aileron span to the wing span and dimension of the aileron.

Since, our wing span value is 2.5m. Now we may easily find the aileron span and its dimensions using design principle of aircraft with parameter's below

- Aileron to wing planform area (S_a/S) = 0.05 – 0.1
- Aileron span (b_a/b) = 0.2 – 0.3
- Aileron chord (C_a/C) = 0.15 – 0.25
- Inboard aileron area (b_{ai}/b) = 0.6–0.8
- Maximum up and down aileron deflection ($\delta_{A_{max}}$) = 30°

Let's consider the average value of aileron span is 0.25

$$\frac{\text{Aileron span}}{\text{Wing span}} = 0.25$$

$$\text{Aileron span} = \text{Wing span} * 0.25$$

$$\text{Aileron span} = (2.5 * 0.25)\text{m}$$

$$\text{Aileron span} = 0.625 \text{ m (for both aileron)}$$

$$\text{For each aileron} = \frac{0.625}{2}\text{m} = 0.313 \text{ m}$$

Generally, the standard ratio of aileron dimension(length: width) is 3:1 or 4:1(depending on design criteria). Here we are choosing the ratio of 4:1 (because long span aileron provides more aerodynamic efficiency, accuracy and stability as well)

Hence, the **length** of aileron is indifferent to aileron span and it is **0.313 m**

and the **width** of aileron should be one-fourth of the length and it is **0.078 m**

7.11 High Lift Devices

In the design of our fixed-wing Unmanned Aerial Vehicle (UAV), we have carefully considered the lift requirements and the associated design parameters that influence the generation of lift. Our analysis indicates that with an ideal coefficient of lift C_L of **1.38** our UAV design demonstrates that it can achieve the necessary lift without the incorporation of high-lift devices such as flaps or slats.

The design of our UAV's wings and the selection of **GA 35A015** Airfoil, combined with the operational flight velocity, ensure that the lift generated meets the UAV's requirements. The calculated coefficient of lift (C_L) confirms that high-lifting devices are not necessary for our UAV, simplifying the design and reducing the overall weight and mechanical complexity. This results in a more efficient and reliable UAV, optimized for its intended mission profile.

7.12 Summary

Features	Estimates
Airfoil	GA 35A015
Wing vertical position	High wing
Wing sweep	No sweep
Taper ratio	1
Twist angle	0°
Incidence angle	2°
Wing planform	Rectangular

Table 7.3: Summary

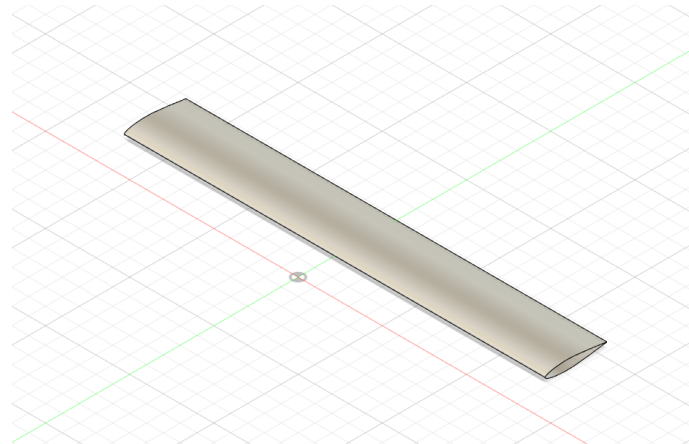


Figure 7.11: Wing CAD

Chapter 8

Fuselage Design

The primary function of fuselage is to house the payload. As the gross takeoff weight has been estimated and also as we have completed initial wing sizing, we now go on to estimate the initial fuselage size. The fuselage size is strictly determined by "real-world constraints"[13].

In this section, we:

1. Determine the fuselage length.
2. Determine the fuselage Width and height.
3. Carry out the segmentation of the fuselage.
4. Give an initial idea of position of various payload components.

We will be sizing our fuselage based on the volume requirements of the payload we will be carrying. The main components of our payload include life jacket, camera, GPS tracker. In addition, the powerplant systems including battery, motor, wiring, communication equipment will also be housed inside the payload.

The dimensions of the payload are detailed in below table8.1.

Component	Dimension (mm)	Volume (mm ³)	Weight (g)
Motor	ϕ 47.4 , L - 38.7	68,255	172
Battery Volume	70 x 80 x 120	6,72,000	1008
Lifejacket	559 x 231 x 231	2,34,27,690	995
Neo 7M	16.6 x 12.3 x 2.6	530.9	12
Arduino	17.78 x 43.18	767.7	7
GPS battery	56 x 18 x 32	32,256	36
LoRA module	80 x 70 x10	56,000	8
Camera (HD 25)	ϕ 76 , L - 109	19,77,896	340

Table 8.1: Component Volume Estimation

In addition to this we will be adding a tolerance of 10% . Now that we have identified the dimensions of the payload, we will go ahead with sizing the fuselage as per these requirements.

8.1 Fuselage Dimensions:

8.1.1 Fuselage Length:

The initial estimate of fuselage length will be developed based on previous comparable aircraft data as listed in table(8.2).

UAV	DTOW (kg)	Fuselage length (mm)
DeltaQuadPro	6.2	751
Blackswift	9.5	1778
SQA eVTOL	9.8	990.5
Atlas AS90X	2.4	750
Bramor C4eye	4.5	960
AR1-Tekever	5	811.1
Albatross	10	733.4

Table 8.2: Comparable UAV data - DTOW and fuselage length

These data points are then plotted and a best fit is obtained. Following this we use the empirical relation as in equation(8.1)[13]:

$$L_f = aW^c \quad (8.1)$$

Based on the best fit data, we have $a = 0.5886$, and, $c = 0.2483$. For our UAV we have design weight of 9.646Kg. This gives the fuselage length as 1033 mm.

But the above length is insufficient for our internal components hence the length was further increased to,

$$\text{Fuselage Length} = 1505 \text{ mm}$$

This length is the overall length involving the nose, mid-section and the rear fuselage.i.e.,

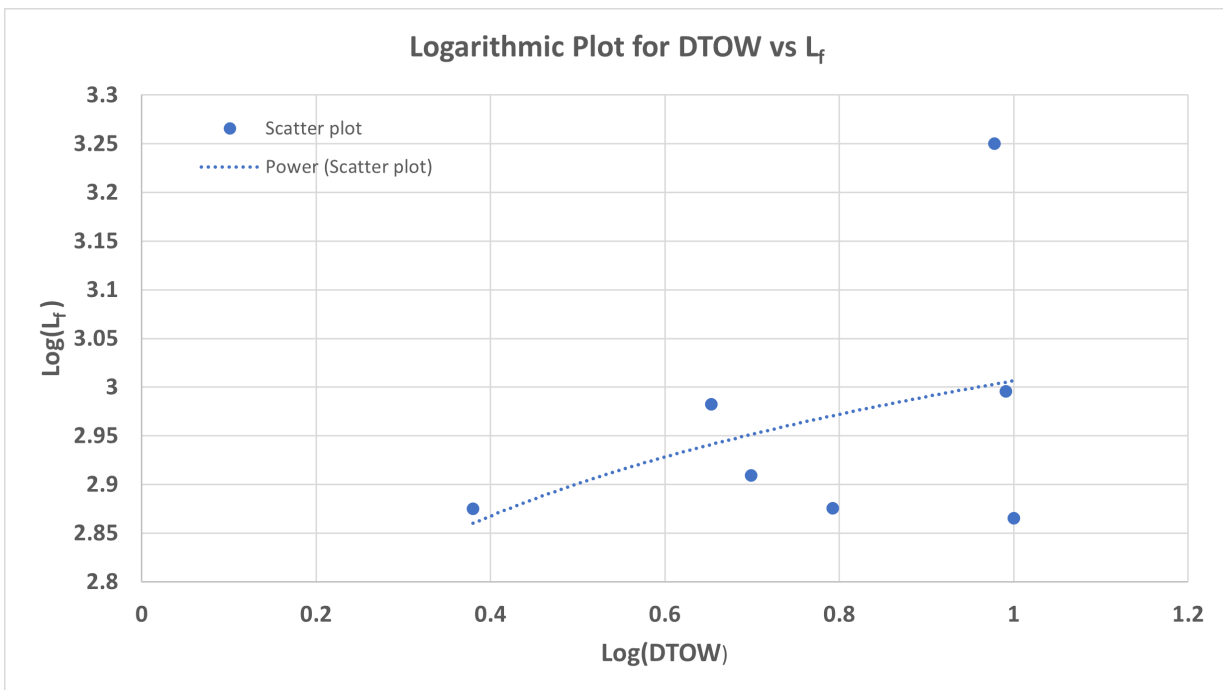
$$L_f = L_{f,nose} + L_{f,mid} + L_{f,rear}$$

8.1.2 Mid-section of Fuselage:

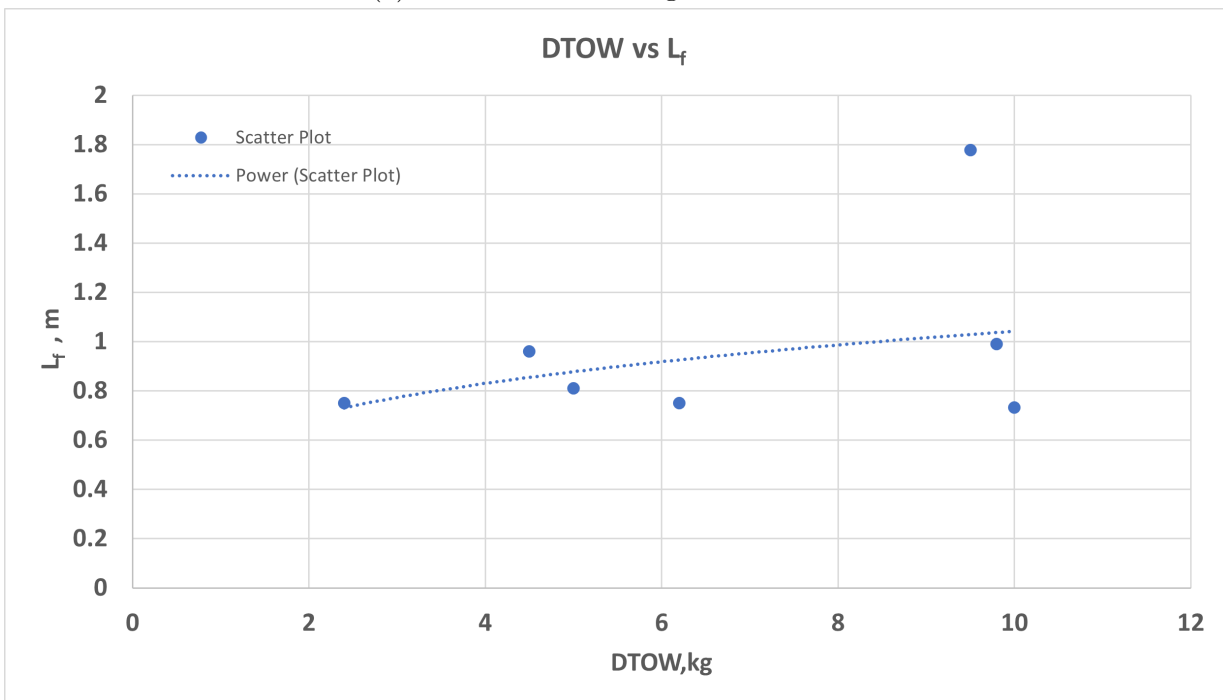
The fuselage midsection will be in rectangular shape, with the length of this section determined by the length of the life jacket. As given by the dimension in(8.1), the length of the life jacket is 559mm. In addition, taking a factor of 10%, the length of the fuselage mid-section comes out to be $L_{f,mid} = 615 \text{ mm}$.

Considering that the Life-jacket has dimensions unsuitable for a Fuselage. We decided to roll up the life jacket and even out the Cross-section of the Life-jacket. By conserving the volume we obtain the dimensions of the cylindrical roll.

We have decided to have the Access door and Bay-door common for the payload, which will be at the bottom of Mid-Fuselage.



(a) Linear best fit in logarithmic scale.



(b) Best fit curve

Figure 8.1: Plots for regression

$$L_{f,mid} = 615 \text{ mm}$$

$$H_{f,mid} = 254 \text{ mm}$$

$$W_{f,mid} = 254 \text{ mm}$$

8.1.3 Up-sweep angle:

The rear fuselage must be able to clear the ground under regular operating conditions. Also, since we have pusher configuration, we'd not need the airflow to be blocked. Hence we cut the rear fuselage by giving an upsweep angle. This angle can be calculated as follows,

$$C_l = C_{l\alpha}(\alpha - \alpha_{L=0}) \quad (8.2)$$

The lift curve slope is taken as 0.1(approximately) and the zero lift angle of attack is -7° . Based on these we obtain, [14]

$$\text{Upsweep angle} = 7 \text{ deg}$$

8.1.4 Nose Section

The Nose is assigned to hold the Camera and the Communication package. Since it also is the Front part of the fuselage which contacts the flow first, hence it is required to be Aerodynamic.

Using the Mid-Fuselage as base dimension for Nose. For the front for now we are taking up it as a spline which will give it aerodynamic shape, exact shape will be obtained after Structural analysis. Hence maintain the smoothness of curvature from Mid-Fuselage, 300mm was chosen as the Nose length.

The positioning of the Communication package is planned as by adding a Horizontal partition and placing them above the Partition while the Camera is below the partition protruding out of the Fuselage.

$$L_{f,nose} = 300 \text{ mm}$$

8.1.5 Rear fuselage length:

The rear fuselage length will be subtraction of nose length and mid fuselage section from the total length. Here, The total length of fuselage is 1505 mm.

Hence, the rear fuselage section length will be,

$$\text{Rear fuselage length} = \text{total length} - (\text{nose length} + \text{mid fuselage})$$

$$\text{Rear fuselage length} = 1505 \text{ mm} - (300 + 615) \text{ mm} = 590 \text{ mm}$$

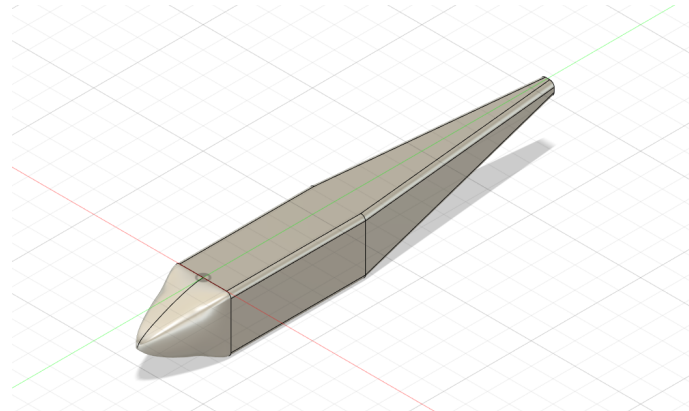


Figure 8.2: Fuselage Isometric View

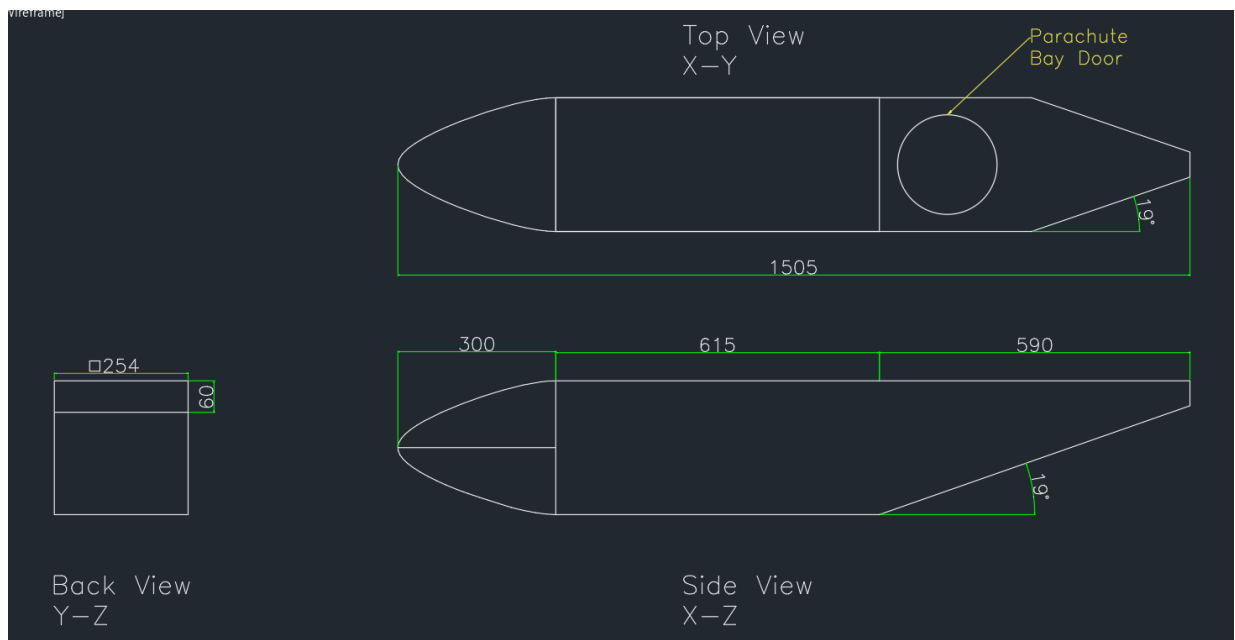


Figure 8.3: Fuselage dimension

8.2 Summary

Fuselage section	Dimension [L x W x H] (mm)
Nose	300
Mid-Section	615 x 254 x 254
Rear	590 x 254 x 254 base with 19° upsweep

Table 8.3: Fuselage Dimensions

Chapter 9

Tail Design and Preliminary Sizing

In this chapter, the tail configuration has been decided, the tail design sizing details have been enumerated and simulations for the same have been provided.

9.1 Tail Configuration

We decided on an inverted V-tail configuration for our plane as we wanted to minimize the blockage in front, which would be higher for a conventional plane because it will have three surfaces blocking the pusher's input airflow compared to two of surfaces of a V-tail.

Traditional V-tail would have adverse roll-yaw coupling, hence we opted for an inverted V-tail as it would have proverse roll-yaw coupling. The only drawback for this configuration is that the controls would be more complex than a conventional design as there is roll yaw coupling.

We explored other configuration like a T-tail, cruciform and H tails but avoided them as they are more susceptible to vibrations as the motor is close to the tail.

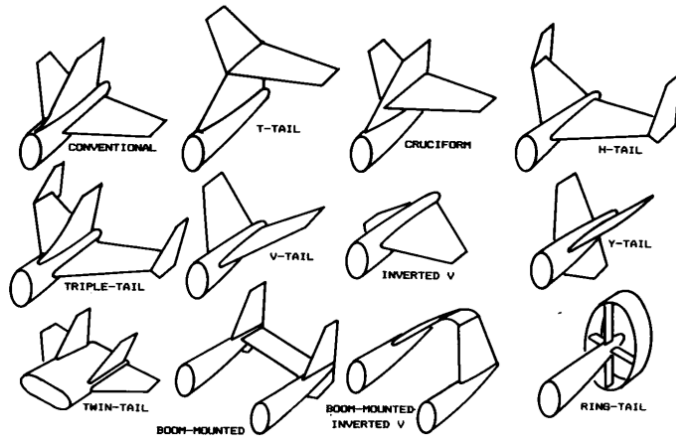


Figure 9.1: Tail config, ref pg.68 [13]

9.2 Average values for parameters

The aircraft whose data are used are . These are similar in weight and configuration to the aircraft we are designing. From the aircraft data collected,

- The horizontal tail volume ratio $V_H = 0.76$
- The vertical tail volume ratio $V_V = 0.007$
- The horizontal tail aspect ratio $AR_h = 5.5$
- The vertical tail aspect ratio $AR_v = 1.8$
- The distance between MAC of wing and that of the horizontal tail $l_h = 1.08$ m
- The distance between MAC of wing and that of the vertical tail $l_v = 0.01$ m
- The average planform area for wing $S_w = 0.68$
- The average chord for wing $c_w = 0.25$ m

9.3 Horizontal Tail

The following section lists the details of the horizontal tail.

9.3.1 Area S_h :

The horizontal tail volume ratio is assumed to be the average of that of the comparable aircraft. Similarly, the distance between MAC of wing and that of the horizontal tail is assumed to be the average of that of the comparable aircraft. Using these values, the horizontal tail area is calculated below:

$$\begin{aligned} V_H &= \frac{S_h l_h}{S_w c_w} \\ \implies S_h &= \frac{V_H S_w c_w}{l_h} = 0.24 \text{ m}^2 \end{aligned} \quad (9.1)$$

9.3.2 Aspect Ratio AR_h :

The aspect ratio for the horizontal tail is assumed to be the average of that of the comparable aircraft. This assumption will be refined in the stability analysis process. Therefore,

$$AR_h = 5.5 \quad (9.2)$$

9.3.3 Taper Ratio λ_h and Sweep Angle Λ_h :

- To minimize fabrication cost and complexity, the taper ratio $\lambda_h = 1$ is considered.
- For low subsonic Mach number flight, a high sweep angle is not required. Hence, we take an unswept horizontal tail with $\Lambda_h = 0^\circ$.

9.3.4 Horizontal Tail Airfoil Selection:

Symmetric airfoils are most commonly used for the horizontal tail. This is to improve the control characteristics of the airplane. In order for the tail to be beyond the compressibility effect, the tail lift coefficient is determined to be less than the wing lift coefficient. To insure this requirement, the

flow Mach number at the tail must be less than the flow Mach number at the wing. This objective will be realized by selecting a horizontal tail airfoil section to be thinner than the wing airfoil section. To this end, the airfoil selected for the horizontal tail is **NACA 0009**.[14]

9.3.5 Horizontal Tail Incidence Angle:

The horizontal tail incidence angle has a significant effect on the stability of the aircraft and its final value will be set after the stability analysis is complete. At this stage of design,

$$i_h = 0^\circ \quad (9.3)$$

9.4 Vertical Tail:

For vertical tail we again go back to the past data, since we wont have the actual idea of tail size and span without performing the stability analysis of the UAV. That being the task for later stage, we chose to use parameters from similar configuration and weight category.

9.4.1 Vertical Tail Area

The vertical tail area is defined as, with analogous meanings to that in the horizontal volume ratio.

$$\begin{aligned} V_V &= \frac{S_v l_v}{S_w c_w} \\ \implies S_v &= \frac{V_V S_w c_w}{l_v} = 0.12 \text{ } m^2 \end{aligned} \quad (9.4)$$

9.4.2 Aspect Ratio of vertical tail

Using the past data we can get the vertical tail aspect ratio to be

$$AR_v = 1.8 \quad (9.5)$$

9.4.3 Vertical tail Sweep Λ_v and Taper Ratio λ_v

For the time being we are sweep and Taper Ratio as zero, and the actual values can be obtained only after stability analysis.

9.4.4 Airfoil selection

Mostly for vertical tails, symmetric airfoils are used, that to thin, as the major function of the tail is to provide stability and not has much to do with the functionalities like that of wings. So we are finalizing on a thin airfoil **NACA 0009** for meeting our requirements.

9.5 Inverted V-tail:

The parameters for the inverted V-tail are calculated using the values of the horizontal and vertical tail as given above.[13]

- For the horizontal tail, span $b_h = \sqrt{AR_h S_h} = 1.14 \text{ m}$.
- For the vertical tail, span $b_v = \sqrt{AR_v S_v} = 0.47 \text{ m}$.
- For the horizontal tail, chord $c_h = S_h/b_h = 0.21 \text{ m}$.
- For the vertical tail, chord $c_v = S_v/b_v = 0.26 \text{ m}$.

The inverted V-tail is designed using the following steps:

- The dihedral angle of the tail, $\theta = \tan^{-1}(2b_v/b_h) = 39.23^\circ$.
- The chord length chosen is the average of the chord lengths c_h and c_v .
Therefore, $c_t = \frac{c_h + c_v}{2} = 0.23 \text{ m}$.
- The tail is symmetric and the area of the tail is equal to the sum of the areas of the horizontal and vertical tail. Therefore, denoting the diagonal length of each tail element as b_t , $2b_t c_t = S_h + S_v$. Therefore, $b_t = 0.77 \text{ m}$.
- The airfoil chosen is the same as that chosen for the horizontal and vertical tail, that is, **NACA 0009**.

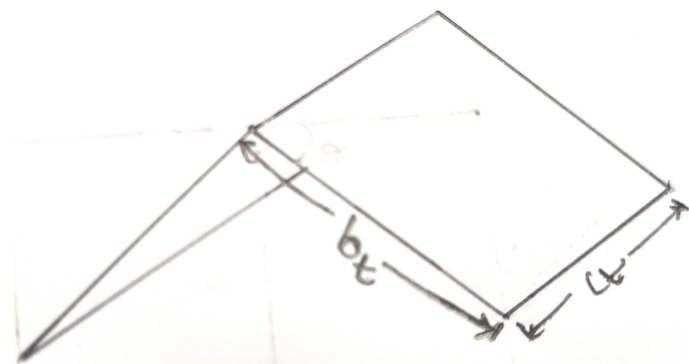
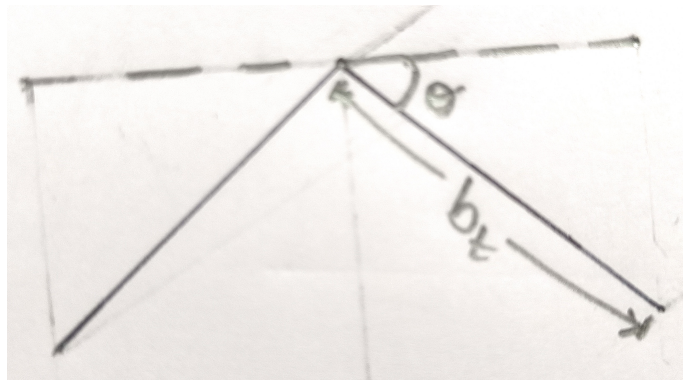


Figure 9.2: Inverted V-tail diagrams

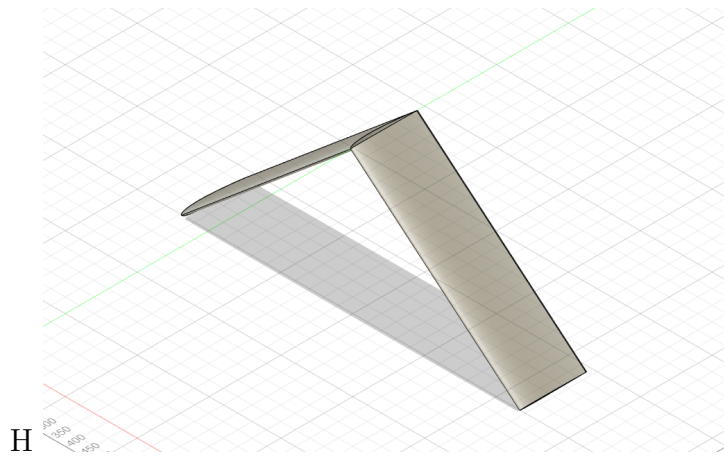


Figure 9.3: Tail CAD

9.6 Summary

So, for this week's task we got the estimates for following parameters, which may change after stability analysis

Parameters	Estimated values
S_h	0.24 m^2
AR_h	5.5
S_v	0.12 m^2
AR_v	1.8
θ	39.23°
b_t	0.77 m
c_t	0.23 m

Table 9.1: Summary

Chapter 10

Landing System Design

10.1 Different landing mechanisms

For a fixed wing UAV ,the landing mechanism is a critical component that ensures the safe return of vehicle to the ground. There are several methods for landing fixed wing UAVs:

- **Conventional landing gear:** This is the most common type of landing mechanism, which involve wheels and require runway for takeoff and landing.
- **Belly landing:** Some fixed wing UAV are designed to land on their belly, sliding along a runway or field. This method eliminates the need for complex landing gear but can be rough on UAV's structure.
- **Parachute system:** The parachute can be deployed to slow down the UAV for soft landing. This method adds weight and requires space within the fuselage but can be used when a runway is not available.
- **Vertical takeoff And landing:** Some fixed wing UAVs incorporate mechanisms for vertical landing, similar to multicopters, which allows them to land without the need for a runway.
- **Automatic landing systems:** Advanced UAVs may use ALS, which employs algorithms and sensors to perform a safe landing autonomously, even under challenging conditions like strong winds.

The landing system we have picked is the **parachute landing system**. This system offers the advantage of **lower weight**. Conventional landing gears tend to be heavier than parachutes used for a desired terminal velocity. This system also **eliminates** the need for a **runway**. The **maintenance** of the system is also relatively easier as a new parachute can be installed as needed conveniently.

10.2 Takeoff mechanism

Fixed wing UAVs need to be accelerated to a minimum controllable airspeed. Since we are not using any landing gears in our design the conventional runway takeoff is out of question. Also, since the UAV is weighing around 10 kg, hand launching will also be difficult. The other alternatives for achieving takeoff include use of catapult mechanisms, such as:

1. **Pneumatic catapult launchers :** Here, compressed air is used to accelerate the launching cradle. A compressor is needed to pressurize the gas, making the setup bulky and difficult to handle.
2. **Hydraulic catapult launchers :** They use oil and compressible gas separated by a piston. Pumping the oil causes the piston to compress the case, which stores energy for launching the UAV. Like pneumatic UAV catapults, hydraulic UAV launchers also require a power supply to operate.
3. **Bungee catapult launchers :** They are simpler than hydraulic or pneumatic launchers, using energy stored in elastic cords. The cord may be stretched manually or by means of an electric motor.

Based on these observations, we have decided to use bungee catapult launch mechanism for launching our UAV and have found a system which we can directly use. It is the scorpion launch system. [44]

10.2.1 How it works:

- The UAV is secured to the catapult with a launch bar. The catapult is loaded with potential energy by pulling back the launch bar to stretch the bungee cords.
- When the UAV is ready to launch, the launch bar is released, and the bungee cords rapidly retract, propelling the UAV forward. This sudden acceleration launches the UAV into the air at a high velocity, typically around 80 knots, depending on the specific system and the weight of the aircraft.
- After the launch, the bungee cords are quickly retracted and reset for the next launch.

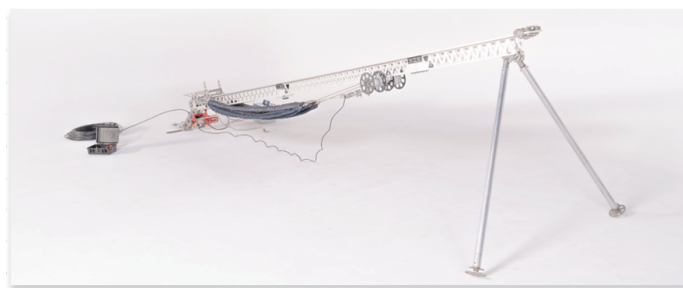


Figure 10.1: Bungee Chord Mechanism.

10.3 Terminal velocity and altitude of deployment

The primary points of consideration when designing a parachute landing mechanism are the terminal velocity to be achieved and the altitude of parachute deployment.

10.3.1 The terminal velocity:

- The terminal velocity is the velocity at which the UAV descends unaccelerated and lands on the ground.
- This velocity must be selected such that the impact of the UAV on the ground doesn't damage the UAV.
- To select this velocity, aircraft and drones of weights similar to our UAV currently using a parachute landing mechanism were analysed. This analysis yielded the following typical range for the terminal velocity: 3 m/s to 4.5 m/s.[41], [43]
- The parachute sizing and terminal velocity selection are coupled. From the parachute sizing considerations described subsequently, a terminal velocity of **3.14 m/s** has been selected for the UAV.

10.3.2 The altitude of parachute deployment:

- The parachute must be deployed at an altitude high enough that the UAV reaches the ground with the desired terminal velocity.
- However, the UAV must also be deployed at an altitude low enough that cross-winds and gusts don't cause a significant change in the location where the drone lands.
- After testing with various values, the altitude of parachute deployment was fixed at **20 metres**. The code used to solve the mathematical model representing the landing is given in the appendix.15

10.3.3 Mathematical model used:

- A two-degree of freedom model is used to represent the system.[45]
- The airplane is treated as a point mass and the lift and drag forces contributed by it are neglected.
- The effect of the wind has been neglected. However, since the terminal velocity fixed is towards the lower end of the range of terminal velocities typically chosen, the UAV should land safely even with the effect of wind.
- The time taken by the parachute to unfurl is neglected and the parachute drag is assumed to act opposite to the velocity vector at all points of time.
- The diagram below shows the model used:

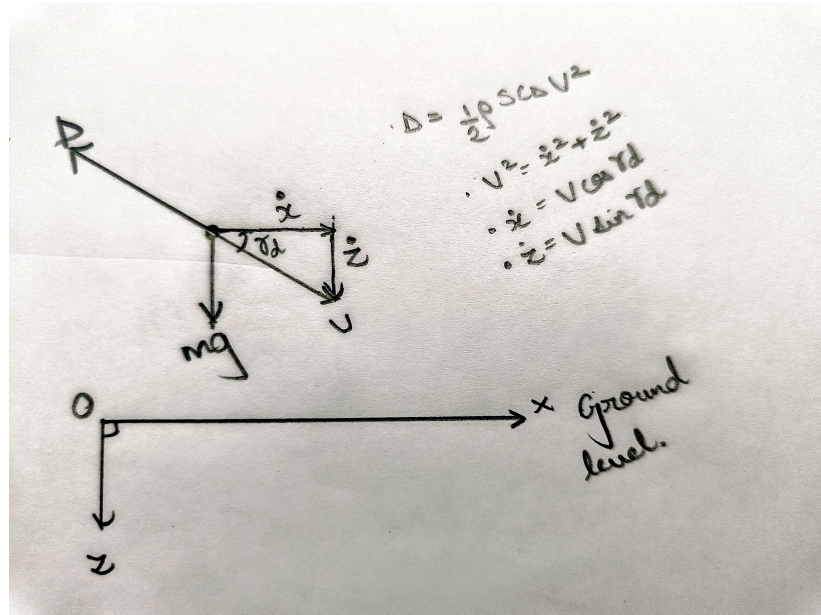


Figure 10.2: Two-degree of freedom trajectory system model

- The equations to be solved are as follows:

$$\frac{dx}{dt} = \dot{x} \quad (10.1)$$

$$\frac{dz}{dt} = \dot{z} \quad (10.2)$$

$$\ddot{x} = -\frac{\rho S C_D}{2m} \dot{x} \sqrt{\dot{x}^2 + \dot{z}^2} \quad (10.3)$$

$$\ddot{z} = g - \frac{\rho S C_D}{2m} \dot{z} \sqrt{\dot{x}^2 + \dot{z}^2} \quad (10.4)$$

- We plan for the aircraft to descend to an altitude of 20 m and cruise with a horizontal velocity of 13.68 m/s for the parachute deployment. The parachute is deployed when the aircraft is operating in this condition. Therefore, the initial conditions taken are as follows:

$$x = 0 \text{ m}$$

$$z = -20 \text{ m}$$

$$\dot{x} = 13.68 \text{ m/s}$$

$$\dot{z} = 0 \text{ m/s}$$

- These equations are solved numerically using the Runge-Kutta fourth order method. 15

10.3.4 Results:

Solving the system described above using the Runge-Kutta fourth order method 15, the results obtained are as follows:

- The x location varies with time as shown in the figure. It can be observed that the UAV lands 2.5 m from the origin in the x direction.

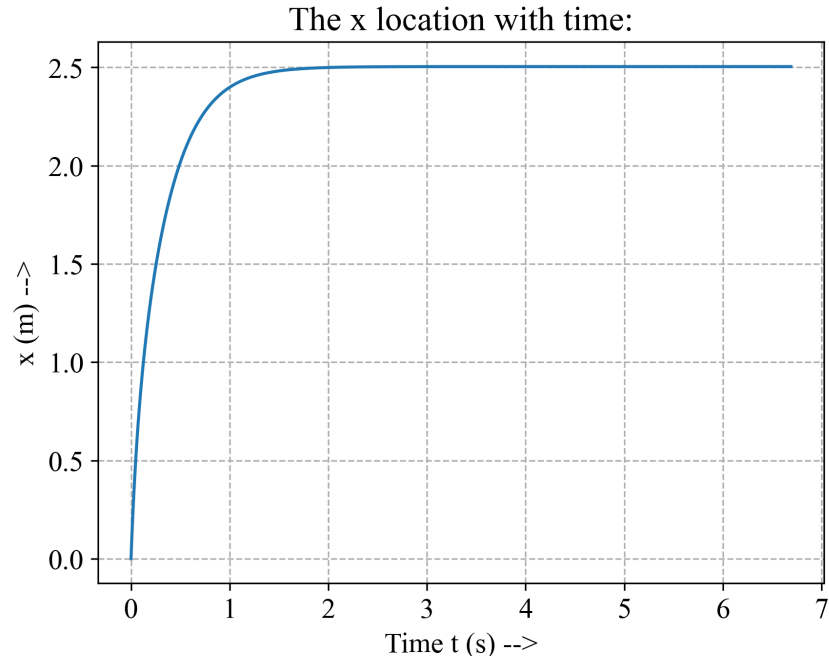


Figure 10.3: The x location variation with time.

- The z location varies with time as shown in the figure. It can be observed that the UAV takes about **6.69 seconds** to land. Only the magnitude of z has been plotted. This represents the altitude.

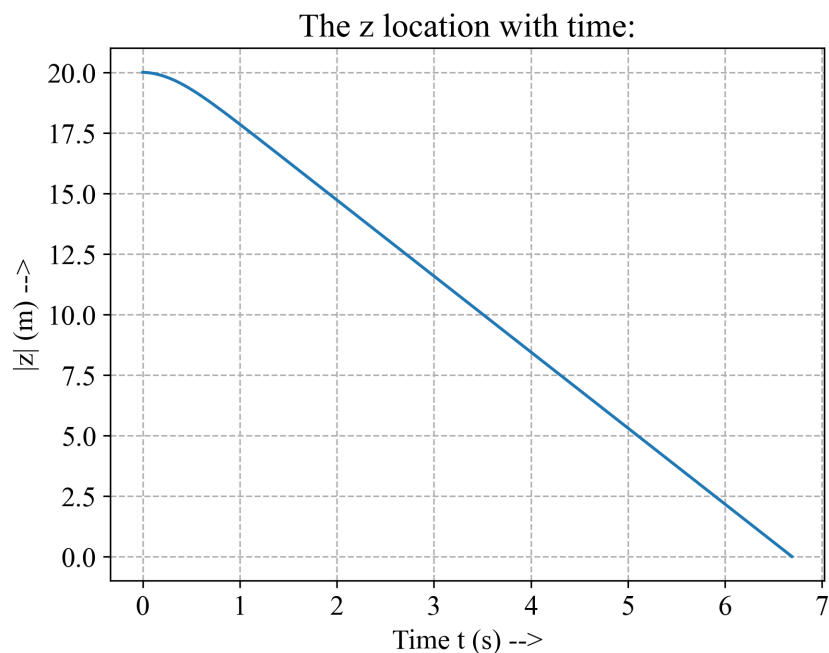


Figure 10.4: The z location variation with time.

- The horizontal velocity \dot{x} varies with time as shown in the figure. The velocity \dot{x} rapidly drops to zero as is required and expected.

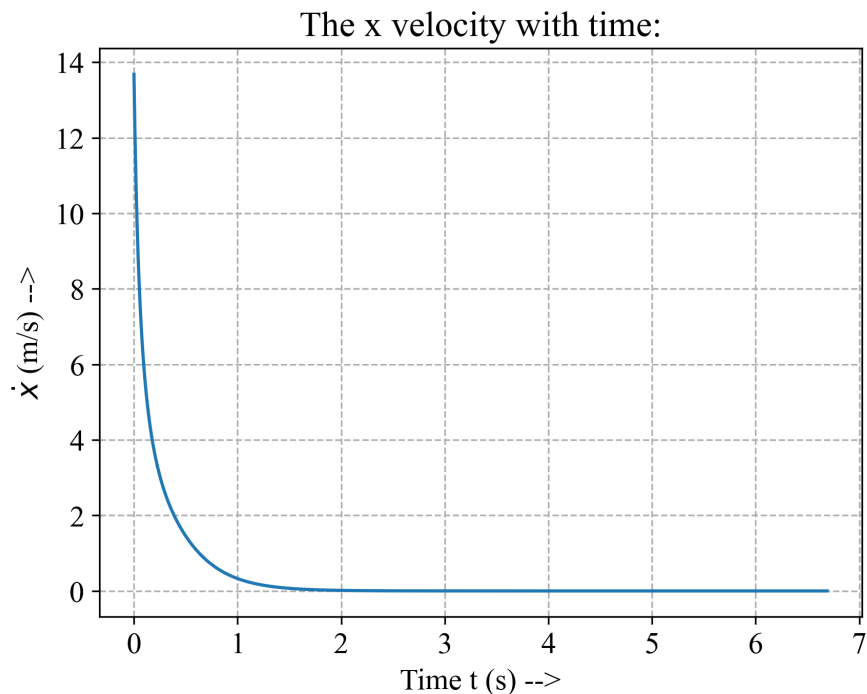


Figure 10.5: \dot{x} variation with time.

- The vertical velocity \dot{z} varies with time as shown in the figure. The velocity \dot{z} increases to the terminal velocity = 3.14 m/s from zero and remains constant at that value. The coordinate system used is as shown in the diagram of the mathematical model used.

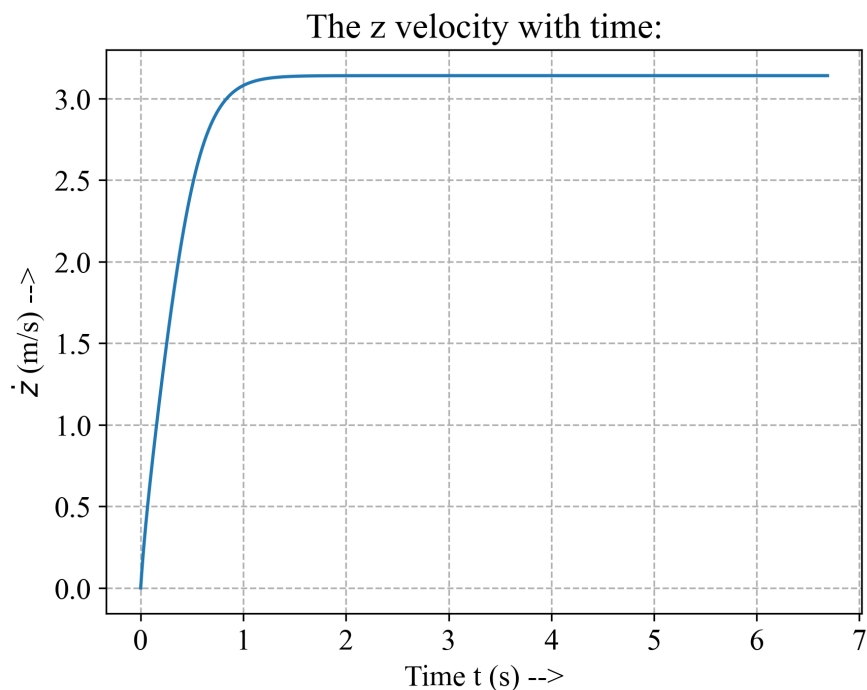


Figure 10.6: \dot{z} variation with time.

- The trajectory followed by the aircraft is plotted in the figure below. The magnitude of z has been plotted. This represents the altitude.

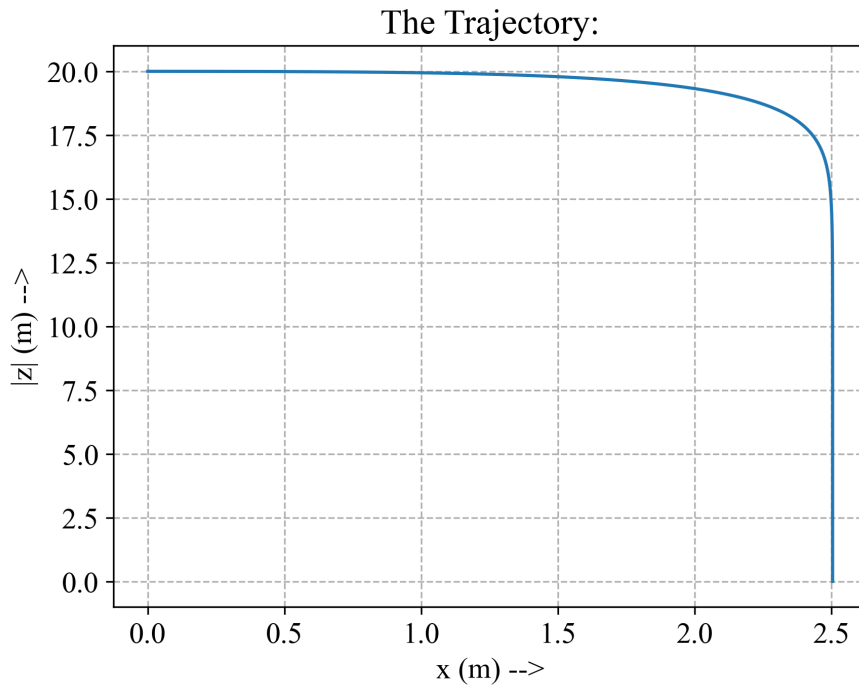


Figure 10.7: UAV Trajectory

10.4 Parachute selection

Based on the requirements we can design/select the parachute, for standardization and easy replacement we planned to go with a pre-designed annular parachute. In order to select the exact size we need to know the terminal velocity which can be obtained by past data as it can be analytically solved for any velocity and until there is any constraint on landing speed we can't have a unique solution. As the calculation depends on how good our structure is in terms of dissipating energy and how much tolerance should be taken. As we will do the structure part later, simultaneously we can recheck our estimates later, for now using these equations we can obtain an area for given terminal velocity which is about 3.14 m/s .

$$S = \frac{2 \times W}{\rho v^2 C_D}$$

$$d = \sqrt{\frac{4S}{\pi}}$$

where,

ρ being the density at 20 m.

d is the parachute diameter.

C_D being the projected one.

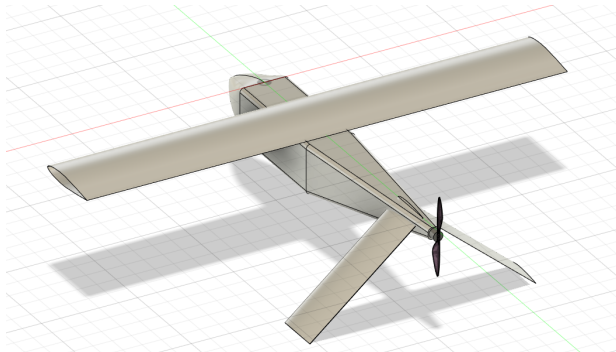
Defining a safe altitude is also required as we should keep our UAV safe ultimately and ensure we give enough margin to achieve that speed.

For our estimated terminal velocity of around 3.14 m/s, we are getting a diameter of around 3 m, assuming the C_D to be approximately 1.23 and projected C_D around 2.2. For getting the specifications regarding the volume and other parameters, we chose [42] and [43] Based on data available we finalized [42], the following table mentions the parameters related to this parachute.

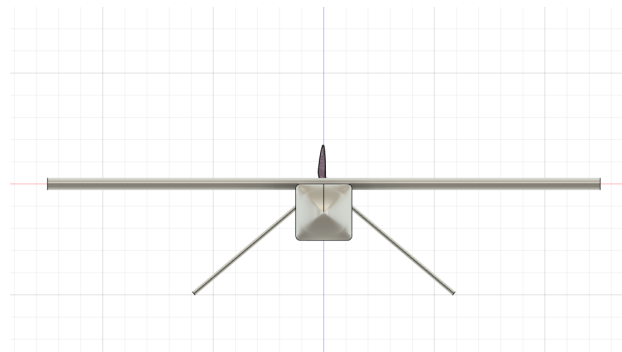
Parameters	Values in inches (")
Length/width	10"
Weight	950 gm
Packing volume	190 cu"
Y-harness length	5/8"
Pilot-chute rope	3/8"
Nylon shock cord	11/16"

Table 10.1: Parachute specifications

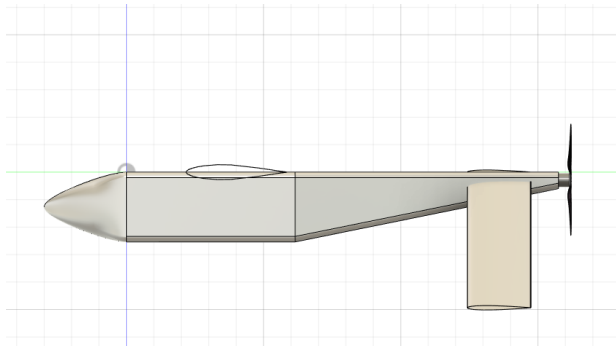
10.5 CAD Models:



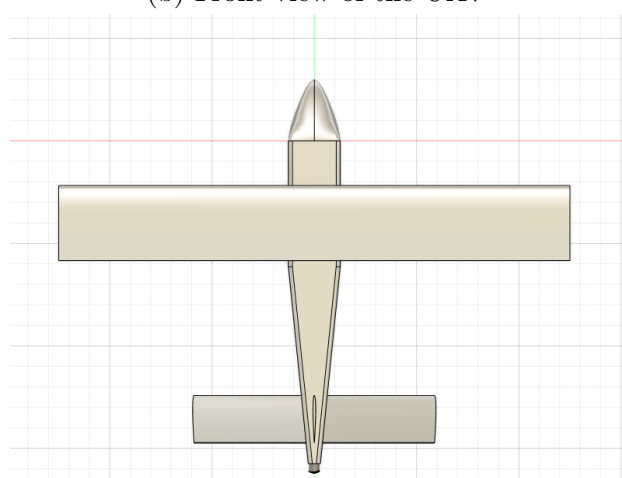
(a) Isometric view of the UAV



(b) Front view of the UAV



(c) Side view of the UAV



(d) Top view of the UAV

Figure 10.8: CAD model of the UAV design proposed

10.6 Summary

Landing System	Parachute system
Terminal velocity	3.14 m/s
Altitude of deployment	20 m
Time to land	6.69 s
Parachute selected	FIXED WING RECOVERY BUNDLE [42]

Table 10.2: Parachute specifications

Chapter 11

Internal Layout & CG Estimate

11.1 Introduction

The chapter is dedicated to justify the positioning of the Internal components and estimating the centre of gravity location of the UAV.

11.2 Internal Layout

11.2.1 Nose

- The nose was proposed to carry the Camera , Battery , ESC and Communications system for the UAV.
- The camera will be protruding out from the bottom.
- Communication, Battery and ESC are planned to be placed above the camera with a horizontal partition separating them.

11.2.2 Mid-Fuselage

The sole aim of Mid-Fuselage is to accommodate the Payloads, that are the Life jacket and GPS.

11.2.3 Rear Fuselage

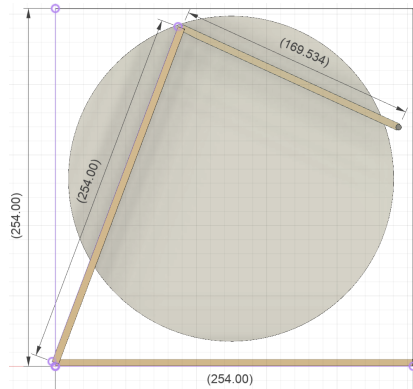
Rear fuselage accommodates motor & parachute.

1. Motor is placed here as we have pusher configuration and outside the fuselage as it is an Outrunner motor which requires to be placed outside of the body.
2. Rear fuselage was designed to have surplus space as the rest of the Fuselage is tightly packed. Parachute is attached to the top of the segment.

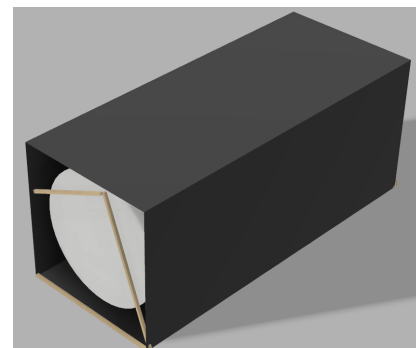
11.2.4 Payload-drop Mechanism

- The payload drop mechanism consists of a single door hinged at one end that opens the lower surface of the fuselage allowing the payload to fall out.
- The dimensions of the door are $615\text{ mm} \times 254\text{ mm}$.

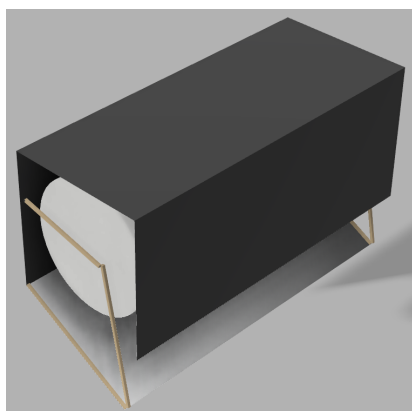
- The mechanism operating the door is essentially a four-bar linkage. Two linkages are provided, one at each end of the door.
- Each of the bars currently has a square cross-section with side length = 5 mm.
- A servo motor (rotary) will be provided at each end to operate the mechanism. The pivot point is shown in the figure about 82 mm below the top surface of the fuselage.
- The following figure shows the working of the mechanism as well as the dimensions of the links.



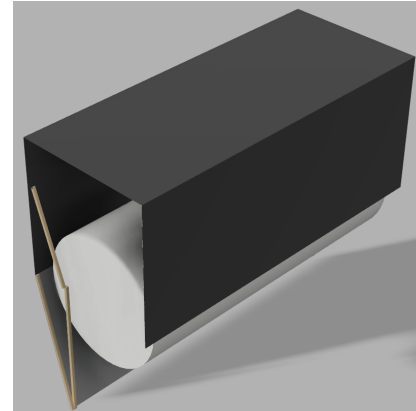
(a) Front view sketch



(b) Payload-drop Mechanism - 1



(c) Payload-drop Mechanism - 2



(d) Payload-drop Mechanism - 3

Figure 11.1: Payload-drop Mechanism

11.2.5 Access Doors

Apart from payload and parachute deployment doors, there are a bunch of doors provided within the UAV to give access to different components which will be helpful considering the maintenance. Also having doors at different locations makes the design redundant and also modular to some extent which is very beneficial to achieve in a complicated system like an UAV. We are planning to have access doors for the Nose

- Communications, Battery and camera : The upper portion of the nose will be attached through screws placing them inside the nose.

Apart from these the access and deployment doors for parachute and payload is the same, this is because they will be the ones used more frequently and relative to other components, so to reduce the failures due to operations we did this simplification.

11.2.6 Parachute deployment door

To deploy the parachute, a door is designed to be on the upper portion of the rear fuselage. As the parachute bundle will be mostly inside a cubical package with the pilot parachute being slightly out of this package, the door will be operated by a servo, the main idea is to use servo to remove a pin which would hold the door in the closed state, one servo is activated, the pin will be released and the gate will stay open, deploying the parachute. The door is planned to keep a little ahead of the centroid of the parachute bundle so that the parachute can be easily extracted. And has a circular shape as of now, which can be seen in the below figures.

11.3 CG Estimation

- It is assumed that the CG coincides with the centroid of the Component.
- Care was taken to place the components with their CG on the X axis in order to eliminate the roll moments due to the CGs having a Y component.
- CG was estimated by using the Weighted mean method where all the internal components and the Structural parts, that are wings , fuselage and tail are also considered

11.3.1 Structural Mass Approximation

Sheet thickness of **0.3 mm** was chosen for Al-6061 alloy to estimate the mass of the Fuselage, tail and wing. While the masses of spars, longerons, ribs and other structural supports were currently unknown, their contribution to mass of the component was accounted by an approximation of 40% mass of total structural weight and redistributed as,

- 20% of tail mass for structural components in tail.
- Difference between additional 40% structural mass and 20% tail mass was redistributed as 65-35 between fuselage and wing.

The Masses and the location of CG for structural components were obtained using the Features of Fusion360.

Structural Component	Stand alone Mass (g)	Overall mass (g)
Wing	1502	1894
Tail	594.5	713.5
Fuselage	1000	1728

Table 11.1: Structural Mass estimation

11.3.2 CG calculation

The following section involves calculation of CG using Eq.(11.1). The coordinates in the tables (11.4) were obtained by appropriately placing the components in CAD model and obtaining its location Fig.(11.2) .

$$X_{j|CG} = \frac{\sum m_i \cdot x_{i,j}}{\sum m_i} \quad (11.1)$$

Structural Component	X_{cg} (mm)	Y_{cg} (mm)	Z_{cg} (mm)
Wing	665.7	127	254
Tail	1,347	127	333.6
Fuselage	578	127	135.1

Table 11.2: CG location of Structural Components

here,

- $X_{j|CG}$ denotes the index notation for X , Y and Z center of gravity
- m_i denotes the mass of i^{th} component and $x_{i,j}$ denotes the j^{th} coordinate of i^{th} mass

It is to be noted that the distances were measured in the following manner,

- X distances were measured from the Nose tip.
- Y distances from the left side of Mid-Section of Fuselage.
- Z distances from the bottom of Mid-Section of Fuselage.

The WHITE-BLACK center mark shows the CG location of a component whereas the YELLOW-BLACK one depicts the CG location of the UAV.

Finally the CG location of the UAV and its coordinates are obtained and illustrated in Fig.(11.3)

Components	Mass (g)
Motor	172
Propeller	25
ESC	26
Battery	1008
Life Jacket	995
GPS	63
Parachute	950
Communication	300
Camera	340

Table 11.3: Components' Masses

11.3.3 CAD Figures

The model for the entire UAV is given in figure 10.8.

Components	X_{cg} (mm)	Y_{cg} (mm)	Z_{cg} (mm)
Motor & Propeller	1522	127	224
Battery & ESC	183	127	162
Life Jacket	607.5	127	127
GPS	607.5	127	127
Parachute	1042	127	230
Communication	263	127	147
Camera	183	127	32

Table 11.4: Components' CG location

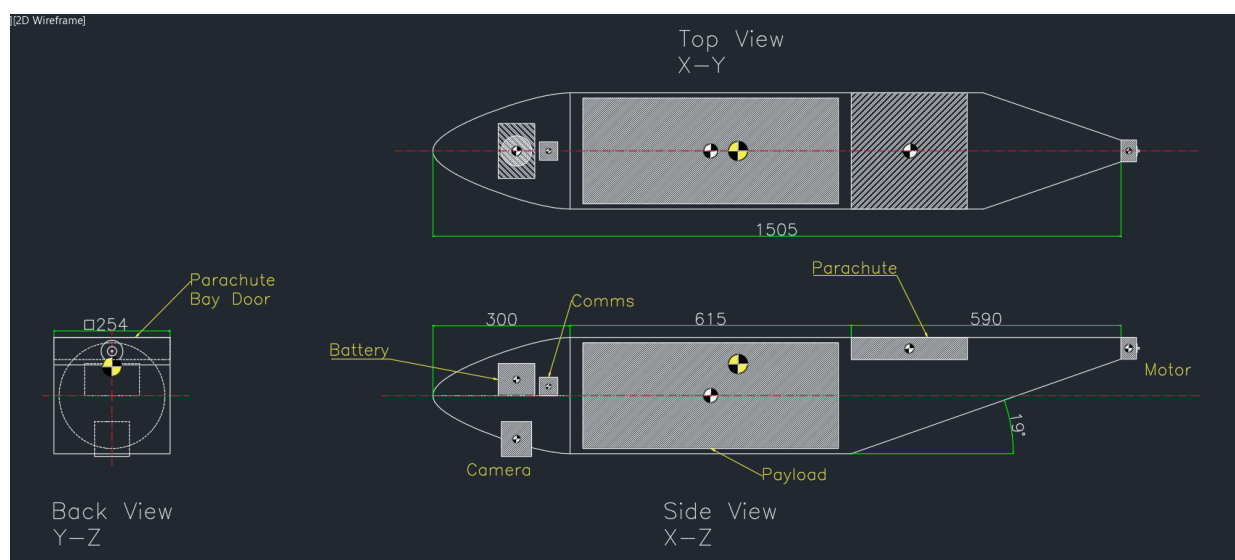


Figure 11.2: Three View diagram of Internal Layout and CG locations

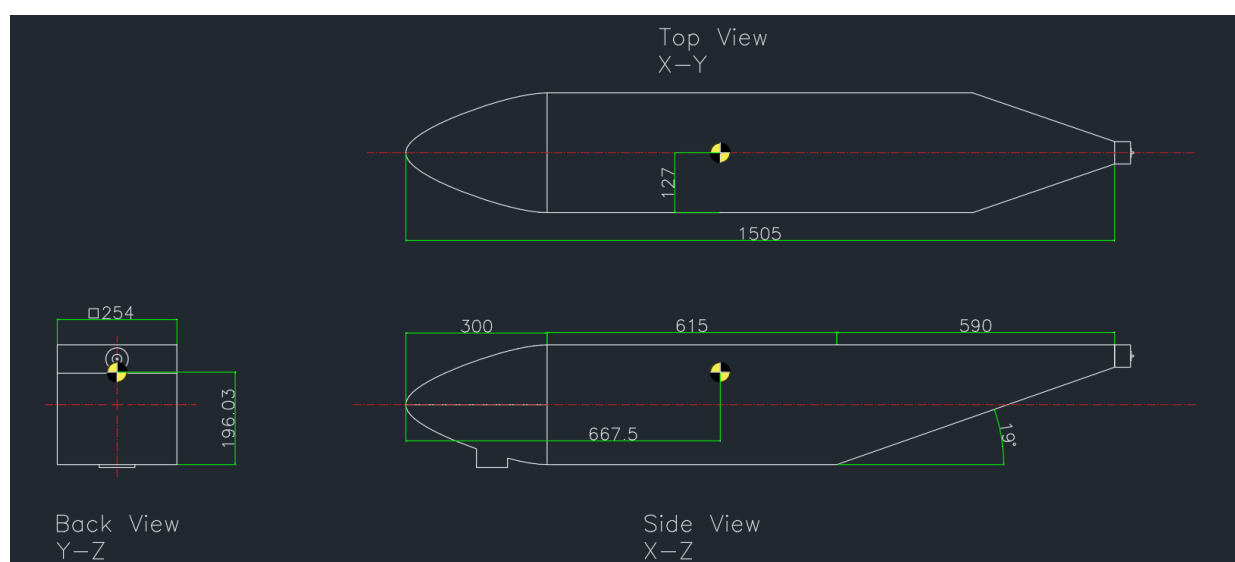


Figure 11.3: CG location

11.4 Summary

Parameters	Quantity
Internal Layout	Nose - Camera, Battery, ESC & Comms Mid-Fuselage - Life Jacket & GPS Rear Fuselage - Parachute & Motor
Payload Drop Mechanism	Single Bay door at the bottom of Mid-Fuselage
Sheet thickness	0.3 mm
Sheet Material	Al-6061
X_{cg}	667.5 mm
Y_{cg}	127 mm
Z_{cg}	196 mm

Table 11.5: Summary - Chapter 11

Chapter 12

Static Stability Analysis

This chapter details the static stability considerations for our aircraft. We analyse and modify our design after taking into account the stability requirements of the UAV.

Static stability: This refers to the initial tendency of the aircraft to return to its original equilibrium configuration upon the application of a disturbance.

Dynamic stability: This refers to the behaviour of the aircraft with time upon disturbance from its original equilibrium configuration.

Within stability analysis, we look into the following:

- Longitudinal static stability
- Directional static stability
- Lateral static stability

where directional static stability and lateral static stability are coupled and longitudinal static stability is independent of the other two.

12.1 Longitudinal Static Stability

For our symmetrical aircraft, the stability analysis may be decoupled into longitudinal and lateral-directional analysis. This section details the longitudinal static stability analysis which refers to the static stability of the pitching motion of the aircraft.[13]

The major contributors to aircraft pitching motion about the CG (centre of gravity) are:

- The wing: The wing pitching-moment contribution includes the lift through the wing aerodynamic center(ac) and the wing moment about the aerodynamic center.
- The tail (mainly horizontal tail): The long moment arm of the horizontal tail times its lift produces a very large moment that is used to trim and control the aircraft.
- The fuselage: The fuselage produces pitching moments which are influenced by the upwash and downwash produced by the wing (difficult to estimate).
- The engine:
 - One term is the thrust times the vertical distance from the CG.
 - Another term is the vertical force produced at the propeller disk due to the turning of the freestream airflow.

- The propwash will influence the effective angle of attack of the tail and possibly the wing. However, as we have opted for a pusher configuration, propwash will not be an influencing factor.

12.1.1 Static Pitch Stability and Neutral Point

- The expression to estimate the location of the neutral point is derived below. The notations and sign conventions shown in figure 12.1 are used.[13] The values are input as per our design.
- The net moment about the CG can be expressed as:

$$M_{CG} = L(X_{CG} - X_{acw}) + M_w + M_{fus} - L_h(X_{ach} - X_{CG}) - Tz_t + F_p(X_{CG} - X_p) \quad (12.1)$$

(Note: We have no flaps.)

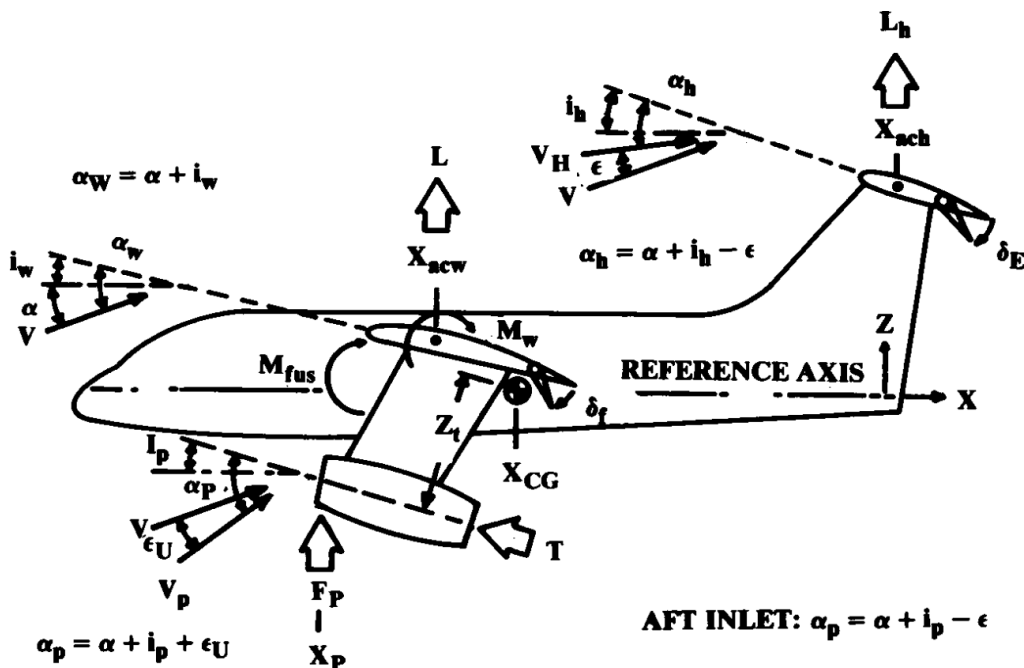


Figure 12.1: Forces acting on the aircraft.

- Simplifying this equation,

$$C_{m_{CG}} = C_L(\bar{X}_{CG} - \bar{X}_{acw}) + C_{m_w} + C_{m_{fus}} - \eta_h \frac{S_h}{S_w} C_{L_h}(\bar{X}_{ach} - \bar{X}_{cg}) - \frac{T}{qS_w} \bar{Z}_t + \frac{F_p}{qS_w} (\bar{X}_{CG} - \bar{X}_p) \quad (12.2)$$

where, $\eta_h = q_h/q$. η_h represents the ratio between the dynamic pressure at the tail and the freestream dynamic pressure. This ranges from about 0.85-0.95. We will assume $\eta_h = 0.95$.

- To analyse the static pitch stability, we analyse the derivative of the pitching moment coefficient. In this expression, the wing pitching moment and thrust terms are dropped as they are essentially constant with respect to angle of attack.

$$C_{m_\alpha} = C_{L_\alpha}(\bar{X}_{CG} - \bar{X}_{acw}) + C_{m_{\alpha_{fus}}} - \eta_h \frac{S_h}{S_w} C_{L_{\alpha_h}} \frac{\partial \alpha_h}{\partial \alpha} (\bar{X}_{ach} - \bar{X}_{CG}) + \frac{F_{p_\alpha}}{qS_w} \frac{\partial \alpha_p}{\partial \alpha} (\bar{X}_{CG} - \bar{X}_p) \quad (12.3)$$

- For longitudinal static stability, C_{m_α} must be negative, $C_{m_\alpha} < 0$, and $C_{m_{CG}}$ at zero angle of attack (C_{m_0}) must be positive, $C_{m_0} > 0$.

- Neutral point: The neutral point is defined as that location of the CG where the pitching moment is independent of the angle of attack ($C_{m_\alpha} = 0$). The neutral point \bar{X}_{np} represents neutral stability and is the most-aft CG location before the aircraft becomes unstable. From equation (12.3):

$$\bar{X}_{np} = \frac{C_{L_\alpha} \bar{X}_{acw} - C_{m_{\alpha_{fus}}} + \eta_h \frac{S_h}{S_w} C_{L_{\alpha_h}} \frac{\partial \alpha_h}{\partial \alpha} \bar{X}_{ach} + \frac{F_{p_\alpha}}{q S_w} \frac{\partial \alpha_p}{\partial \alpha} \bar{X}_p}{C_{L_\alpha} + \eta_h \frac{S_h}{S_w} C_{L_{\alpha_h}} \frac{\partial \alpha_h}{\partial \alpha} + \frac{F_{p_\alpha}}{q S_w}} \quad (12.4)$$

$$C_{m_\alpha} = -C_{L_\alpha} (\bar{X}_{np} - \bar{X}_{CG}) \quad (12.5)$$

- Static margin: The distance in percent MAC from the neutral point to the CG ($\bar{X}_{np} - \bar{X}_{CG}$).
- It is common to neglect the inlet or propeller force term F_p to determine "power-off" stability. Power effects are then accounted for using a static margin allowance based upon test data for a similar aircraft. Typically these allowances for power-on will reduce the static margin by about 4-10% for propeller aircraft. We will proceed by neglecting the propeller force terms.

$$\bar{X}_{np} = \frac{C_{L_\alpha} \bar{X}_{acw} - C_{m_{\alpha_{fus}}} + \eta_h \frac{S_h}{S_w} C_{L_{\alpha_h}} \frac{\partial \alpha_h}{\partial \alpha} \bar{X}_{ach}}{C_{L_\alpha} + \eta_h \frac{S_h}{S_w} C_{L_{\alpha_h}} \frac{\partial \alpha_h}{\partial \alpha}} \quad (12.6)$$

12.1.2 Lift coefficient slopes - Wing and Tail

- The lift coefficient slopes for the wing and the tail have been found from the graphs available for the corresponding airfoils.[1]
- We use Prandtl's classical lifting line theory to relate the three dimensional coefficients of lift and their variation to the two dimensional coefficients of lift.[9]

$$C_{L_\alpha} = \frac{C_{l_\alpha}}{1 + (C_{l_\alpha}/\pi AR)(1 + \tau)} \quad (12.7)$$

The value of τ is taken from the graph attached below.[10],[3]

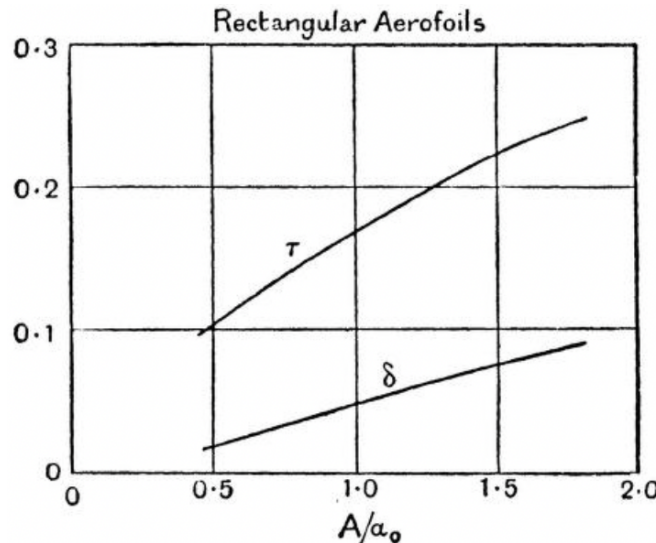


Figure 12.2: τ variation plot - A is the aspect ratio and $a_0 = C_{l_\alpha}$.

- For the wing, the airfoil is GA 35A015, $\tau = 0.18$:

$$C_{L_{\alpha_w}} = \frac{C_{l_{\alpha_w}}}{1 + (C_{l_{\alpha_w}}/\pi AR_w)(1 + \tau)} = 0.081/\text{deg} \quad (12.8)$$

- For the horizontal tail, the airfoil is NACA 0009, $\tau = 0.14$:

$$C_{L_{\alpha_h}} = \frac{C_{l_{\alpha_h}}}{1 + (C_{l_{\alpha_h}}/\pi AR_h)(1 + \tau)} = 0.086/\text{deg} \quad (12.9)$$

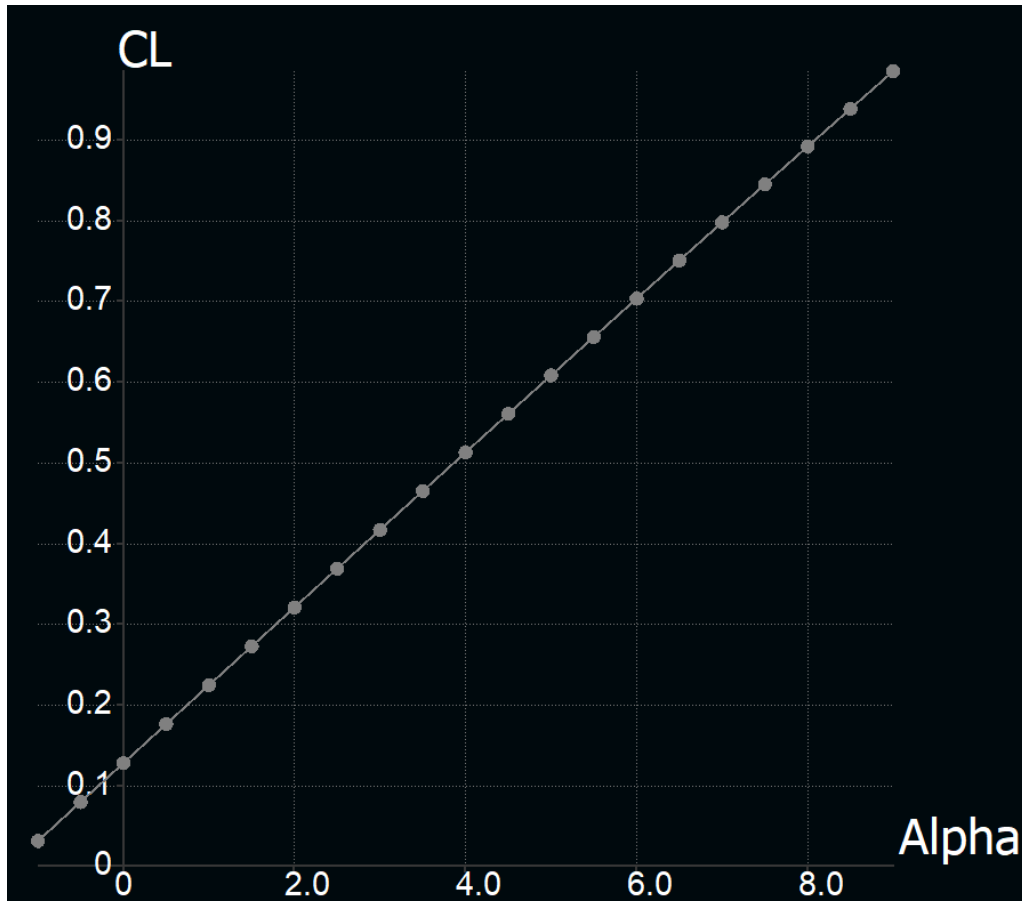


Figure 12.3: CL vs Alpha using XFLR5

12.1.3 Effect of the Fuselage

The pitching-moment contribution of the fuselage can be approximated using the following relation from NACA TR 711.

$$C_{m_{\alpha_{\text{fus}}}} = \frac{K_f W_f^2 L_f}{c S_w} / \text{deg} \quad (12.10)$$

where,

- K_f is the empirical pitching moment factor that may be obtained from the figure below. Using the online plot digitizer tool [3], $K_f = 0.013$.
- $W_f = 254 \text{ mm}$ is the maximum width of the fuselage.
- $L_f = 1875 \text{ mm}$ is the length of the fuselage.

Therefore,

$$C_{m_{\alpha_{\text{fus}}}} = 0.005 / \text{deg}$$

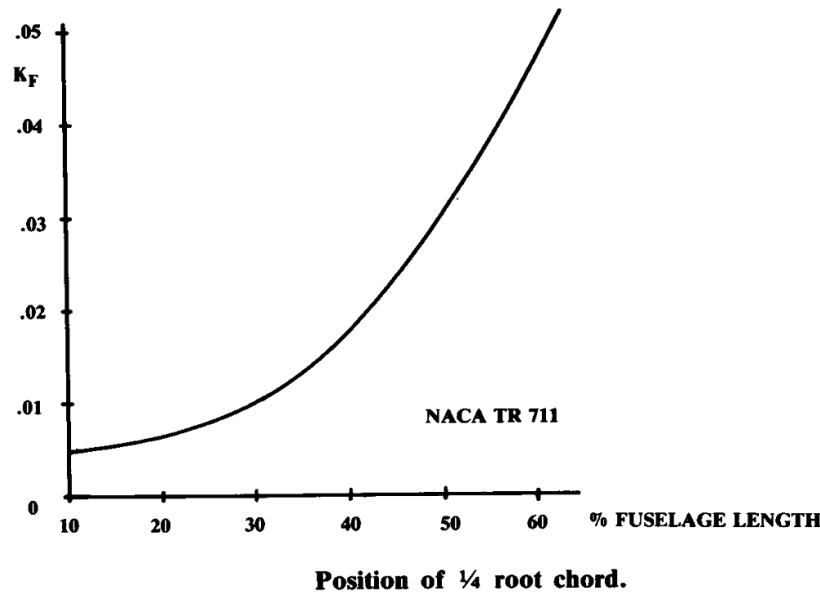


Figure 12.4: K_f vs. Position of 1/4 root chord

12.1.4 Effect of Downwash

- Downwash is defined as the downward deflection of an airstream by an aircraft wing due to wingtip vortices. Hence, the direction of flow incident on the tail differs from the direction of the freestream velocity by downwash angle ϵ . The downwash decreases the tail angle of attack.
- The change of the tail angle of attack with respect to the absolute angle of attack is as follows:

$$\frac{\partial \alpha_h}{\partial \alpha} = 1 - \frac{\partial \epsilon}{\partial \alpha} \quad (12.11)$$

- The change in the downwash angle with respect to the absolute angle of attack $\frac{\partial \epsilon}{\partial \alpha}$ can be estimated using figure 12.5. As the graph for our aspect ratio ($AR = 6.8172$) is not directly available, linear interpolation is used. The height of the tail as labelled in figure 12.5, $Z_t = 0$ for our aircraft. Therefore, $m = \frac{Z_t}{b/2} = 0$. As our design has no taper, taper ratio $\lambda = 1$. From the current fuselage dimensions, $r = \frac{l_t}{b/2} = 0.75388$. Using the plot digitizer software [3] and figure 12.5,

$$\frac{\partial \epsilon}{\partial \alpha} = 0.43$$

Therefore,

$$\frac{\partial \alpha_h}{\partial \alpha} = 1 - \frac{\partial \epsilon}{\partial \alpha} = 0.57$$

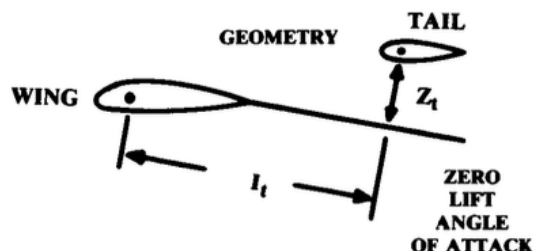
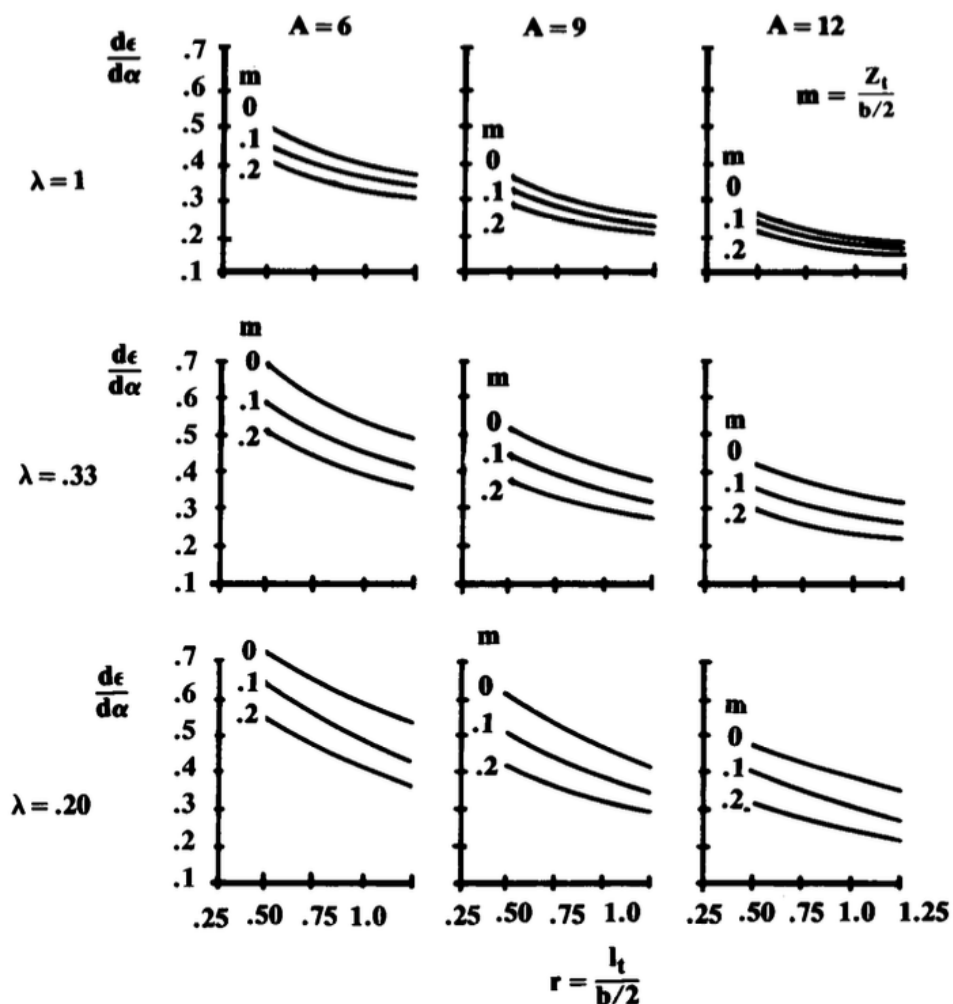


Figure 12.5: Downwash estimation

12.1.5 Tail contribution

For getting the tail contribution, we first of all need to know the configuration of it. **keeping in mind the analysis we changed the previous preference of the tail from an inverted Vee-tail to conventional one**, the reason is to keep analysis simple, also not much information is available regarding the V-tail specifically.

Summary of new tail design

Since we started the design for tail using conventional design as a base and use projection method to find dimensions for V-tail our previous calculations hold true for conventional tail design and the summary of all the tail parameters is given below.

Parameters	Estimated values
Airfoil	NACA 0009
S_h	0.24 m^2
AR_h	5.5
S_v	0.12 m^2
AR_v	1.8
λ_h	1
Λ_h	0°
λ_v	1
Λ_v	0°
b_h	1.14 m
c_h	0.21 m
b_v	0.47 m
c_v	0.26 m

Table 12.1: Summary

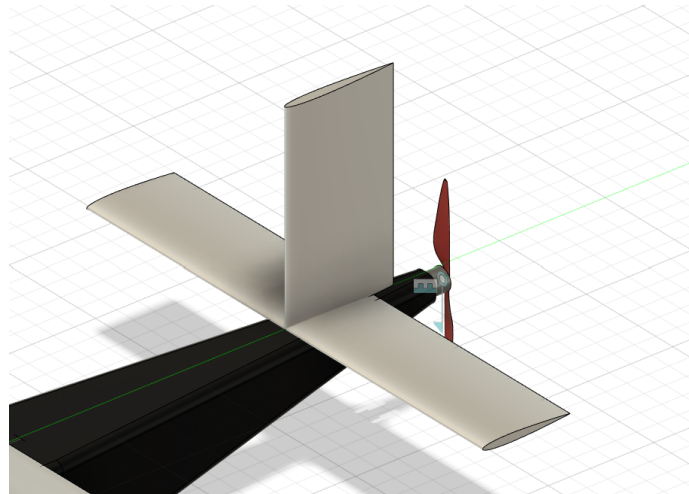


Figure 12.6: New tail CAD

For longitudinal stability

Regarding the longitudinal stability, the tail(horizontal stabilizer) being a significant contributor as discussed before. So to get the moment of the lift generated from the horizontal stabilizer we use the following equation

$$C_{M_{\alpha t}} = -Cl_{\alpha t} \left[\alpha \left(1 - \frac{\partial \epsilon}{\partial \alpha} \right) - (i_t + \epsilon_0) \right] \quad (12.12)$$

For lateral stability

In lateral direction, we have 2 moments which are roll and yaw moment, these come into picture when the aircraft faces a side-slip(β) which is taken positive in clockwise direction when seen from above. This β leads to a angle of attack for the vertical tail, based on the coefficients we'll look into specific cases and the response of the aircraft to them.

For yaw moment

considering positive side-slip, we get a lift force on the left hand side of the tail, which because of the long tail arm tries to rotate the aircraft in clockwise direction. This coefficient is defined as C_{N_β} which comes out to be positive as it tries to yaw about positive z-direction.



Figure 12.7: C_{N_β} plot

For roll moment

Considering positive side-slip as described before, we have lift force in left hand as the vertical tail has the centre of pressure off-centered with CG of the aircraft thus leading to roll moment, this vertical arm being small, the moment turns out to be negative it is defined as C_{L_β}

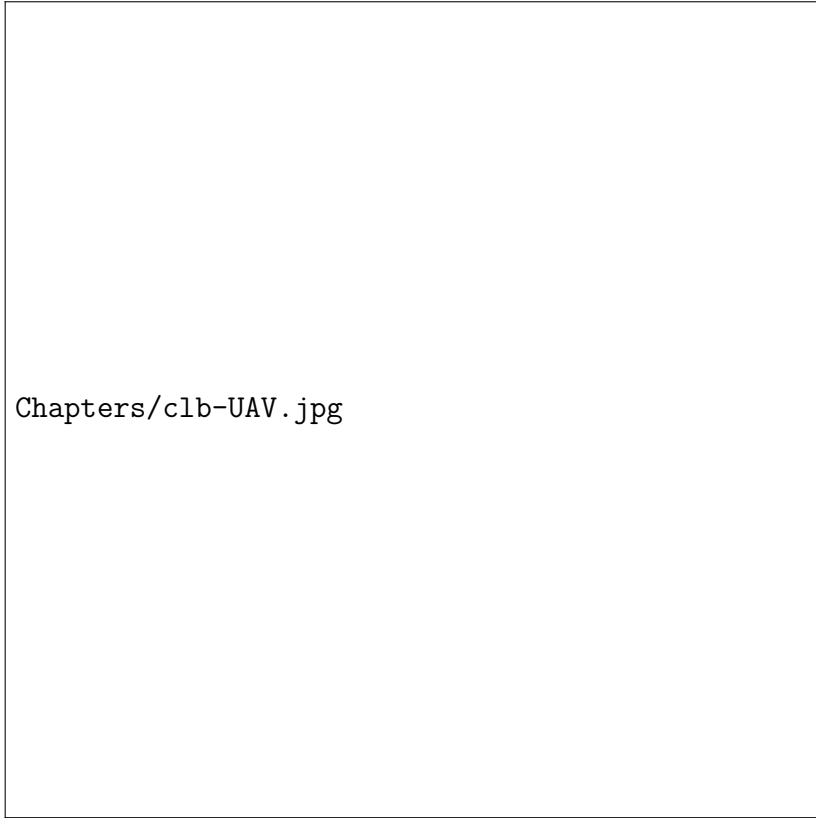


Figure 12.8: C_{L_β} plot

12.1.6 Neutral Point and Static Margin:

Using equation 12.6,

$$\bar{X}_{np} = 2.06$$

$$X_{np} = 755 \text{ mm}$$

The static margin,

$$\bar{X}_{np} - \bar{X}_{CG} = 8.63\%$$

From the simulations,

$$\bar{X}_{np} = 1.96$$

$$X_{np} = 717.4 \text{ mm}$$

The static margin,

$$\bar{X}_{np} - \bar{X}_{CG} = 13.65\%$$

The results from the analytical expression and the simulations are similar and we have a stable configuration. The deviations can be attributed to the assumptions and interpolations taken for the theoretical calculations.

- $C_{m_0} = 0.072$
- The slope $C_{m_\alpha} = -0.014 / \text{deg}$
- During steady state operation without any control input, $C_m = 0$ at $\alpha = 5.1^\circ$. For the airfoil selected for the wing, aerodynamic efficiency is maximum when $\alpha = 5.5^\circ$. Hence, during steady state cruise, without any control input, the aerodynamic efficiency is nearly maximum.

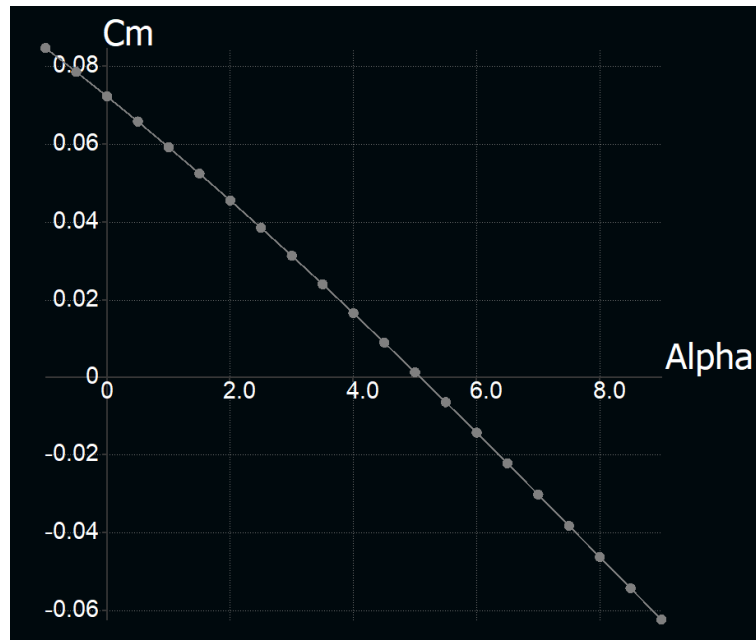


Figure 12.9: CM vs Alpha plot using XFLR5

12.2 Gust Strength:

Since our UAV operating environment is ocean, we need to consider the gust that our UAV might get exposed to and size our control surfaces so as to withstand the gust strength.

As per meteorology, gust is defined as the sudden increase in the wind speed above the average windspeed. More specifically, wind speed must temporarily peak above 16 knots (about 8.23 m/s) after accelerating by at least 9–10 knots (about 4.63 to 5.14 m/s) to qualify as a gust.

Based on the 40% rule of thumb as given in [2], the following table (12.2) shows the potential gust that we can expect for different average windspeeds.

Average Wind Speeds (Knots)	Gust Strength to be planned for (knots)	Wind warning
10	14	
15	21	
20	28	
26-33	36-45	Strong wind
34-47	48-65	Gale force
48-63	67-88	Storm force
64 or more	90 or more	Hurricane force

Table 12.2: Average wind speeds and the corresponding gust speeds

Now taking into consideration our mission profile as well as the size of our UAV, we are looking at a expected gust in the range of about 28 Knots, which corresponds to 14.5 m/s. The reason for considering this as the upper limit is because any higher value of gusts has a potential to even capsize a sailboats, so the values would be unrealistic.

Gust strength that should be planned for = 28Knots(about 14.5 m/s)

12.3 Horizontal and Vertical Control Surfaces

12.3.1 The Elevator

To stabilize the aircraft horizontally, elevator design is a must along with the tail design. And to design a elevator with high stabilize accuracy, the required parameter's approximate numerical value is needed.[14]

Most of the aircraft with high accuracy and performance, specially military aircraft maintain the unchanged value of elevator span-to-tail span ratio so that it may occur flow separation of entire flow passes through tail.

For deflection angle more than 20 to 25 degrees, may severely cause of loss elevator effectiveness. And a small deflection of elevator downward close to the horizontal stall, may invites the flow separation and loss of pitch control effectiveness.

For smaller and similar aircraft the geometrical parameters and properties remain unchanged. Such as, for Cessna 182 light aircraft with the weight of 1406 kgs, S_e/Sh is 0.38, C_e/Ch is 0.44 and deflection is (Down, Up=22,25).

To measure the fundamental requirement of elevator effectiveness, we need three non-dimensional derivatives:

$$C_{m_{\delta_E}} = \frac{\partial C_m}{\partial \delta_E} = -C_{L_{\alpha_h}} \eta_h \bar{V}_H \frac{b_E}{b_h} \tau_e \quad (12.13)$$

$$C_{L_{\delta_E}} = \frac{\partial C_L}{\partial \delta_E} = C_{L_{\alpha_h}} \eta_h \frac{S_h}{S_w} \frac{b_E}{b_h} \tau_e \quad (12.14)$$

$$C_{L_{h_{\delta_E}}} = \frac{\partial C_{L_h}}{\partial \delta_E} = \frac{\partial C_{L_h}}{\partial \alpha_h} \frac{\partial \alpha_h}{\partial \delta_E} = C_{L_{\alpha_h}} \tau_e \quad (12.15)$$

$C_{m_{\delta_E}}$ = aircraft pitching moment coefficient with respect to elevator deflection.

$C_{L_{\alpha_h}}$ = horizontal tail lift curve slope.

\bar{V}_H = horizontal tail volume coefficients

η_h = the ratio of horizontal tail dynamic pressure to freestream dynamic pressure.

τ_e = angle of attack effectiveness of the elevator.

$C_{L_{\delta_E}}$ = elevator deflection to aircraft lift

$C_{L_{h_{\delta_E}}}$ = elevator to tail lift

In general form, the typical values of elevator parameters are below:

- Elevator-to-tail planform area ratio (S_E/S_h) = 0.15 – 0.4
- Elevator chord-to-tail chord ratio (c_E/c_h) = 0.2 – 0.4
- Elevator span-to-tail span ratio (b_E/b_h) = 0.8–1
- Maximum up-elevator deflection ($-\delta_{E_{max}}$) = -25°
- Maximum down-elevator deflection ($\delta_{E_{max}}$) = $+20^\circ$

Since, our estimated H-Tail span is 1141.67 mm and chord is 207.45 mm. According to reference value, let's take the average value from above range for span and it is 0.9 and for chord length, the average value is 0.3

$$\frac{\text{Elevator span}}{\text{H-Tail span}} = 0.9$$

Elevator span = H-Tail span * 0.9 = 1027.503 mm

$$\frac{\text{Elevator chord}}{\text{H-Tail chord}} = 0.3$$

Elevator chord = H-tail chord * 0.3 = 62.245 mm

Hence, the elevator **length or span** is **1027.503 mm**.

And the elevator **width or chord length** is **62.235 mm**.

12.3.2 The Rudder

In the design of the rudder, four parameters must be determined:

1. Rudder area (S_R)
2. Rudder chord (C_R)
3. Rudder span (b_R)
4. Maximum rudder deflection ($\pm\delta_{R_{\max}}$)
5. location of inboard edge of the rudder (b_{R_i})

The aircraft side force is primarily a function of dynamic pressure, vertical tail area (S_V), and in the direction of the vertical tail lift (L_V):

$$L_V = qS_V C_{L_V} \quad (12.16)$$

where C_{L_V} is the vertical tail lift coefficient and is a function of vertical tail airfoil section, sideslip angle, and rudder deflection. The vertical tail lift coefficient is linearly modeled as

$$C_{L_V} = C_{L_{V0}} + C_{L_{V\beta}}\beta + C_{L_{V\delta_R}}\delta_R \quad (12.17)$$

The aircraft aerodynamic yawing moment is a function of dynamic pressure, wing area (S), and wing span (b), and is defined as

$$N_A = qSC_{n_b} \quad (12.18)$$

where C_N is the yawing moment coefficient and is a function of aircraft configuration, sideslip angle, rudder deflection, and aileron deflection. The yawing moment coefficient is linearly modeled as,

$$C_n = C_{n_o} + C_{n_\beta}\beta + C_{n_{\delta_A}}\delta_A + C_{n_{\delta_R}}\delta_R \quad (12.19)$$

The parameter $C_{n_{\delta_R}}$ is referred to as the aircraft yawing moment coefficient due to rudder deflection derivative and is also called the rudder yaw control power. The rudder yaw control effectiveness is mainly measured by the rate of change of yawing moment with respect to rudder deflection angle. In a non-dimensional form,

$$C_{n_{\delta_R}} = \frac{\partial C_n}{\partial \delta_R} \quad (12.20)$$

The directional control derivative ($C_{n_{\delta_R}}$) depends strongly on the vertical tail size, vertical tail moment arm, and is determined by:

$$C_{n_{\delta_R}} = -\frac{C_{L_\alpha} V^2 \eta_V \tau_r}{b_R b_V} \quad (12.21)$$

where $C_{L_\alpha} V$ denotes the vertical tail lift curve slope, V_V is the vertical tail volume coefficient, and η_V is the vertical tail dynamic pressure ratio ($\frac{q_V}{q_\infty}$). The parameter τ_r is referred to as the rudder angle of attack effectiveness parameter and is a function of rudder chord-to-vertical tail chord ratio ($\frac{C_R}{C_V}$). It is determined through Figure 12.12. The contribution of the rudder size to the rudder control effectiveness is reflected by the rudder angle of attack effectiveness τ_r . The vertical tail volume coefficient :

$$V_V = \frac{l_V S_V}{b_S} \quad (12.22)$$

In general form, the typical values of rudder parameters are below:

- Rudder volume to tail volume ratio (S_R/S_V) = 0.15 – 0.6
- Rudder span-to-vertical tail span ratio (b_R/b_V) = 0.8 - 1.0
- Rudder chord-to-vertical tail chord ratio (C_R/C_V) = 0.2 – 0.6
- Maximum rudder deflection ($\pm \delta_{R_{max}}$) = $\pm 30^\circ$

Since, estimated value of rudder span is 466.06 mm and chord length is 257 mm .

Let's consider the average value from range for the span and chord as well.

Rudder span-to-vertical tail span ratio (b_R/b_V) = 0.9

Rudder span = $466.06 * 0.9 = 419$ mm

Rudder chord-to-vertical tail chord ratio (C_R/C_V) = 0.4

Rudder chord = vertical tail chord * 0.4 = 103 mm

Finally, the rudder **span** is **419 mm**

And the rudder **chord length** is **103 mm**

12.4 Summary

Parameters	Value
$C_{L_{\alpha_w}}$	$0.081 \deg^{-1}$
$C_{L_{\alpha_h}}$	$0.086 \deg^{-1}$
$C_{m_{\alpha_{fus}}}$	$0.005 \deg^{-1}$
$\partial\epsilon/\partial\alpha$	0.43
$\partial\alpha_h/\partial\alpha$	0.57
C_{m_0}	0.072
C_{m_α}	$-0.014 \deg^{-1}$
X_{NP}	717 mm
X_{CG}	667 mm
Static Margin	13.65%
C_{l_β}	<0
C_{n_β}	>0
Gust Strength	28 knots
S_E/S_h	0.275
c_E	62.2
b_E	1027 mm
Elevator deflection	-25 deg , +20 deg
S_R/S_V	0.375
b_R	419 mm
c_R	103 mm
Rudder deflection	± 30 deg

Table 12.3: Summary : Stability

12.5 Tail parameters (updated)

Using the concepts of static stability we modified the dimensions of the tail which was earlier made using the data we gathered from similar air-crafts. The important quantity to be determined for getting the size of the tail, specially horizontal was the horizontal volume ratio in moment equation about y axis. The condition to get Vh was as follows

$$C_{M_\alpha} = 0.018 - 0.042Vh$$

and

$$C_{M_0} = 0.073Vh$$

So these were the two equations we got analytically from the moment equation. Choosing a reasonable value for the slope of the moment (C_{M_α}) can give us the value of V_h . For our UAV the value was $-0.012/\text{deg}$. which gave a V_h of 0.711, these lead to the following values

- $l_{ht} = 0.635 \text{ m}$
- $C_{ht} = 0.27 \text{ m}$
- $b_{ht} = 1.39 \text{ m}$
- $S_{ht} = 0.376 \text{ m}^2$

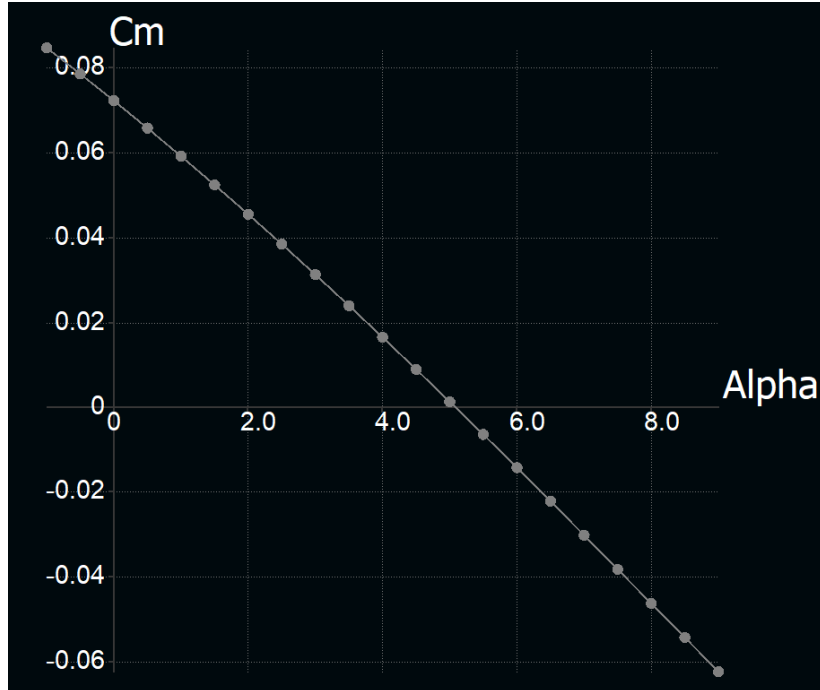


Figure 12.10: C_{M_α} updated plot

These are optimised values as the tail arm and area were linked together, thus we tried to get a value that gave us a reasonable static margin, which was about **13.6 %**. For the vertical tail parameters, we used the roll and yaw moment equations, them being coupled we tried to use simulations which lead to following trends. As there is no correct choice that has to be made here, any combination that satisfies the moment conditions keeping them under a certain limit can be used for the design purpose. That limit for C_{L_β} is from 0.02 to 0.1 and for C_{N_β} is -0.01 to -0.05 Further by using control surfaces, these can be brought into the range more accurately.

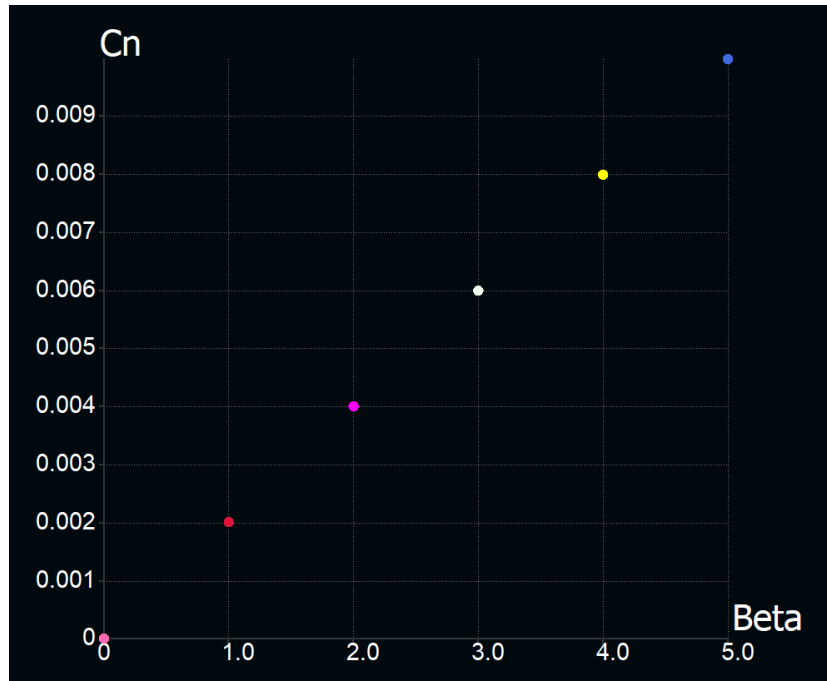


Figure 12.11: C_{N_β} updated plot

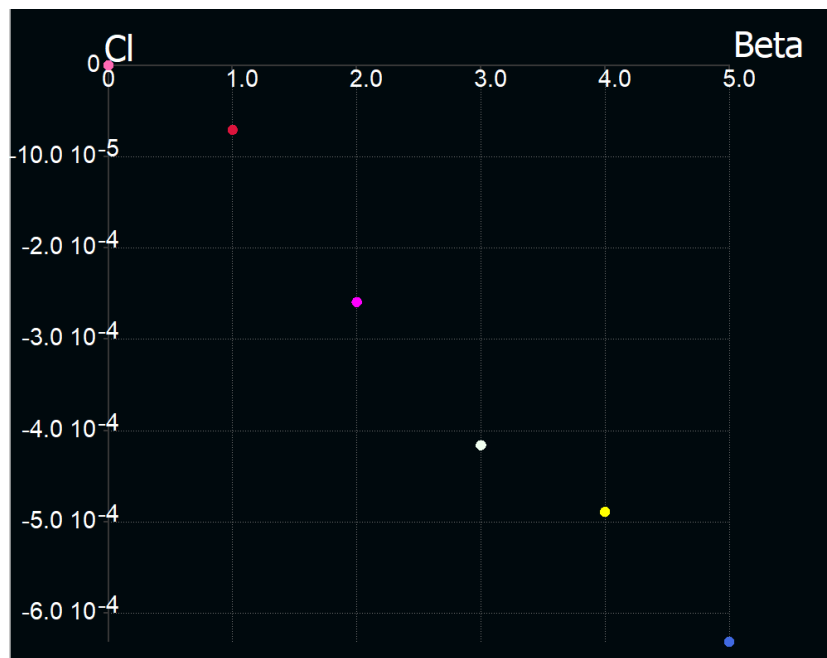


Figure 12.12: C_{L_β} updated plot

Chapter 13

Performance Analysis

This chapter details the theoretical performance parameters of the aircraft designed. At this stage, the configuration and the design has been fixed and only minute changes, if any, shall be made.

13.1 Parasite drag estimation:

There are two methods for estimating parasite drag.

1. Equivalent skin friction method.
2. Component build-up method.

In our report we will be using component build-up method to estimate the parasite drag. In this method parasite drag of each component is estimated using flat-plate skin friction coefficient (C_f) and the form factor (FF) that estimates pressure drag due to viscous separation.

$$C_{D_0} = \frac{\sum(C_{f_c} FF_c S_{wet_c})}{S_{ref}} \quad (13.1)$$

where subscript "c" indicates values for each component.

13.1.1 Skin friction coefficient:

The skin friction coefficient depends on mach number and Reynolds number. The skin friction coefficient for a laminar flow is given as:

$$C_{f,laminar} = \frac{1.328}{Re^{0.5}} \quad (13.2)$$

where,

$$Re = \frac{\rho v l}{\mu} \quad (13.3)$$

"l" is the characteristic length. For wing and tail it is the mean aerodynamic chord and for fuselage it is the total length. Skin friction coefficient for turbulent flow is given as:

$$C_{f,turbulent} = \frac{0.455}{(\log Re)^{2.58}(1 + 0.144M^2)^{0.65}} \quad (13.4)$$

As our UAV will be flying at 200m altitude and at 18 m/s velocity, the atmospheric condition's at this altitude are as follows:

- Density = 1.202 kg/m^3
- Temperature = 286.85K
- Viscosity (μ) = 0.00001806 Pa-s.

Another important factor affecting the skin friction drag is the extent to which UAV has laminar flow over its surfaces. Raymer([13]) mentions fuselage to have fully turbulent flow, while wings and tails have 10-20% of laminar flow. So the overall skin friction coefficient will be calculated as:

$$C_f = K_{laminar} C_{f,laminar} + (1 - K_{laminar}) C_{f,turbulent} \quad (13.5)$$

where, $K_{laminar}$ is the laminar fraction and is 0 for fuselage and 0.2 for wing and tail.

Component	Reynolds number	$C_{f,laminar}$	$C_{f,turbulent}$	C_f
Wing	4.39×10^5	0.002	0.005	0.0046
Fuselage	2.5×10^5	0.001	0.004	0.004
Horizontal tail	2.48×10^5	0.001	0.006	0.005
Vertical tail	3.08×10^5	0.0024	0.0056	0.005

Table 13.1: Skin friction coefficient

13.1.2 Wetted area(S_{wet}):

The wetted area for all the components are obtained from the three view diagrams and the CAD model of our UAV and is tabulated as follows:

Component	$S_{wet} (m^2)$
Wing	1.88
Fuselage	1.17
Horizontal tail	0.96
Vertical tail	0.49

Table 13.2: Wetted area

13.1.3 Form factor:

Form factor is used to estimate the pressure drag due to viscous separation. These are calculated based on empirical relations. For wing and tail the empirical relation used to estimate form factor is given as follows:

$$FF = \left(1 + \frac{0.6}{\left(\frac{x}{c}\right)_c} \left(\frac{t}{c} \right) + 100 \left(\frac{t}{c} \right)^4 \right) (1.34M^{0.38}(\cos \Lambda)^{0.28}) \quad (13.6)$$

For fuselage

$$FF = 0.9 + \frac{5}{f^{1.5} + \frac{f}{400}} \quad (13.7)$$

where,

$$f = \frac{l}{d} = \frac{l}{\sqrt{\frac{4}{\pi} A}} \quad (13.8)$$

The form factor for different components is shown below;

Components	Form Factor (FF)
Wing	3.53
Fuselage	3.53
Horizontal tail	4.09
Vertical tail	4.09

Table 13.3: Form factor

13.1.4 Final calculations:

Now that we have estimated the skin friction coefficient, wetted area and form factor for all the components, the overall parasite drag coefficient is computed as per equation (13.1).

Components	C_f	Wetted area (m^2)	Form factor(FF)
Wing	0.005	1.88	3.53
Fuselage	0.004	1.17	3.53
Horizontal tail	0.005	0.96	4.09
Vertical tail	0.005	0.5	4.09

Table 13.4: Component build-up for parasite drag calculation

So, the total parasite drag comes out to be,

$$C_{D_0} = 0.024$$

13.2 Drag Polar:

For plotting the drag polar, we require the Oswald's efficiency which is calculated based on the aspect ratio as per the following relation([7]):

$$e = 1.78(1 - 0.045AR^{0.68}) - 0.64 \quad (13.9)$$

Our UAV has aspect ratio of 6.82. The Oswald's efficiency factor based on this aspect ratio is

$$e = 0.844$$

The value of K can be evaluated based on the Oswald's efficiency factor as

$$K = \frac{1}{\pi e AR} \quad (13.10)$$

$$K = 0.055$$

Now, the drag polar equation can be written as :

$$C_D = 0.024 + 0.055 C_L^2 \quad (13.11)$$

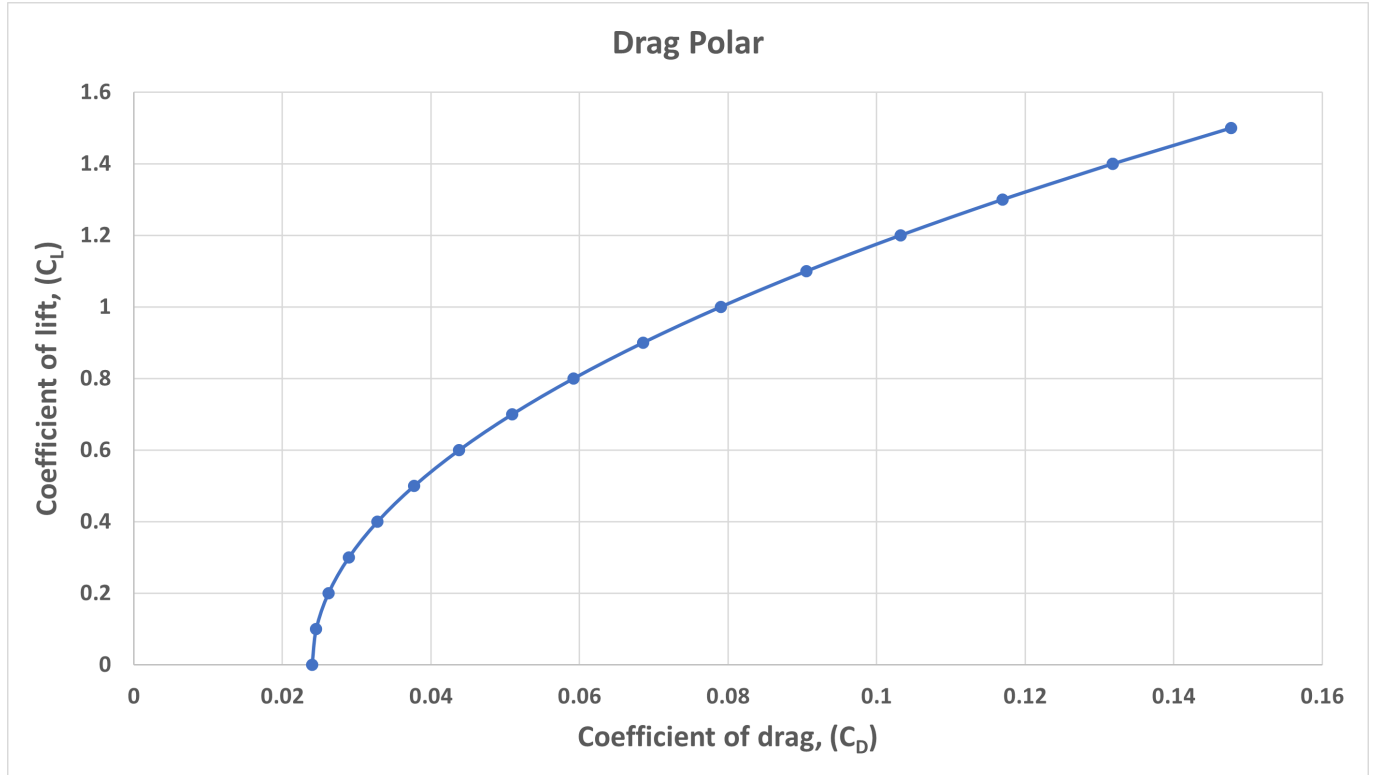


Figure 13.1: Drag Polar

13.3 The $V - n$ diagram

The greatest loads acting on the aircraft are the lift forces during maneuvers. We define the load factor n as the ratio of the lift acting on the aircraft to its weight to express the loads acting on the aircraft.

$$n = \frac{L}{W} \quad (13.12)$$

The $V - n$ diagram is used to define the maximum structural loads that the aircraft is designed to withstand. It is a plot of the load factor n against the velocity V . The aircraft may operate at all points within the curve defined. The code for the plot - 15.

- Given a velocity V , $n_{\max} = \frac{1}{2W} \rho V^2 S C_{L_{\max}}$
- Given a velocity V , $n_{\min} = \frac{1}{2W} \rho V^2 S C_{L_{\min}}$
- The positive and negative limits of the load factor restrict the coefficient of lift at which the aircraft may operate.
- For cruise or climb, the minimum load factor must be 1 ($L \geq W$).

- The aircraft maximum speed, or dive speed, at the right of the $V - n$ diagram represents the maximum dynamic pressure that the aircraft can structurally withstand. For our UAV, $V_{\max} = 20.35 \text{ m/s}$.
- Only the wing lift is considered in the diagram as the contributions from other components are small. For the maximum and minimum lift coefficients, we use the airfoil values since the values after correcting for 3D effects using theoretical equations give approximately the same results. Therefore,

$$C_{L_{\max}} = C_{l_{\max}} = 1.15 \quad (13.13)$$

$$C_{L_{\min}} = C_{l_{\min}} = -1.14 \quad (13.14)$$

- The density is taken as the density at cruise altitude, $\rho = 1.207 \text{ kg/m}^3$. This gives a safer envelope.

The limiting values for the load factor depend upon the expected use of the aircraft. The limits taken have been chosen from available data.[13]

$$n_{\text{positive}} = 3$$

$$n_{\text{negative}} = -1.5$$

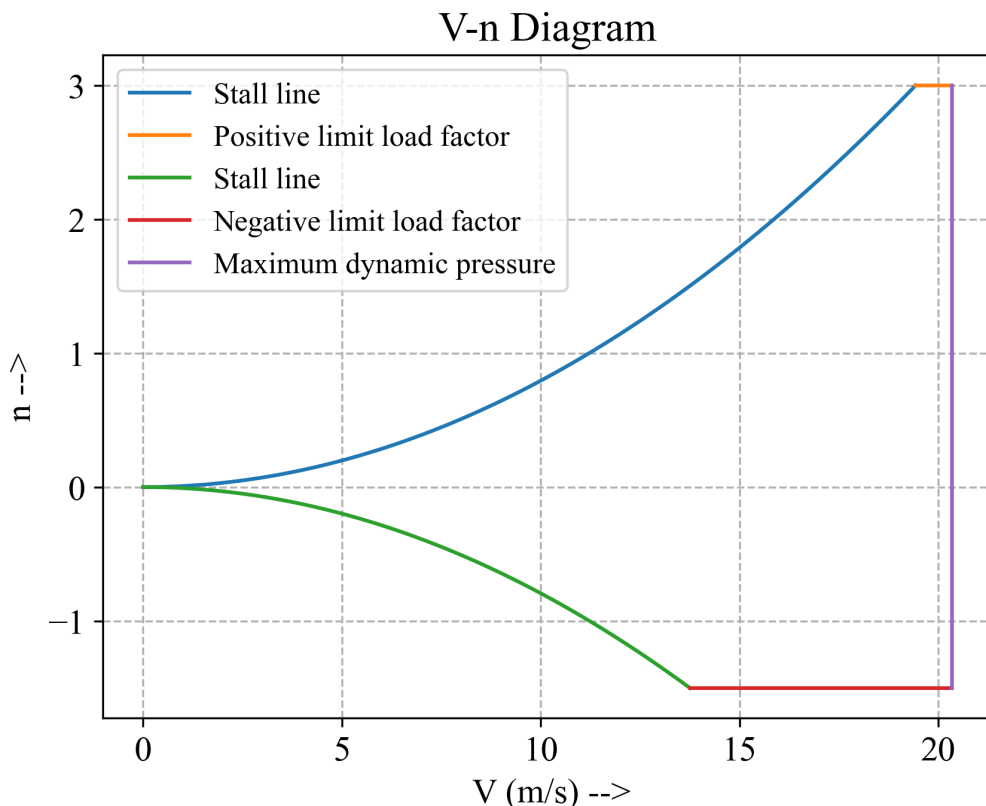


Figure 13.2: $V - n$ Diagram

13.4 Gust load diagram

The loads experienced when the aircraft encounters a strong gust can exceed the maneuver loads in some cases. When an aircraft experiences a gust, the effect is an increase (or) decrease in the angle of attack.

The change in angle of attack is approximately W_g divided by V .

$$\Delta\alpha = \tan^{-1} \left(\frac{W_g}{V} \right) \quad (13.15)$$

The change in lift is proportional to the gust velocity,

$$\Delta L = 0.5 \times \rho V S C_{L\alpha} W_g \quad (13.16)$$

The change in load factor is then

$$\Delta n = \frac{\Delta L}{W} = 0.5 \times \rho V \frac{S}{W} C_{L\alpha} W_g \quad (13.17)$$

The above equations are based on the assumption that an aircraft instantly encounters gust and that it instantly affects the entire aircraft. These assumptions are unrealistic.

Gusts tend to follow a cosine-like intensity increase as the aircraft flies through. To account for this a statistical "gust alleviation factor" (K) is applied to measured gust data (U_{de}). Hence $W_g = K \times U_{de}$. Where,

$$K = \frac{0.88\mu}{5.3 + \mu} \quad (13.18)$$

and

$$\mu = \frac{2(\frac{W}{S})}{\rho g c C_{l\alpha}} \quad (13.19)$$

We have considered standard gust data of 20 ft/s and 15 ft/s as given in [13].

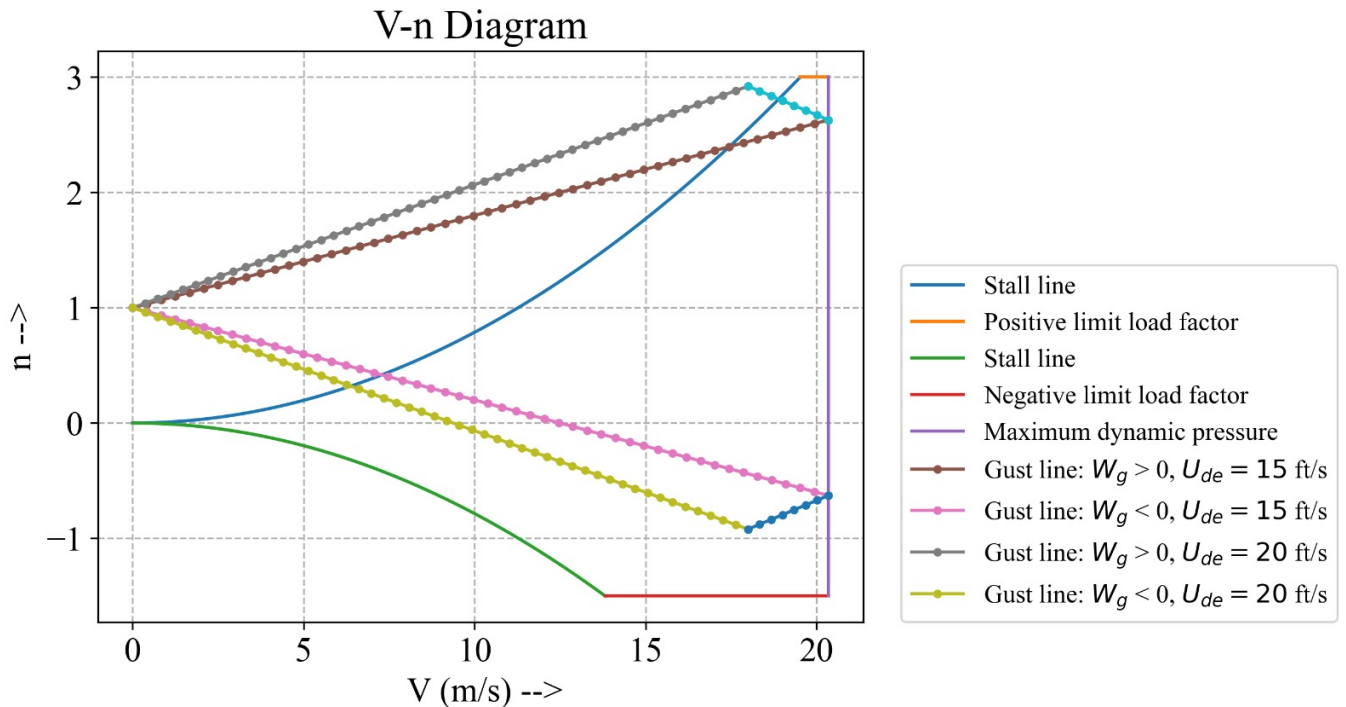


Figure 13.3: Flight Envelope

13.5 The Drag Bucket

$\frac{C_L}{C_D}$ vs C_L curve helps analyse the Regime of minimum power required to fly, the region corresponds to the peak of the curve where drag is minimum, this region is also called as 'The drag bucket' which corresponds to $\frac{C_D}{C_L}$ vs C_L curve. For our UAV the bucket lies in [0.3 - 0.6] C_L .

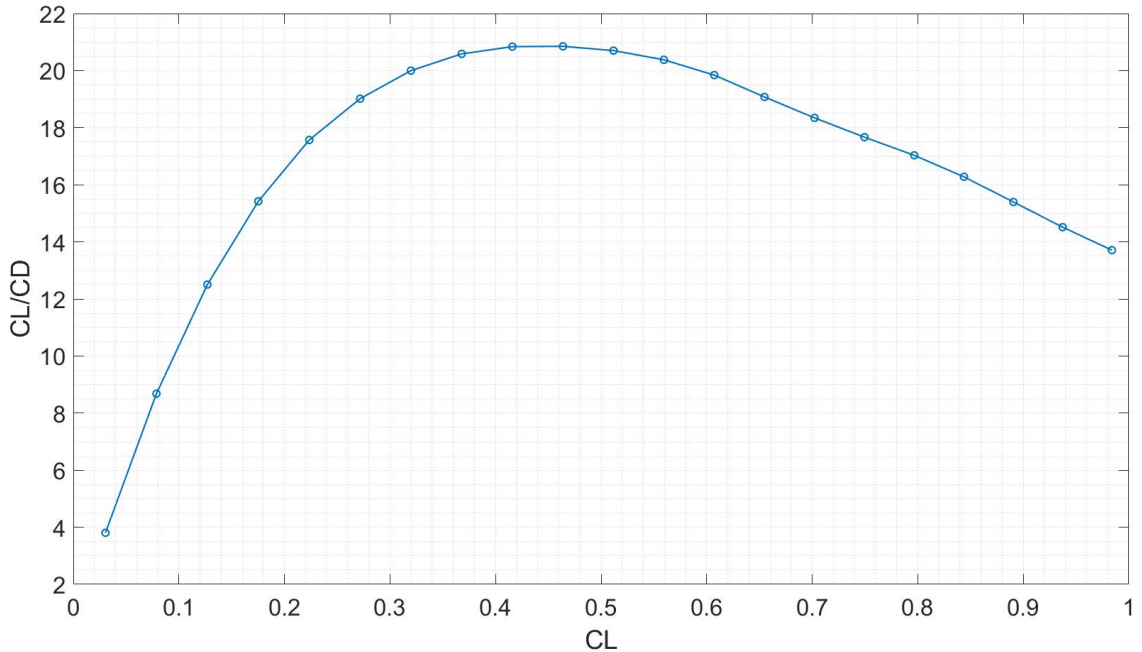


Figure 13.4: $\frac{C_L}{C_D}$ vs C_L

13.6 Power requirement

As we know before that that the power estimates help us to select the maximum and climb velocities and sometimes angle of take off and so on. The UAV being propelled by a propeller has the property of producing constant power even when the speed is changed(maintaining the same altitude). These can be some of the reasons why we need to check if the power requirements still satisfy, these can have a large impact on plane's performance and ultimately may lead to failure.

These are some aspects where the power calculations can be helpful to give us the insight of what we can achieve with the setup.

- Maximum velocity at cruise
- Rate of climb

Before proceeding further we would like to discuss the procedure as to how we are going to calculate the power requirements and further parameters from these values.

So previously the power requirements were taken from the mission profile, where we took the values based on the energy consumption in each stage and by making the assumption that the flight is steady we solved the equilibrium equations to get an estimate. In this estimate the skin friction drag was initially assumed based on the data and was finalised using analytical formulas during the weight estimation. Simultaneously using the equilibrium equations we were able to get energy required for each phase based on the geometry. Now as our information regarding the aircraft and the battery has improved we planned to use the following way to determine the power.

- Estimation of C_{D_0} using the contributions from different components ??
- Power estimation using the battery

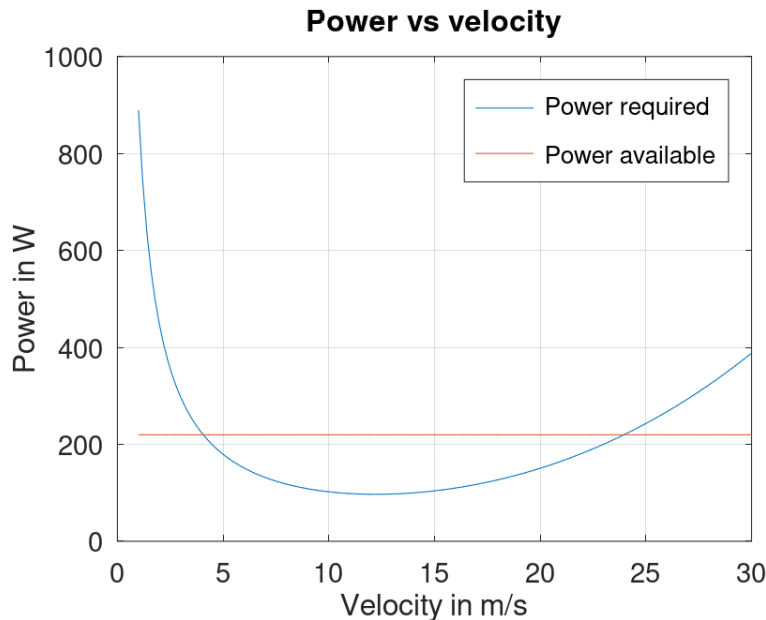


Figure 13.5: Power-velocity curve

13.6.1 Maximum velocity estimate

In order to get the maximum velocity in the cruise mode we did the following thing.

$$W = \frac{1}{2} \rho v^2 S C_L \quad T = \frac{1}{2} \rho v^2 S C_D \quad C_D = C_{D_0} + K C_L^2$$

For cruise, the available power(energy precisely) is obtained through the battery pack, for which we'll be using Li-ion cells in the order of 6 series and 4 parallels.(A being the Amp rating in Ah)

$$P = \Sigma V A = 4 \times 6 \times 3.7 \times 3.5 = 310.8 Wh$$

Thus giving us the power supplied by the battery, putting on the propeller efficiency we get

$$P_a = \eta P = 0.495 \times 310.8 = 153.85 Wh$$

Using the above equations, we can get the maximum cruise velocity. This will be the point at which the available power is same as that of the required power. This is shown in the below equation

$$153.85 = 0.5 \times 1.207 \times v^3 \times S \times C_D \times t_{cr}$$

This yields out the maximum velocity to be around **23 m/s**

13.6.2 Rate of climb

For rate of climb, the equation we use is as follows

$$ROC = \frac{P_a - DV}{W} = V \sin \alpha$$

Solving this equation analytically becomes a tough task so, the best way to get it could be a simulation, that will also help us in solving other parameters which are related to stability.

Chapter 14

Summary

14.1 Mission Profile

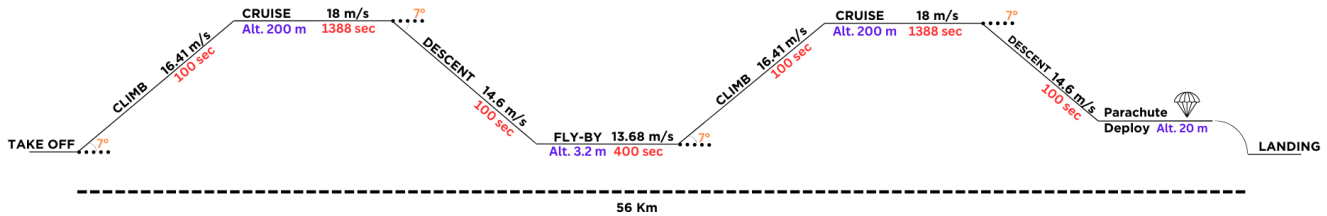


Figure 14.1: Mission Profile

14.2 Payload

Payloads	
Life-Jacket	As first response of safety
GPS	To pinpoint the location of Stranded person
Camera	To survey and search for those lost in Sea

14.3 Preliminary weight estimate

Preliminary weight estimation	
Parameter	Values
A	0.894172
L	-0.086047
Takeoff weight	12.1kg
Empty weight	8.76kg
Battery weight	1.88kg
Payload weight	1.5kg

14.4 Wing Loading

Wing loading estimate	
Parameter	Values
Cruise Velocity	18 m/s
Stall Velocity	12.22 m/s
Maximum velocity	22 m/s
Aspect ratio	7.21
Cruise altitude	200m
$C_{L_{max}}$	1.5
C_{D_0}	0.016
K	0.05
Wing loading	89 N/m ²
Wing area	1.07 m ²
Wing span	2.5m

14.5 Secondary weight estimate

Secondary weight estimate	
Parameter	Value
Takeoff weight	8.4kg
Payload weight	1.5kg
Battery weight	1.06kg
Energy requirement	316 Wh/kg
Maximum thrust required	25N
Wing area	0.92 m^2
Aspect ratio	6.8

14.6 Powerplant Description

Power-Plant	
Motor	MN4112-KV320
Propeller	16" × 5.4"
Propeller Efficiency (η_P)	0.478
ESC	2-6S , 40A
Battery	6S4P Li-ion

14.7 Wing Design

Wing	
Parameters	Value
Airfoil	GA 35A015
Position	High Wing
Distance of LE from Nose	509.5 mm
Span	2.5 m
Chord	0.3667 m
Taper ratio	1.0
Sweep angle	0.0°
Twist angle	0.0°
Dihedral angle	0.0°

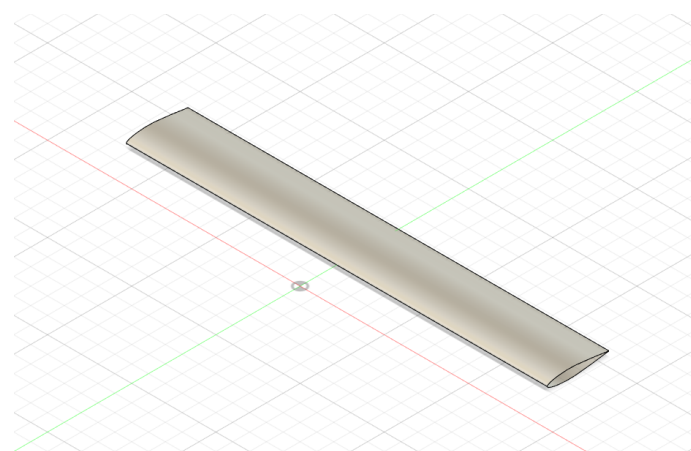


Figure 14.2: Wing

14.8 Fuselage Design and Tail Design

Fuselage Dimensions	
Parameters	Value
Nose Dimension	Length : 300 mm Cross section : $254 \times 254 \text{ mm}^2$ Shape - Conical
Mid-Fuselage Dimension	Length : 615 mm Cross section : $254 \times 254 \text{ mm}^2$
Rear Fuselage Dimension	Length : 590 mm Cross section : $254 \times 254 \text{ mm}^2$
Upsweep angle	19°
Overall Fuselage Length	1505 mm

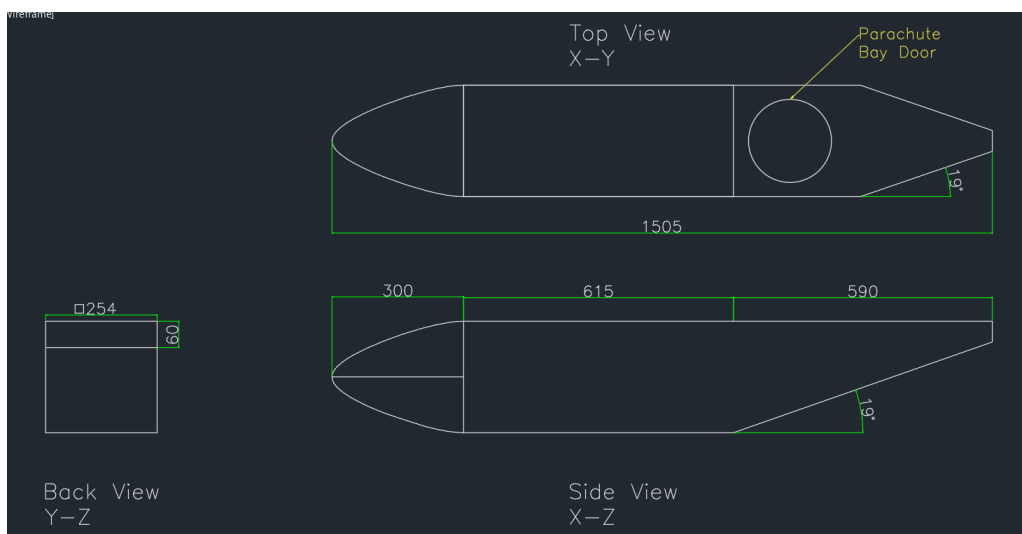


Figure 14.3: Fuselage

Tail	
Parameters	Values
Airfoil	NACA 0009
Distance of Tail LE from Nose	1542 mm
S_h	0.376 m^2
AR_h	5.16
S_v	0.12 m^2
AR_v	1.8
λ_h	1
Λ_h	0°
λ_v	1
Λ_v	0°
b_h	1.39 m
c_h	0.270 m
b_v	0.466 m
c_v	0.257 m

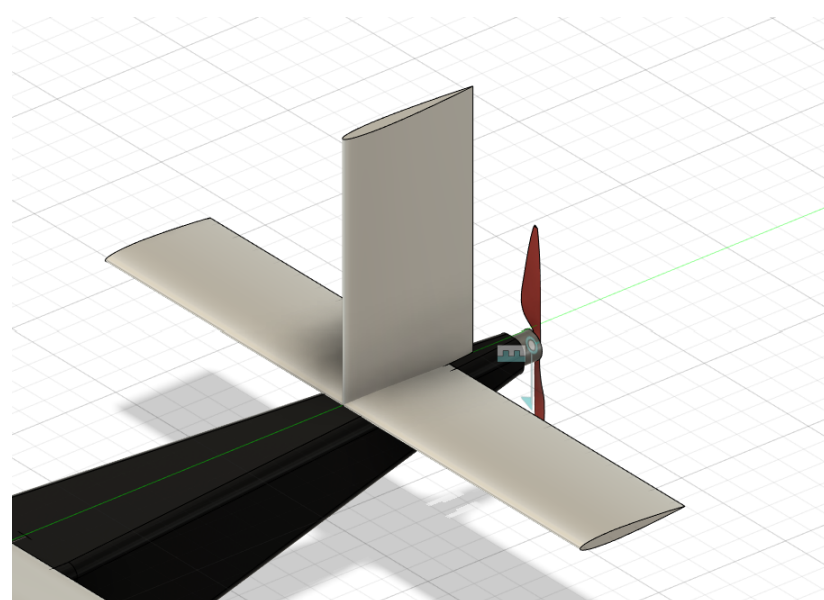


Figure 14.4: Tail

14.9 Internal Layout

Internal Layout	
Component	Position [(X,Y,Z) mm]
Camera	(183 , 127 , 32)
Battery & ESC	(183 , 127 , 162)
Communications	(263 , 127 , 147)
Life-jacket	(607.5 , 127, 127)
GPS	(607.5 , 127, 127)
Parachute	(1042 , 127 , 229.87)
Motor & Propeller	(1521.9 , 127 , 224)

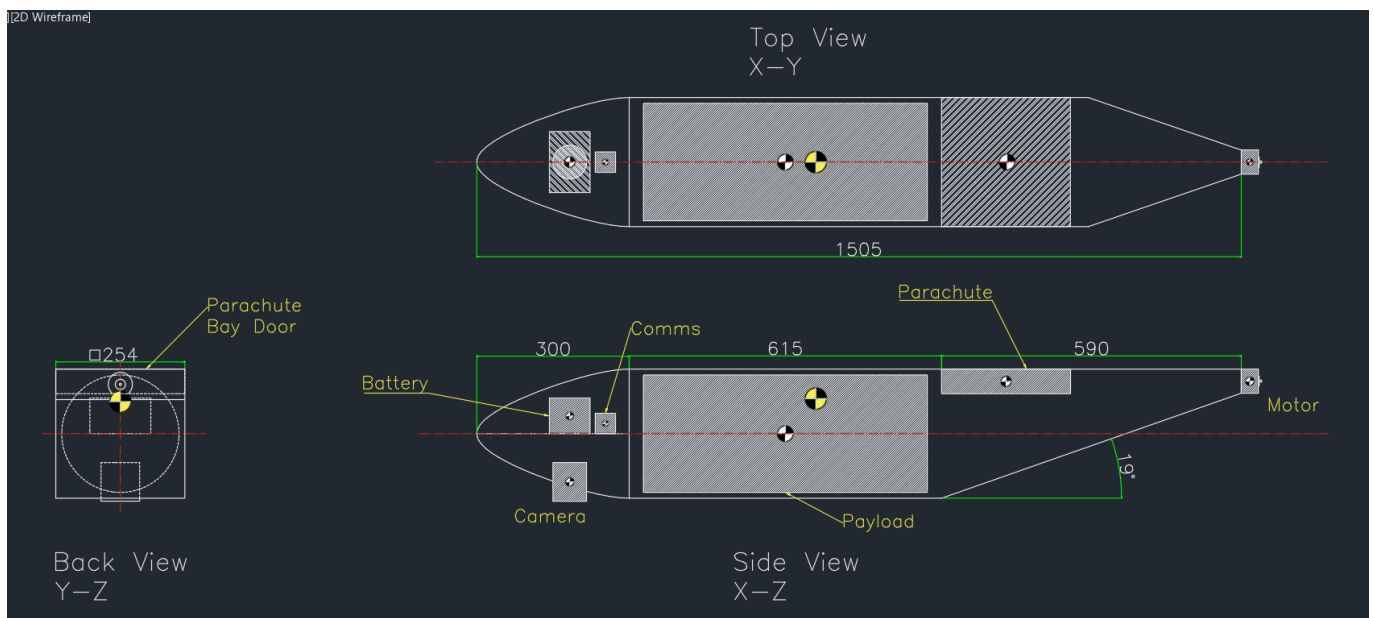


Figure 14.5: Internal Layout of Components

14.10 Takeoff and Landing Mechanisms

- Takeoff mechanism: Bungee catapult launch mechanism has been selected to launch our UAV.
- Parachute landing system: The landing mechanism chosen is a parachute landing system.
 - Altitude of parachute deployment = 20 m.
 - Terminal velocity = 3.14 m/s.
 - x - location upon landing = 2.5 m from deployment location.
 - Time to land = 6.69 s.
 - Parachute selected: FIXED WING RECOVERY BUNDLE [42]

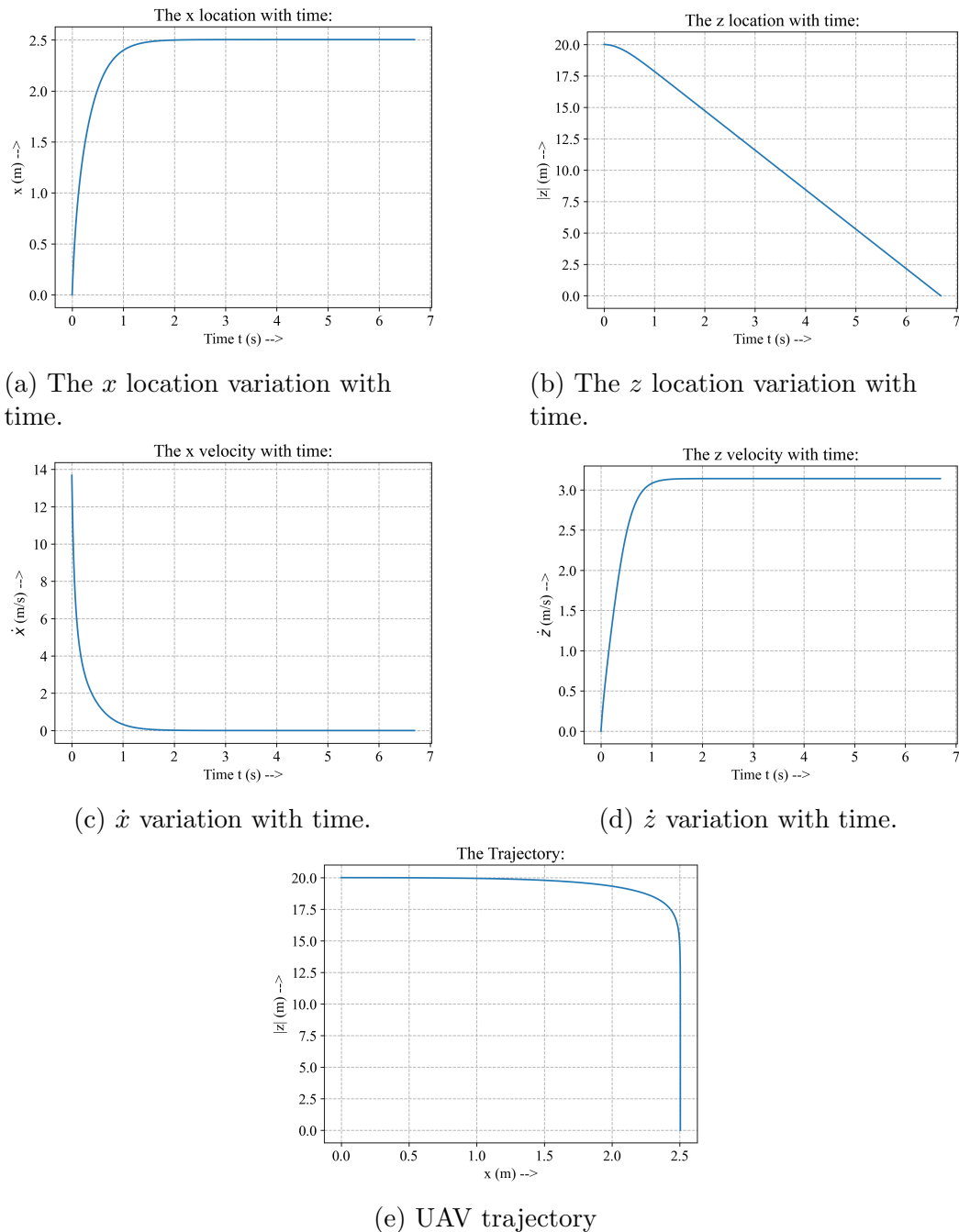


Figure 14.6: Parachute deployment - Two degree-of-freedom model results.

14.11 CG Location & Masses

To approximate the Structural mass, **Al6061** sheet material was used with thickness of **0.3 mm**.

The measurements are from :-

1. X : Measured from Nose-tip
2. Y : Port side of Mid-Fuselage
3. Z : Floor of Mid-Fuselage

CG Location	
Parameter	Distance (mm)
X_{CG}	668
Y_{CG}	127
Z_{CG}	196

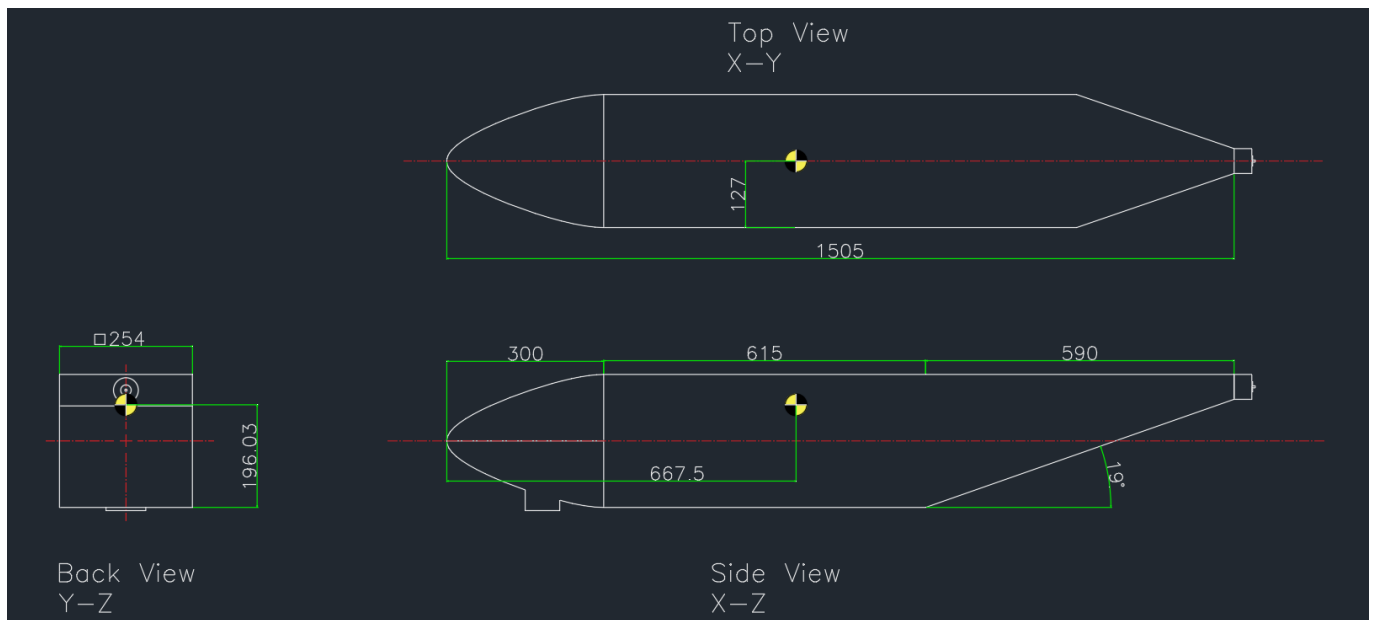


Figure 14.7: UAV CG location

Total Mass = 8215.33 grams

Mass Distribution : Structures	
Component	Mass (g)
Wing	1895
Horizontal Tail	451
Vertical Tail	262
Nose	519
Mid-Fuselage	864
Rear-Fuselage	346
Total Structural Mass	4336

Mass Distribution : Components	
Component	Mass (g)
Camera	340
Communications	300
ESC	26
Battery	1008
Life-Jacket	995
GPS	63
Parachute	950
Propeller	25
Motor	172
Total Component Mass	3879

14.12 Stability Analysis

Static Stability Analysis	
Parameters	Value
$C_{L\alpha_w}$	0.081 deg^{-1}
$C_{L\alpha_h}$	0.086 deg^{-1}
$C_{m\alpha_{fus}}$	0.005 / deg
$\delta\epsilon/\delta\alpha$	0.43
$\delta\alpha_h/\delta\alpha$	0.57
C_{m_0}	0.072
X_{NP}	717 mm
Static Margin	13.65%
C_{l_β}	<0
C_{n_β}	>0
Gust Strength	28 knots
S_E/S_h	0.275
c_E/c_h	0.3
b_E/b_h	0.9
Elevator deflection	-25 deg , +20 deg
S_R/S_V	0.375
b_R/b_V	0.9
c_R/c_V	0.4
Rudder deflection	± 30 deg

14.13 Performance Analysis

Performance parameters	
Parameter	Value
C_{D_0}	0.024
Oswald's efficiency, e	0.84
K	0.05
Max velocity	20.4 m/s
ROC	2.5 m/s

14.14 CAD model

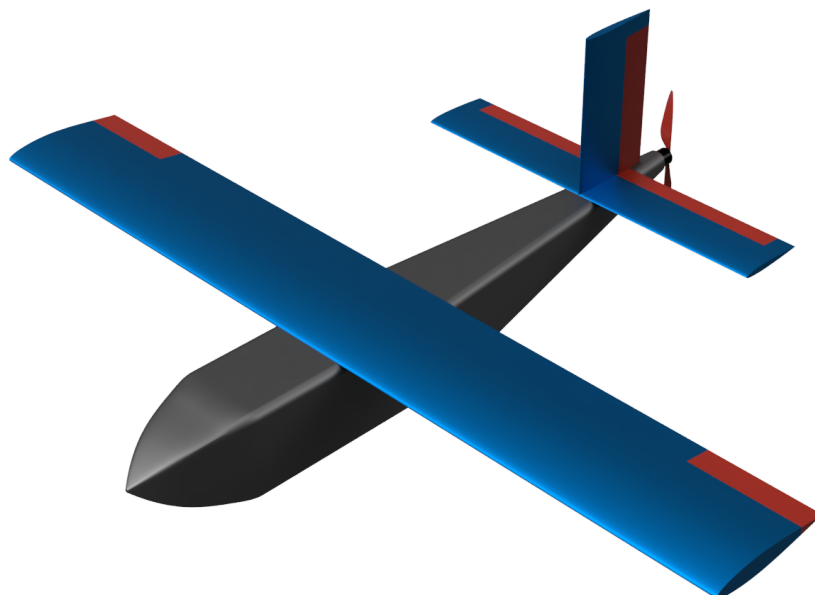


Figure 14.8: Isometric view of the UAV model

Bibliography

Website References

- [1] *BigFoil.com.* <https://bigfoil.com>.
- [2] *Gust reference.* <http://www.bom.gov.au/marine/knowledge-centre/reference/wind.shtml>.
- [3] *Plot Digitizer.* <https://apps.automeris.io/wpd/>.
- [4] *Sinking of MV Sewol - Wikipedia.* https://en.wikipedia.org/wiki/Sinking_of_MV_Sewol.
- [5] *Sweep Angle & Mach Angle relation.* <https://aviation.stackexchange.com/questions/88292/why-should-mach-wave-angle-be-less-than-wing-sweep-angle>.
- [6] *WHO.* <https://www.who.int/news-room/detail/drowning>.

Book References

- [7] Ö. Dündar et al./Engineering Science and Technology, an International Journal 23 (2020) 1182–1193.
- [8] L.W. Traub, Range and endurance estimates for battery-powered aircraft. J. Aircr. 48 (2) (2011) 703–707. doi: 10.2514/1.C031027.
- [9] J.D. Anderson. *Fundamentals of Aerodynamics*. McGraw-Hill Education, 2010. ISBN: 9780073398105. URL: <https://books.google.co.in/books?id=xwY8PgAACAAJ>.
- [10] H. Glauert. *The Elements of Aerofoil and Airscrew Theory*. Cambridge Science Classics. Cambridge University Press, 1983.
- [11] Snorri Gudmundsson. “Chapter 15 - Thrust Modeling for Propellers”. In: *General Aviation Aircraft Design (Second Edition)*. Butterworth-Heinemann, p. 624. ISBN: 978-0-12-818465-3. URL: <https://www.sciencedirect.com/science/article/pii/B978012818465300015X>.
- [12] Jr John D. Anderson. *Aircraft Performance and design*. McGraw-Hill.
- [13] Daniel P. Raymer. *2nd edition, Aircraft Design: A conceptual approach*.
- [14] Mohammad H Sadrey. *Table 4.2 (pg 127) , Aircraft design: A systems engineering approach*. 2012.
- [15] *SAR with UAV*. International Science Index, Marine and Environmental Sciences Vol:9, No:2, 2015 waset.org/Publication/10001953.

Image References

- [16] *Fig3.3R.* http://eng.chinamil.com.cn/CHINA_209163/WeaponryEquipment/News_209182/9328294.html.

UAV References

- [17] *Albatross UAV*. <https://www.appliedaeronautics.com/albatross-uav/>.
- [18] *AR1 TEKEVER*. <https://pdf.aeroexpo.online/pdf/tekever-ltd/ar1/183596-9086.html>.
- [19] *Atlas AS90X*. <https://www.c-astral.com/en/unmanned-systems/atlas-as90x>.
- [20] *Blackswift S2*. <https://bst.aero/black-swift-s2-uas/>.
- [21] *Bramor C4eye*. <https://www.c-astral.com/en/unmanned-systems/bramor-c4eye>.
- [22] *Deltaquad Pro*. <https://www.deltaquad.com/vtol-drones/view/>.
- [23] *MH900 Mav Tech*. <https://www.mavtech.eu/en/products/mh900/>.
- [24] *SQA eVTOL*. <https://www.c-astral.com/en/unmanned-systems/sqa-evtol>.
- [25] *V220 UAV*. <https://garuda.io/v220/>.

Battery & ESC References

- [26] *AIR 40A 2-6S Multi-Rotor UAV Drone ESC*. <https://store.tmotor.com/product/air-40a-6s-esc.html>.
- [27] *LG 18650 Li-ion cell*. <https://robu.in/product/lg-18650-mj1-3500mah-3c-li-ion-battery/>.
- [28] *Lithium batteries*. https://www.doitpoms.ac.uk/tlplib/batteries/batteries_lithium.php.

Gimbal References

- [29] *SIYI A2 mini*. <https://shop.siyi.biz/products/siyi-a2-mini>.
- [30] *SIYI A8 mini*. <https://shop.siyi.biz/products/siyi-a8-mini>.
- [31] *SIYI ZR 10*. <https://shop.siyi.biz/products/siyi-zr10>.
- [32] *Trillium Gimbal HD 25*. <https://www.trilliumeng.com/gimbals/hd25>.
- [33] *Trillium Gimbal HD 40*. <https://www.trilliumeng.com/gimbals/hd40>.
- [34] *Trillium Gimbal HD 45*. <https://www.trilliumeng.com/gimbals/hd45>.

Life Jacket References

- [35] *Solas Life Jacket*. <https://mustangsurvival.com/products/adult-4-one-solas-life-jacket-mv8040>.

Motor References

- [36] *MN4110 UAV Multi-Motor KV300/KV400*. <https://store.tmotor.com/product/mn4110-motor-navigator-type.html>.
- [37] *MN4112 UAV Multi-Motor KV320*. <https://store.tmotor.com/product/mn4112-motor-navigator-type.html>.

Propeller References

- [38] *Electric Propulsion System Sizing for Small Solar-powered Electric Unmanned Aerial Vehicle*. https://www.researchgate.net/publication/308329590_Electric_Propulsion_System_Sizing_for_Small_Solar-powered_Electric_Unmanned_Aerial_Vehicle.

- [39] *Propeller 16" x 5.4"*. https://store.tmotor.com/product/polish-carbon-fiber-16x5_4-prop.html.
- [40] *Propeller 16" x 8"*. <https://store.tmotor.com/product/ts16x8-prop-polymer-straight.html>.

Parachute References

- [41] *DJI Matrice 300 RTK – Drone Parachute System*. <https://www.aeromotus.com/product/dji-matrice-300-rtk-drone-parachute-system/>.
- [42] *Fruitychute*. <https://shop.fruitychutes.com/collections/fixed-wing-bundle/products/fixed-wing-recovery-bundle-44lbs-20kg-15fps>.
- [43] *Parachute Catalog*. <https://drive.google.com/file/d/1tRN5wuVD5FuG4vigv49o2hApgWr96n2j/view?usp=drivesdk>.
- [44] *Scorpion launch*. <https://www.elevonx.com/solutions/elevonx-scorpion/>.
- [45] *The Aerodynamics of Parachutes (Pages 27, 28)*. <https://apps.dtic.mil/sti/tr/pdf/ADA184620.pdf>.

Chapter 15

Appendix

2.A.1: Weight fraction and DTOW code

```
1 #Curve-fitting for Empty weight fraction VS. DTOW:  
2  
3 #Creating figures.  
4 f1=figure(); hold on;  
5 f2=figure(); hold on;  
6  
7 #Array of DTOW values:  
8 W0 = [2.4, 4.5, 5, 6.2, 9.5, 9.8, 10, 13.5]  
9  
10 #Array of empty weight fraction values:  
11 WeW0 = [0.875, 0.7777778, 0.7, 0.8064516, 0.7578947, 0.8673469, 0.56, 0.7777778]  
12  
13 #Vectors to store the values of log(W_0), log(W_e/W_0):  
14 v11=(log(W0))'  
15 v12=(log(WeW0))'  
16  
17  
18 ###Linear Regression Algorithm:  
19  
20 #Adding a column of all ones.  
21 mv11=[v11, [ones(8,1)]]  
22  
23 #Finding [L; log(A)].  
24 X=inv((mv11')*mv11)*(mv11')*v12  
25  
26 printf("L = %f \n", X(1))  
27 printf("A = %f \n", exp(X(2)))  
28  
29 #Compute the predicted values of log(W_e/W_0).  
30 y1=mv11*(X)  
31  
32 #Compute the predicted values of W_e/W_0.  
33 y = exp(y1)  
34  
35  
36 ###Plots:  
37  
38 #Plot of log(W_e/W_0) VS. log(W_0):  
39 figure(f1);  
40 scatter(v11, v12, 16, "filled")  
41 plot(v11,y1, "m")
```

```

42
43 #Making the legend.
44 legend({ "Aircraft Data", "Linear Regression"}, "location", "southwest")
45 grid on
46 #Titling the figure.
47 title("Empty Weight Fraction VS. DTOW")
48 #Labelling the axes.
49 xlabel("log(W_0) -->")
50 ylabel("log(W_e/W_0) -->")
51 set(gca, "fontsize", 10)
52 #Saving the plot.
53 print(f1, "-r500", "WeightFract_Linear.png")
54
55 #Plot of W_e/W_0 VS. W_0:
56 figure(f2);
57 scatter(W0, WeW0, 16, "filled")
58 plot(W0, y, 'm')
59
60 #Making the legend.
61 legend({ "Aircraft Data", "Model output"}, "location", "southwest")
62 grid on
63 #Titling the figure.
64 title("Empty Weight Fraction VS. DTOW")
65 #Labelling the axes.
66 xlabel("W_0 -->")
67 ylabel("W_e/W_0 -->")
68 set(gca, "fontsize", 10)
69 #Saving the plot.
70 print(f2, "-r500", "WeightFract.png")

```

2.A.2 Code for weight estimation

```
1 % The code for initial weight estimate
2 clc
3 clear all
4 w = zeros(100,1); # The array of W0 values
5 wb = zeros(size(w)(1),1); # The array to get the battery weight estimates
6 count=zeros(size(w)(1),1); # Counter
7 a = 0.894172; # from previous code
8 l = -0.086; # from previous code
9 w(1) = 8; # First weight guess
10 wp = 1.5; # Payload weight
11 wb(1) = 1.7277; # First battery weight guess
12 for i = 1:size(w)(1)
13     count(i)=i-1;
14     w(i+1) = wp/(1-[(wb(i)/w(i))+a*(w(i)^l)]);
15     # Derived fromt the weight fraction equation
16     [wb(i+1)] = tot_power (w(i+1));
17     # above step calculates the battery weight for each total weightS
18     if (abs(w(i+1)-w(i))<1e-6); # checks for convergence
19         disp("The final total weight is"),disp(w(i+1))
20         % Displays the final total weight of the battery
21         disp("The final battery weight is"),disp(wb(i+1))
22         % Displays the weight of battery based on the total weight w(i+1)
23         break
24     endif
25 endfor
26 plot(count(1:i,1), w(1:i,1), 'linewidth', 0.8, 'b');
27 set(gca , 'fontsize', 16);
28 title('Weight estimation');
29 xlabel('Iterations');
30 ylabel('Weight (Kg)');
31 legend('Weight');
32 grid on;
```

The function used to calculate power is mentioned below

```
1 % The code for total power calculation
2 function [P] = tot_power (w)
3     E = 145.7119368+(0.5774166*(w^2)) + (0.9479*(w^1.25)) +
4     (9.12966*(w^0.25)) + (0.053*(w^1.25)) + 0.343*(w^1.5) + (4.6884*(w^0.5));
5     # The E is the total energy consumption including all phases
6     P = E/160;
7     # 160 is the battery energy density
8 endfunction
```

3.A.1 Linear regression for L/D estimation

```
1 # This is the code for L/D max vs root(ARwet)
2 clc
3 clear all
4 AR = [2.132007164 2.015639336 1.469693846 2.070196678 1.206673363
5 2.4079742 1.145793457 1.886621541];
6 LD = [20.49313833 18.84778314 12.0417142 20.32570455 20.06377629
7 22.05813283 13.74679004 21.49744899];
8 k = size(LD)(2); # THe length of the vector
9 X = [AR; ones(1,k)]; # A vector of 2*9
10 #t This will do the regression to get the best fit line
11 # Using Gaussian elimination method to get m and c values
12 M = LD*(X')*inv(X*(X'));
13 Y = M*X;# The equation for best fit line
14
15 # creates uniformly distributed points for the values of AR and L/D
16 x = linspace(0.5,3,30);
17 y = linspace(10,30,30);
18 c = 17.348; # choosen L/D max value based on data
19 figure(1)
20 # Used to do scatter plot
21 scatter(AR,LD,'g','linewidth',1.2,'o')
22 hold on
23 # Plots the regression line
24 plot(x,M(1)*x+M(2),'m--','linewidth',1.2)
25 hold on
26 #Plots the choosen point
27 plot((c - M(2))/M(1),'rx','linewidth',1.5)
28 hold on
29 #plots the boundary lines
30 plot(1,y,'b.',2,y,'b.')
31 hold off
32 set(gca , 'fontsize', 11);
33 title('L/D vs sqrt{AR_{wet}}');
34 xlabel('sqrt(AR_{wet})');
35 ylabel('L/D max');
36 legstr = {'Data','Regression','Choosen point','lower limit','upper limit'};
37 legend(legstr,'location','southeast');
38 grid on
39 saveas(figure(1),'ldmax-ar.png')
```

4.A.1 Wing loading and Ceiling height calculations

```
1 # The file to get wing loading for all phases
2 function [L_st, L_m, Lc1, Lc2, L_lo, L_c, H] = wing_loading(Vst, Clm, Vm, Cd0,
3 K, P_W, g, LDm, Vc) # Using the above values
4 r0 = 1.225; # sea level density
5 # For (Vstall) wing loading
6 L_st = 0.5*r0*Vst^2*Clm;
7 # For cruise (max velocity) wing loading
8 Cl = sqrt(Cd0/K);
9 L_m = 0.5*1.207*Vm^2*Cl;
10 # For climb-1
11 Cl_c = sqrt(3*Cd0/K);
12 f = @(W_S) 2.302 - (sin(g)+1.1547/LDm)*sqrt(2*W_S/(r0*Cl_c)) ;
13 Lc1 = fzero(f,0.5)
14 # For climb-2 After payload drop
15 Cl_c = sqrt(3*Cd0/K);
16 f = @(W_S) 2.6266 - (sin(g)+1.1547/LDm)*sqrt(2*W_S/(r0*Cl_c)) ;
17 Lc2 = fzero(f,0.5)
18 # For Loiter
19 L_lo = 0.5*r0*Vc^2*Cl_c;
20 # For ceiling height
21 H = -6055.462*log(1/P_W)*sqrt(2*L_m/1.225)*[0.7436*Cd0*(pi*K)^0.75];
22 R = 287;
23 T = 298;
24 # For ceiling wing loading
25 rc = r0*exp(-9.81*H/(R*T)); # Ceiling density
26 Vch = sqrt(r0/rc)*Vc;
27 L_c = 0.5*rc*Vc^2*Cl;
28 endfunction
29 # [L_st, L_m, Lc1, Lc2, L_lo, L_c, H] = wing_loading(12.22,1.5,22,0.0157,
30 0.053,119*18,5*pi/180,17.35546,18)
```

5.A.1 Secondary Weight Estimate

```
1 #Weight Estimation:
2
3
4 #Importing libraries:
5 import sympy as sym
6 from scipy.optimize import fsolve
7 import numpy as np
8 import matplotlib
9 import matplotlib.pyplot as plt
10 import math
11
12
13 #Selecting the font size and type to be used in the figure.
14 font={ 'family' : 'Times New Roman',
15         'weight' : 'normal',
16         'size' : '14'}
17
18 #Setting the selected font properties.
19 matplotlib.rcParams('font', **font)
20
21
22 #Data for the aircraft:
23 AR = 5.84112
24 S = 1.07
25 LDmax = 16.54
26 CLmax = 1.5
27
28 #kg
29 W0 = 12.142
30 Wb1 = 0.048
31 W0_old = 1000
32 Wp = 1.5
33
34 n_prop = 0.478
35
36 e = 1.78*(1-0.045*(AR**0.68)) - 0.64
37 K = 1/(np.pi*e*AR)
38 CDO = 0.25/(K*LDmax*LDmax)
39 gamma = 5*np.pi/180
40
41 En_dens = 269.79 #Wh/kg
42
43 A = 0.894172
44 L = -0.086047
45
46
47 #Storage variables:
48 W0_iter = []
49 n_iter = []
50 i = 0
51
52
53 #To obtain the battery specifications:
54 def ret_Wb(W0):
55
56     W0 = W0*9.81 #Newton
57
58     #Climb-1:
59     v_c11 = 1.2*np.sqrt(2*W0/(1.225*S*CLmax))
```

```

60     L = W0*np.cos(gamma)
61     CL = 2*L/(1.225*S*v_cl1*v_cl1)
62     D = 0.5*1.225*S*v_cl1*v_cl1*(CDO + K*CL*CL)
63     T = W0*np.sin(gamma) + D
64     Pcl1 = T*v_cl1
65     Ecl1 = Pcl1*120/3600
66
67 #Cruise:
68 v_cruise = 18
69 CL = 2*W0/(1.207*v_cruise*v_cruise*S)
70 T = 0.5*1.207*v_cruise*v_cruise*S*(CDO + K*CL*CL)
71 Pcr = T*v_cruise
72 Ecr = Pcr*2700/3600
73
74 #Loiter:
75 v_loit = v_cl1
76 CL = 2*W0/(1.225*v_loit*v_loit*S)
77 D = 0.5*1.225*v_loit*v_loit*S*(CDO + K*CL*CL)
78 Ploit = D*v_loit
79 Eloit = Ploit*(540/3600)
80
81 #Climb-2:
82 W0 = W0 - 1.5*9.81
83 v_cl2 = 1.2*np.sqrt(2*(W0)/(1.225*S*CLmax))
84 L = W0*np.cos(gamma)
85 CL = 2*L/(1.225*S*v_cl2*v_cl2)
86 D = 0.5*1.225*S*v_cl2*v_cl2*(CDO + K*CL*CL)
87 T = W0*np.sin(gamma) + D
88 Pcl2 = T*v_cl2
89 Ecl2 = Pcl2*120/3600
90
91 #Descent:
92 Edes = Ecl1
93
94 #Total:
95 Etot1 = Ecl1 + Ecr + Eloit + Ecl2 + Edes
96
97 #Miscellaneous requirements:
98 Emis = 0.2*Etot1
99
100 #Final energy:
101 Ereq = 1.2*Etot1
102 Efinal = Ereq/n_prop
103
104 #Battery weight and number:
105 W_battery = Efinal/En_dens
106 Battery_number = math.ceil(W_battery/Wb1)
107 W_battery = Battery_number*Wb1
108
109 return W_battery, Battery_number
110
111
112 #Iterations for W0:
113 for j in range(3000):
114     if(i%10 == 0):
115         n_iter.append(i)
116         W0_iter.append(W0)
117
118     i = i + 1
119

```

```

120     W0_old = W0
121     Wb, nb = ret_Wb(W0)
122     W0 = Wp/(1 - (Wb/W0) - A*(W0**L))
123
124
125 #Output Block:
126 print("Final DTOW: " + str(W0) + " kg")
127 print("Final number of batteries: " + str(nb))
128 print("Final battery weight: " + str(Wb) + " kg")
129
130
131 #Plotting Block:
132 plt.plot(n_iter, W0_iter, '.-')
133 plt.title("Iterations for DTOW $W_0$")
134 plt.ylabel("DTOW $W_0$ (kg)-->")
135 plt.xlabel("Iteration number -->")
136 plt.grid(linestyle = "--")
137 plt.savefig("W0iter", dpi = 300, bbox_inches = 'tight')
138 plt.show()

```

6.A.1 Secondary Weight Estimate with Wing Loading Convergence

```
1 #Weight Estimation:
2
3
4 #Importing libraries:
5 import sympy as sym
6 from scipy.optimize import fsolve
7 import numpy as np
8 import matplotlib
9 import matplotlib.pyplot as plt
10 import math
11
12
13 #Selecting the font size and type to be used in the figure.
14 font={ 'family' : 'Times New Roman',
15        'weight' : 'normal',
16        'size' : '14'}
17
18 #Setting the selected font properties.
19 matplotlib.rc('font', **font)
20
21
22 #Data for the aircraft:
23 AR = 5.84112
24 S = 1.07
25 LDmax = 16.54
26
27 ###
28 CLmax = 1.5
29 v_cruise = 18
30
31 #kg
32 W0 = 12.142
33 Wb1 = 0.048
34 W0_old = 1000
35 Wp = 1.5
36
37 n_prop = 0.478
38
39 e = 1.78*(1-0.045*(AR**0.68)) - 0.64
40 K = 1/(np.pi*e*AR)
41 CDO = 0.25/(K*LDmax*LDmax)
42
43 gamma = 7*np.pi/180
44
45 En_dens = 269.79 #Wh/kg
46 b = 2.5
47
48 A = 0.894172
49 L = -0.086047
50 ###
51
52 #Storage variables:
53 W0_iter = []
54 n_iter = []
55 i = 0
56
57 #Function for wing loading:
```

```

58 def WingLoading(W0, CDO, K):
59
60     W0 = W0*9.81
61     CL = np.sqrt(CDO/K)
62     W_S = 0.5*1.207*v_cruise*v_cruise*CL
63     Sref = W0/W_S
64     Swet = 3*Sref
65     ARref = b*b/Sref
66     ARwet = b*b/Swet
67     LDmax = 5.339*np.sqrt(ARwet) + 9.0769
68
69     e = 1.78*(1-0.045*(ARref**0.68)) - 0.64
70     K = 1/(np.pi*e*ARref)
71     CDO = 0.25/(K*LDmax*LDmax)
72
73     return W_S, Sref, K, CDO
74
75
76 #To obtain the battery specifications:
77 def ret_Wb(W0, S, K, CDO):
78
79     W0 = W0*9.81 #Newton
80
81     #Climb-1:
82     v_c11 = 2/np.sin(gamma)
83     L = W0*np.cos(gamma)
84     CL = 2*L/(1.225*S*v_c11*v_c11)
85     D = 0.5*1.225*S*v_c11*v_c11*(CDO + K*CL*CL)
86     Tcl1 = W0*np.sin(gamma) + D
87     Pcl1 = Tcl1*v_c11
88     Ecl1 = Pcl1*100/3600
89
90     #Cruise:
91     v_cruise = 18
92     CL = 2*W0/(1.207*v_cruise*v_cruise*S)
93     T = 0.5*1.207*v_cruise*v_cruise*S*(CDO + K*CL*CL)
94     Pcr = T*v_cruise
95     Ecr = Pcr*2777.77/3600
96
97     #Fly-by:
98     v_flyby = 0.76*v_cruise
99     CL = 2*W0/(1.225*v_flyby*v_flyby*S)
100    T = 0.5*1.207*v_flyby*v_flyby*S*(CDO + K*CL*CL)
101    Pfb = T*v_flyby
102    Efb = Pfb*400/3600
103
104    #Climb-2:
105    W0 = W0 - 1.5*9.81
106    v_c12 = v_c11
107    L = W0*np.cos(gamma)
108    CL = 2*L/(1.225*S*v_c12*v_c12)
109    D = 0.5*1.225*S*v_c12*v_c12*(CDO + K*CL*CL)
110    T = W0*np.sin(gamma) + D
111    Pcl2 = T*v_c12
112    Ecl2 = Pcl2*100/3600
113
114    #Descent:
115    Edes = Ecl1
116
117    #Total:

```

```

118     Etot1 = Ecl1 + Ecr + Efb + Ecl2 + Edes
119
120     #Miscellaneous requirements:
121     Emis = 0.2*Etot1
122
123     #Final energy:
124     Ereq = 1.2*Etot1
125     Efinal = Ereq/n_prop
126
127     #Battery weight and number:
128     W_battery = Efinal/En_dens
129     Battery_number = math.ceil(W_battery/Wb1)
130     W_battery = Battery_number*Wb1
131
132     return W_battery, Battery_number, Ecl1, Ecr, Efb, Ecl2, Tcl1
133
134
135 #Iterations for W0:
136 for j in range(3000):
137     if(i%10 == 0):
138         n_iter.append(i)
139         W0_iter.append(W0)
140
141     i = i + 1
142
143
144     W0_old = W0
145     W_S, S, K, CDO = WingLoading(W0, CDO, K)
146     Wb, nb, Ecl1, Ecr, Efb, Ecl2, Tcl1 = ret_Wb(W0, S, K, CDO)
147     W0 = Wp/(1 - (Wb/W0) - A*(W0**L))
148
149
150 #Output Block:
151 print("\n \n \n")
152 print("Final DTOW: " + str(W0) + " kg")
153 print("Final number of batteries: " + str(nb))
154 print("Final battery weight: " + str(Wb) + " kg")
155
156
157 #Plotting Block:
158 plt.plot(n_iter, W0_iter, '.-')
159 plt.title("Iterations for DTOW $W_0$")
160 plt.ylabel("DTOW $W_0$ (kg)-->")
161 plt.xlabel("Iteration number -->")
162 plt.grid(linestyle = "--")
163 plt.savefig("W0iter", dpi = 300, bbox_inches = 'tight')
164 plt.show()

```

10.A.1 Parachute Landing Calculations

```
1 #Parachute landing calculations:
2
3 #Importing libraries:
4 import sympy as sym
5 from scipy.optimize import fsolve
6 import numpy as np
7 import matplotlib
8 import matplotlib.pyplot as plt
9 import math
10
11 #Selecting the font size and type to be used in the figure.
12 font={ 'family' : 'Times New Roman',
13         'weight' : 'normal',
14         'size' : '14'}
15
16 #Setting the selected font properties.
17 matplotlib.rc('font', **font)
18
19 #RK4 Method:
20 def RK4(fun, dt, X0):
21
22     f1 = fun(X0)
23     f2 = fun(X0 + 0.5*dt*f1)
24     f3 = fun(X0 + 0.5*dt*f2)
25     f4 = fun(X0+dt*f3)
26
27     X_out = X0 + dt*(f1 + 2*f2 + 2*f3 + f4)/6
28
29     return X_out
30
31 #Equations to solve:
32 def Equations(X):
33     dx = X[2]
34     dz = X[3]
35     ddx = -a*X[2]*np.sqrt(X[2]*X[2] + X[3]*X[3])
36     ddz = g - a*X[3]*np.sqrt(X[2]*X[2] + X[3]*X[3])
37     return np.array([dx, dz, ddx, ddz])
38
39 #Initializations:
40 X0 = np.array([0, -20, 13.68, 0]) #Initial conditions
41 g = 9.81
42 a = g/(3.14**2)
43 dt = 0.01
44 N = 670
45
46 X = np.zeros([4, N])#Storage matrix
47 t = np.zeros(N)
48 X[:, 0] = X0
49
50 for i in range(N-1):
51
52     t[i+1] = (i+1)*dt
53
54     Xout = RK4(Equations, dt, X0)
55     X[:, i+1] = Xout
56     X0 = Xout
57
58 #Plotting Block:
59 plt.plot(t, X[0])
```

```

60 plt.title("The x location with time:")
61 plt.ylabel("x (m) -->")
62 plt.xlabel("Time t (s) -->")
63 plt.grid(linestyle = "--")
64 plt.savefig("Xt", dpi = 300, bbox_inches = 'tight')
65 plt.show()
66
67 plt.plot(t, abs(X[1]))
68 plt.title("The z location with time:")
69 plt.ylabel("|z| (m) -->")
70 plt.xlabel("Time t (s) -->")
71 plt.grid(linestyle = "--")
72 plt.savefig("Zt", dpi = 300, bbox_inches = 'tight')
73 plt.show()
74
75 plt.plot(t, X[2])
76 plt.title("The x velocity with time:")
77 plt.ylabel("$\dot{x}$ (m/s) -->")
78 plt.xlabel("Time t (s) -->")
79 plt.grid(linestyle = "--")
80 plt.savefig("Xvelt", dpi = 300, bbox_inches = 'tight')
81 plt.show()
82
83 plt.plot(t, X[3])
84 plt.title("The z velocity with time:")
85 plt.ylabel("$\dot{z}$ (m/s) -->")
86 plt.xlabel("Time t (s) -->")
87 plt.grid(linestyle = "--")
88 plt.savefig("Zvelt", dpi = 300, bbox_inches = 'tight')
89 plt.show()
90
91 plt.plot(X[0], abs(X[1]))
92 plt.title("The Trajectory:")
93 plt.ylabel("|z| (m) -->")
94 plt.xlabel("x (m) -->")
95 plt.grid(linestyle = "--")
96 plt.savefig("Traj", dpi = 300, bbox_inches = 'tight')
97 plt.show()

```

13.A.1 $V - n$ Diagram

```
1 #V-n diagram:
2
3 #Importing libraries:
4 import sympy as sym
5 from scipy.optimize import fsolve
6 import numpy as np
7 import matplotlib
8 import matplotlib.pyplot as plt
9 import math
10
11 #Selecting the font size and type to be used in the figure.
12 font={ 'family' : 'Times New Roman',
13         'weight' : 'normal',
14         'size' : '16'}
15
16 #Setting the selected font properties.
17 matplotlib.rc('font', **font)
18
19
20 p = 1.207
21 S = 0.9168
22 Clmax = 1.1460
23 Clmin = -1.1441
24 W = 8.2153*9.81
25 Vmax = 20.35
26
27 Vp = np.sqrt(2*3*W/(p*S*Clmax))
28 Vn = np.sqrt(2*1.5*W/(p*S*abs(Clmin)))
29
30 V_list1 = np.linspace(0, Vp, 100)
31 V_list2 = np.linspace(Vp,Vmax, 100)
32 V_list3 = np.linspace(0, Vn, 100)
33 V_list4 = np.linspace(Vn,Vmax, 100)
34 n_list_pos1 = np.zeros(len(V_list1))
35 n_list_neg1 = np.zeros(len(V_list3))
36 n_list_pos2 = np.zeros(len(V_list2))
37 n_list_neg2 = np.zeros(len(V_list4))
38
39
40 for i, V in enumerate(V_list1):
41     n_list_pos1[i] = (0.5*p*Clmax*S*V*V/W)
42
43 for i, V in enumerate(V_list2):
44     n_list_pos2[i] = 3
45
46 for i, V in enumerate(V_list3):
47     n_list_neg1[i] = (0.5*p*Clmin*S*V*V/W)
48
49 for i, V in enumerate(V_list4):
50     n_list_neg2[i] = -1.5
51
52
53 #Plotting Block:
54 plt.plot(V_list1, n_list_pos1, label = "Stall line")
55 plt.plot(V_list2, n_list_pos2, label = "Positive limit load factor")
56 plt.plot(V_list3, n_list_neg1, label = "Stall line")
57 plt.plot(V_list4, n_list_neg2, label = "Negative limit load factor")
58 plt.plot([V_list2[-1], V_list4[-1]], [n_list_pos2[-1], n_list_neg2[-1]], label =
      "Maximum dynamic pressure")
```

```

59
60
61 #Gust load diagram:
62 Clalpha_wing = 4.6352
63 Wg = 0.55*0.3048*15
64
65 term = 0.5*p*Clalpha_wing*Wg
66 term0 = W/S
67 V = np.linspace(0, Vmax, 50)
68
69 n_pos = 1+term*V/term0
70 n_neg = 1 - term*V/term0
71
72 plt.plot(V, n_pos, '.-', label = "Gust line: $W_g$ > 0, $U_{de} = 15$ ft/s")
73 plt.plot(V, n_neg, '.-', label = "Gust line: $W_g$ < 0, $U_{de} = 15$ ft/s")
74
75 #####
76
77 Wg = 0.55*0.3048*20
78
79 term = 0.5*p*Clalpha_wing*Wg
80 V = np.linspace(0, 18, 50)
81
82 n_pos1 = 1+term*V/term0
83 n_neg1 = 1 - term*V/term0
84
85 plt.plot(V, n_pos1, '.-', label = "Gust line: $W_g$ > 0, $U_{de} = 20$ ft/s")
86 plt.plot(V, n_neg1, '.-', label = "Gust line: $W_g$ < 0, $U_{de} = 20$ ft/s")
87 plt.plot(np.linspace(V[-1], Vmax, 8), np.linspace(n_pos1[-1], n_pos[-1], 8), '.-')
88 plt.plot(np.linspace(V[-1], Vmax, 8), np.linspace(n_neg1[-1], n_neg[-1], 8), '.-')
89 #####
90
91 plt.title("V-n Diagram")
92 plt.ylabel("n -->")
93 plt.xlabel(" V (m/s) -->")
94 plt.grid(linestyle = "--")
95 plt.legend(fontsize = '12', loc = (1.05,0))
96 plt.savefig("VnDiagram", dpi = 300, bbox_inches = 'tight')
97 plt.show()

```

13.A.2 Re-estimation of power

```
1 # Power requirement plot
2 clc
3 clear all
4 v = linspace(1, 30, 150);
5 r = 1.207;
6 n = 0.495;
7 K = 0.055;
8 S = 2.5*0.3667;
9 CDO = 0.024;
10 Pa = 3.7*5*4*6*ones(1, size(v)(2)); # Power supplied by the battery in W
11 Pr = (0.5*r*(v.^3)*S).*[CDO .+ K*(2*9.65*9.8 ./ (r*(v.^2)*S)).^2];
12 plot(v,Pr)
13 hold on
14 plot(v,n*Pa)
15 set(gca , 'fontsize' , 14);
16 ylabel('Power in W')
17 xlabel('Velocity in m/s')
18 title('Power vs velocity')
19 legend('Power required','Power available')
20 grid on
21 hold off
22 saveas(figure(1), 'power-analysis.png')
```

Contributions

Week 1:

- Section 1: Reva, Bhavesh
- Section 2: Reva
- Section 3.1, 3.2 - Vinay
- Section 3.3 - Chinmay, Sarwar
- Section 4 - Akash

Week 2:

- Section 2.1 : Akash
- Subsection 2.2.1 : Reva
- Subsection 2.2.2 : Chinmay , Sarwar
- Subsection 2.2.3 : Vinay , Khushboo
- Subsection 2.2.4 : Bhavesh
- Subsection 15 : Reva
- Subsection 15 : Bhavesh
- References : Bhavesh, Sarwar, Chinmay, Vinay

Week 3:

- section 3.1,3.2 : Bhavesh
 - table 3.1 : Vinay
 - section 3.3 : Reva
 - section 3.4 : Akash, Chinmay
 - section 3.4.5 : Sarwar, Khushboo
 - section 15 : Bhavesh
 - section 3.2 Desmos code : Akash
- Verification and data correction : All

Week 4:

- section 4.1 - 4.3 : Reva
 - section 4.4 - 4.6 : Vinay
 - section 4.7 : Khushboo, Reva
 - code 15 : Bhavesh
- Editing of prev week's report 3.4: Akash, Sarwar, Chinmay
- section 3.5 : Bhavesh

Week 5:

-section 5.2: Reva
-section 5.1.1 and 5.1.2 : Chinmay
-section 5.1.3, 5.1.4, 5.1.5 and 5.1.6 : Vinay
-code 15: Reva
-summary 5.3: Chinmay, Khushboo
-presentation: Bhavesh (pg 1-7,10 & 11), Akash (pg 10), Sarwar (pg 8 & 9)

Week 6:

Reva : code 15, section 7.1
Vinay : sections 6.1, 7.2 & 7.3
Akash : section 7.8
Bhavesh : sections 7.7,7.9 & writing of 6.2, 6.3
Chinmay : figures 6.1 & 7.7, sections 7.4, 7.5 & 7.6
Sarwar : section 7.10
Khushboo : section 7.11

Week 7:

Reva : Sections 9.2, 9.3, 9.5
Vinay : Section 8.1.1 , Section 8.1.2, Section 8.1.3
Akash :Section 9.1
Bhavesh : sections 9.4, 9.1 and calculations of parameters
Chinmay : Section 8.1.4, Figure ??
Sarwar : Section 8.1.5
Khushboo : Table 8.1

Week 8:

Akash, Vinay, Reva, Chinmay, Bhavesh, Sarwar: Ideation
Reva: Sections 10.1, 10.3, 10.6, 15
Bhavesh: Section 10.4
Khushboo: Section 10.1
Akash: Section 10.5

Week 9:

Akash: 11.3.1
Bhavesh: 11.2.5, 11.2.6
Vinay : 11.1
Reva : 11.2.4
Chinmay : 11.3.2 , 11.3.3

Week 10:

Reva : Sections 12.1.1, 12.1.2, 12.1.3, 12.1.4, 12.1.6

Vinay : Section 12.2

Akash :Section 12.1.5

Bhavesh : Section 12.1.5

Chinmay : Section 12.1.6, 12.4, CG value iterations, all simulations.

Sarwar : Section 12.3.1

Khushboo : Section 12.3.2

Week 11:

Vinay : Section 13.1 , 13.2

Reva : Sections 13.3, code 15, 14.1, 14.10, Final presentation preparation.

Bhavesh : Section 13.6 and code 15

Sarwar : Final presentation preparation.

Chinmay : Chapter 14, Final presentation preparation.